Substrate specificities of outer membrane proteases of the omptin family in *Escherichia coli, Salmonella enterica,* and *Citrobacter rodentium*

Andrea Portt, McGill University, Montreal

October 9th, 2010

A thesis submitted to McGill University in partial fulfillment of the requirements of the degree of Master's in Microbiology

Table of Contents

List of abbreviations

α_2-AP – α_2-Antiplasmin

A/E – Attaching and Effacing

AMP – Antimicrobial Peptide

C18G – Cysteine 18 Glycine, an 18 amino acid synthetic antimicrobial peptide

CFU – Colony Forming Unit

CHAPS – 3-[(3-Cholamidopropyl)dimethylammonio]-1-propanesulfonate, a zwitterionic detergent

CIHR – Canadian Institutes for Health Research

CMI – les Concentrations Minimales Inhibitrices

DTT – Dithiothreitol

ECM – ExtraCellular Matrix

EDTA – Disodium ethylenediaminetetraacetate dihydrate, a chelating agent

EHEC – EnteroHemorrhagic *E. coli*

EPEC – EnteroPathogenic *E. coli*

HGT – Horizontal Gene Transfer

LB – Luria-Bertani broth

LD_{50} – Lethal Dose of a pathogen for 50 % of mice infected

LEE – Locus of Enterocyte Effacement pathogenicity island

LPS – Lipopolysaccharide

MAC – Membrane Attack Complex

mCRAMP – Mouse Cathelicidin-Related AntiMicrobial Peptide

MIC – Minimal Inhibitory Concentration

NPN - 1-N-PhenylNaphthylamine

NSERC – Natural Sciences and Engineering Research Council

OM – Outer Membrane

OMP - Outer Membrane Protein

PAM – les Peptides AntiMicrobiens

PBS – Phosophate-Buffered Saline

Plg – Plasminogen

RDEC – Rabbit Diarrhoeagenic *E. coli*

RT-qPCR – Real-Time Quantitative Polymerase Chain Reaction

Sarcosyl – N-Lauroyl-Sarcosine

SCV – *Salmonella*-Containing Vacuole

SDS-PAGE – Sodium Dodecyl Sulphate PolyAcrylamide Gel

T3SS – Type 3 Secretion System

TFPI – Tissue Factor Pathway Inhibitor

TSB – Tryptic Soy Broth

uPA – Urokinase Plaminogen Activator

UTI – Urinary Tract Infection

Abstract

Outer membrane proteins (OMPs) of the omptin family are present in some Gram-negative bacteria. Omptins protect cells by cleaving antimicrobial peptides (AMPs). For example, the *Escherichia coli* OmpT and OmpP impart resistance by cleaving the AMP protamine, and PgtE of *Salmonella enterica* was also reported to cleave AMPs. Despite identification of many *in vitro* substrates, few physiological substrates have been tested. Our laboratory recently identified the omptin CroP of *Citrobacter rodentium*, which cleaves the murine α-helical AMP mCRAMP and the similarly α-helical synthetic AMP C18G. We examined AMPs as substrates of several omptins. OmpT, OmpP, and CroP cleave the AMP C18G more effectively than PgtE, leading to higher minimal inhibitory concentrations (MICs). This suggests that AMP cleavage is an important function of OmpT, OmpP, and CroP during infection. Based on initial results, we attempted to compare and contrast specificity and catalytic activity of C18G cleavage by purified CroP and PgtE.

Les protéines de la membrane externe de la famille omptin se trouvent dans quelques bactéries à Gram négatif. En coupant les peptides antimicrobiens (PAMs), les omptins protègent les bactéries. Par exemple, les omptins OmpT et OmpP d'*Escherichia coli,* et l'omptin PgtE de *Salmonella enterica,* coupent les PAMs. Malgré l'indentification de plusieurs substrats *in vitro*, peu de substrats physiologiques ont été découverts. Dans notre laboratoire, on a identifié l'omptin CroP de *Citrobacter rodentium,* qui coupe le PAM murin mCRAMP. On décrit ici l'activité de plusieurs omptins contre les PAMs. OmpT, OmpP et CroP coupent le PAM C18G plus efficacement que PgtE, ce qui mène à des concentrations minimale inhibitrices (CMIs) plus haute. Ces résultats suggèrent que l'activité catalytique d'OmpT, OmpP, et CroP est importante lors de l'infection. À la suite des résultats préliminaires, on a tenté de comparer la spécificité et l'activité catalytique contre C18G des protéases purifiées CroP et PgtE.

Acknowledgements

The author gratefully acknowledges her supervisor, Dr. Hervé Le Moual, for his careful guidance through every stage of this work. Thanks are due to Dr. Valerie Le Sage for her hard work with *C. rodentium* in the lab and in preparing the Molecular Microbiology manuscript. Dr. Samantha Gruenheid provided guidance and technical training. Dr. Benoit Cousineau offered insight as a committee member. Special thanks are due to Jenny-Lee Thomassin, who produced the LL-37 cleavage data in Figure **9**. I would also like to recognize my labmates Charles Viau for his encouragement and his wealth of biochemical knowledge, and Daniel Ting for his balanced perspective in all things microbiological and philosophical. Charles and Daniel also worked with Mg^{2+} to stabilize the outer membrane in NPN assays. Under the supervision of Dr. France Daigle at the Université de Montréal, Christine LePage and Sébastien Sabbagh undertook the RT-qPCR work and construction of the *S. enterica ΔpgtE* mutant. Dr. James Taylor and Richard Wargachuk were a consistent source of advice throughout this project. Thanks are also due to my parents, Cam Portt and Rena Burkholder, as well as Allen Larocque, Laura Canty, Carmen Evans, and Peter F. Woodford, author of Scientific Writing for Graduate Students.

The Government on Ontario financially supported this work in the form of the Ontario-Quebec Exchange Fellowship. The Canadian Institutes for Health Research (CIHR), McGill University, and the Natural Sciences and Engineering Research Council (NSERC) of Canada provided additional funding.

Contributions of Authors

Dr. Valerie Le Sage and our supervisor Dr. Hervé Le Moual undertook the majority of the scientific direction, laboratory work, and writing of the Molecular Microbiology paper attached to this thesis, see page 80. Under the supervision of Dr. Samantha Gruenheid, Lei Zhu produced the *C. rodentium phoPQ* knockout. Christine Lepage undertook RT-qPCR experiments under the supervision of Dr. France Daigle. Andrea Portt produced the *C. rodentium croP* knockout, contributed data to Figures 1c, 3a, 5a, and 6, produced Table 1, and helped edit the manuscript. Charles Viau contributed β-galactosidase data for the effect of AMPs on activation of PhoPQ in *C. rodentium*.

Literature review

1. OM proteins

The outer membrane (OM) of Gram-negative bacteria is the surface that interacts with the environment and the eukaryotic host, and consequently many OM proteins (OMPs) are crucial for bacterial virulence[1]. OMPs have many roles in pathogenic Gram-negative bacteria. OMPs interact with the host as antigens, receptors or adhesins, and proteases. For example, the pH 6 antigen, of *Yersinia pestis* has antigenic properties, but it also promotes adhesion to human epithelial cells via binding to phosphatidylcholine[2]. OM proteases may cleave bacterial or host substrates. SepA is a *Shigella* OM protease of the autotransporter family. Autotransporters transport and release one of their own domains, resulting in secretion of the extracellular domain[3]. The secreted portion of SepA contributes to tissue invasion[4]. The omptin family of OM proteases also have proteolytic properties that are key to pathogenesis for enteric bacteria. Their unique catalytic site makes them ideal subjects for study because a better understanding of their function may lead to development of therapeutic agents that limit pathogenesis.

2. Omptins

Omptin proteases are transmembrane β-barrels 70 Å in length. Their 10 anti-parallel β-strands are connected by 4 short periplasmic loops and 5 longer extracellular loops (Figure **1**). Whilst the periplasmic loops have no known function, the sequences of the extracellular loops determine the specificity of the different omptins. These loops extend just above the outer edge of rough lipopolysaccaride (LPS) (Figure **2**), forming the active site groove[5]. Residues at the bottom of the active site grove also influence specificity, as altering the charge of the S1 site greatly affects the specificity of the *E. coli* omptin OmpT[6]. Slight modifications in loop and active site groove sequence have given rise to distinct specificities among omptins of different bacterial species, which are beneficial to the species' own method of pathogenesis, as described in Section **6**. Omptin proteases are anchored in the OM by 2 rings of aromatic residues that associate

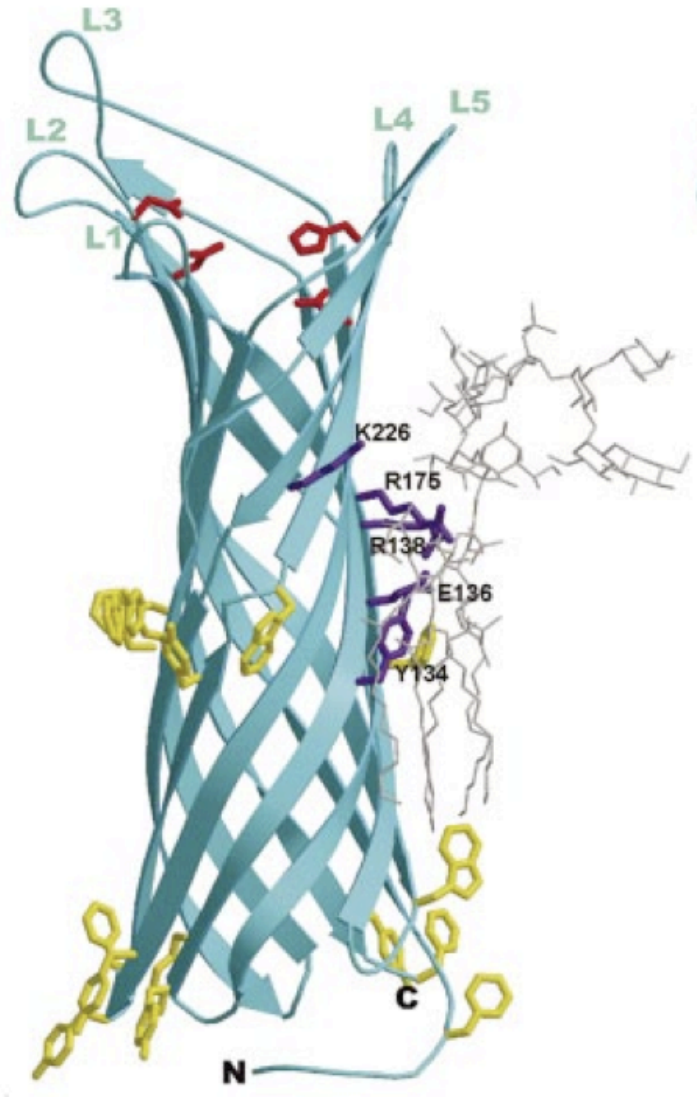

Figure 1: Structure of OmpT showing catalytic residues in red, LPS-associated residues in violet, and aromatic residues in yellow. Reproduced with permission from EMBO J 2001 vol. 20 (18) pp. 5033-9.

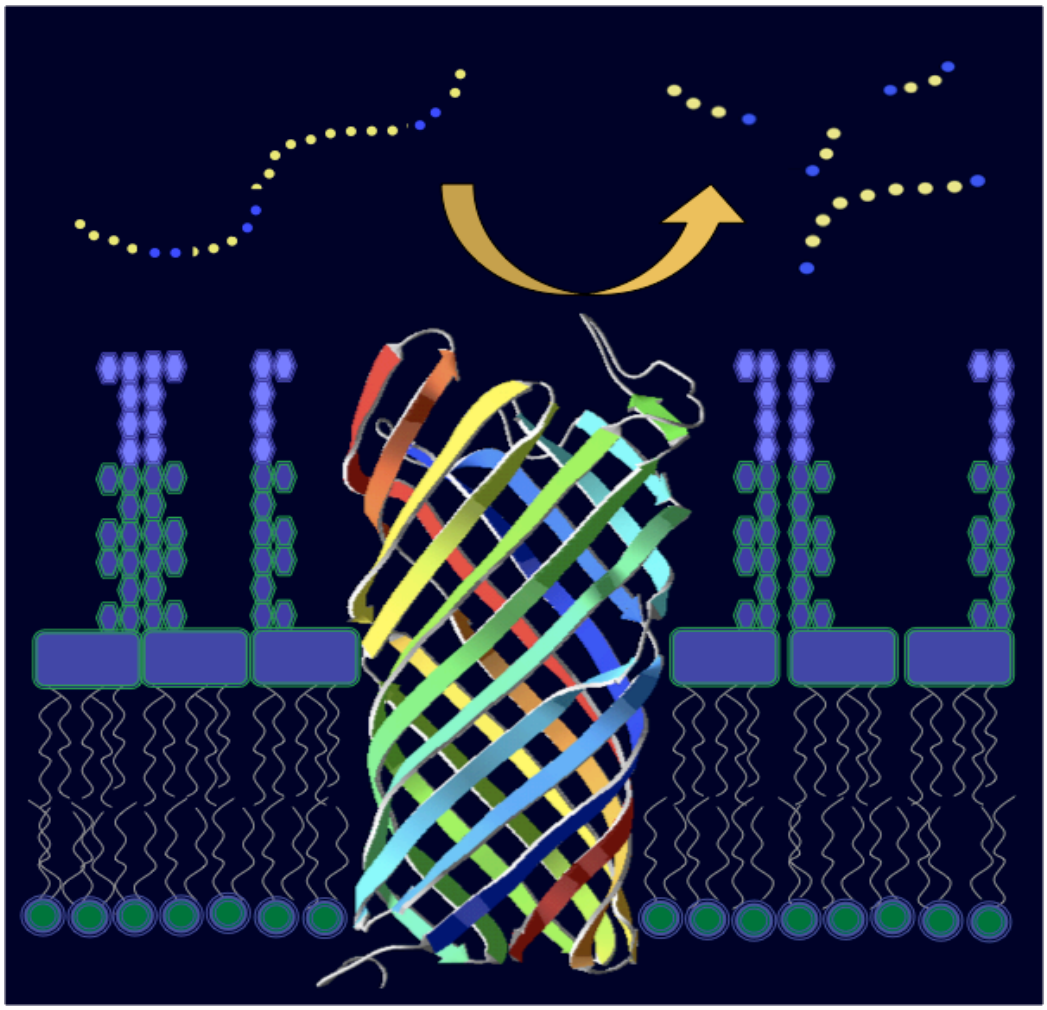

Figure 2: CroP is an integral OM protease. The outer loops of the β-barrel extend just beyond the rough LPS. We propose that CroP cleaves and inactivates AMPs at the OM during A/E pathogenesis. This CroP model was rendered using the Swiss Model First Approach Method with the existing OmpT structure as a template.

with the hydrophobic portions of the outer leaflet, shown in yellow in Figure **1**. The unique catalytic site is highlighted in red. It consists of an Asp-Asp pair and a His-Asp pair. Omptins strongly prefer to cleave between two basic residues, Arg-Arg, Arg-Lys, Lys-Arg, or Lys-Lys. Proteolytic cleavage is thought to involve a water molecule positioned between the first Asp residue and the His residue. The His-Asp dyad then activate the water molecule, which performs a nucleophilic attack on the scissile amino acid bond[5]. The Asp-Asp, His-Asp proteolytic mechanism is highly conserved among omptins[5], however omptin homologues in *Erwinia amylovora* and *Yersinia pseudotuberculosis* carry catalytic site mutations and their functions are unknown[7].

The omptins OmpT, PgtE of *Salmonella enterica* and Pla of *Y. pestis*, have a dual interaction with LPS. On one hand, they are not functional without it. LPS associates with OmpT at conserved residues: Tyr134, Arg 138, Arg175, and Lys226, shown in purple in Figure **1**. LPS does not induce major structural changes to OmpT, and it is instead believed to induce subtle conformational changes that align the catalytic dyads[5]. The requirement for LPS likely prevents proteolysis of cytoplasmic or periplasmic proteins during production and transport to the OM[8]. On the other hand, long LPS reduces omptin activity. The O-antigen of smooth LPS sterically hinders access of protein substrates to the active site, but does allow autoproteolysis[9] and cleavage of peptide substrates. Loss of function in the presence of O-antigen may seem counter-intuitive, given the importance of O-antigen in serum resistance. However, during infection of macrophages, *S. enterica* reduces the length of its O-antigen, which may allow PgtE full functionality[8]. Additionally, *Y. pestis* does not express smooth LPS, so Pla activity is not inhibited[9].

Another distinctive property of omptin proteases is their capacity for autoproteolysis. Autoprocessing has been documented for OmpT, PgtE, and Pla. Autoprocessing between Lys217 and Arg218 results in a 31 kDa form of OmpT[10]. Mutants Lys217Thr and Gly216Lys/Lys217Gly did not autoproteolyse, and had only 40% and 70% of wildtype activity respectively[11]. Kukkonen *et al.* found 3 forms of PgtE: α-, β-, and γ-PgtE. They concluded that the β-, and γ-PgtE resulted

from autoprocessing at Arg154. Proteolytically inactive PgtE mutants did not form β-PgtE or γ-PgtE[9]. In a similar study, residue Lys262 of loop 5 was identified as the autoprocessing site of Pla. *E. coli* expressing non-autoprocessing Pla mutants Glu217Ser and Phe215Tyr were reported to retain plasminogen (Plg) cleavage and α_2-antiplasmin inactivation. However, compared to the wild-type, the mean Plg activation rates were 52 % for E217S and 42 % for F215Y[12]. Overall these data suggest that the native sequence is required for full enzymatic activity.

3. Omptin substrates

a. Antimicrobial peptides

Several omptins have been shown to cleave antimicrobial peptides (AMPs). AMPs are innate immune molecules that belong to many different homologous groups and are produced by all domains of life. For example different AMPs are produced by bacteria to kill other species of bacteria, and by insects or mammals to fight infection[11]. They are potent killers of Gram-positive, Gram-negative, and fungal pathogens[13] and in vertebrates they form a bridge between innate and adaptive immunity by acting as direct antimicrobials at the same time as stimulating the host's adaptive immune response[12].

The best-studied AMPs are defensins and α-helical AMPs. β-defensins are expressed in the gut[11], and α-defensins are present in high quantities in human neutrophils[14]. Disulphide bonds make defensins resistant to proteolytic inactivation[14]. Protective α-helical AMPs are expressed by epithelial cells on skin, on mucosal surfaces of the stomach and colon[15], and within macrophages[16]. This group includes the cathelicidins. The human cathelicidin AMP is LL-37 (LLGDFFRKSKEKIGKEFKRIVQRIKDFLRNLVPRTES[14]). Mice express mouse cathelicidin-related AMP, (mCRAMP, GLLRKGGEKIGEKLKKIGQKIKNFFQKLVPQPEQ[17]). Cathelicidin genes are influenced by exposure to bacterial products. For example, gastric epithelial cells recognize *Helicobacter pylori* and respond by up-regulating LL-37 expression[18], and *Shigella* down-regulates cathelicidin in a rabbit infection model[19].

Cathelicidins employ an overall positive charge and their amphipathic structure to kill bacteria by associating with the negatively charged OM, forming pores, disrupting cytoplasmic membrane integrity, and targeting cytoplasmic components[14]. Their lack of disulphide bonds and the presence of scissile dibasic bonds make them more sensitive to proteolytic inactivation than defensins.

Other AMPs discussed in this work are protamine (MPRRRRSSSRPVRRRRRPRVSRRRRRRGGRRRR[20]) and C18G (ALYKKLLKKLLKSAKKLG[21]). Protamine is isolated from salmon sperm. It lacks the amphipathic structure of α-helical AMPs, but is often used as a less expensive model for action of α-helical AMPs[22]. C18G is a synthetic peptide. Darveau *et al.* developed C18G by truncating and and altering the amino acid sequence of human platelet factor IV, to increase the AMP's α-helicity [21,23]. It is not a physiological substrate, but since it forms this cathelicidin-like α-helix[24], and is readily synthesized, it is used in this work and others as a substitute for LL-37 or mCRAMP.

Bacteria have developed protection from AMPs via efflux pumps, OM alterations, and peptidolysis[25]. As an example, *Neisseria meningitidis* exports LL-37 via its MtrCDE drug resistance exporter. Also*, S. enterica* reduces the attraction between the negatively charged OM and positively charged AMPs by incorporating positively charged aminoarabinose into its lipid A[25]. Finally, omptins are reported to protect *E. coli* and *S. enterica* from AMPs by proteolytic cleavage *in vitro* [26,27,28].

b. Blood clotting proteins and extracellular matrix

Plasminogen and α_2-antiplasmin

In addition to cleaving AMPs, omptins are believed to undermine regulation of blood clotting. Figure **3** illustrates the interactions of the plasminogen (Plg) system with the host Plg activator and with omptins. Plg is a proenzyme that circulates in the blood at a concentration of 180 μg/mL. In the healthy host, it is converted into the serine protease plasmin via cleavage by urokinase Plg activator, which is located on the macrophage surface. This facilitates macrophage migration in the extracellular space because plasmin not only

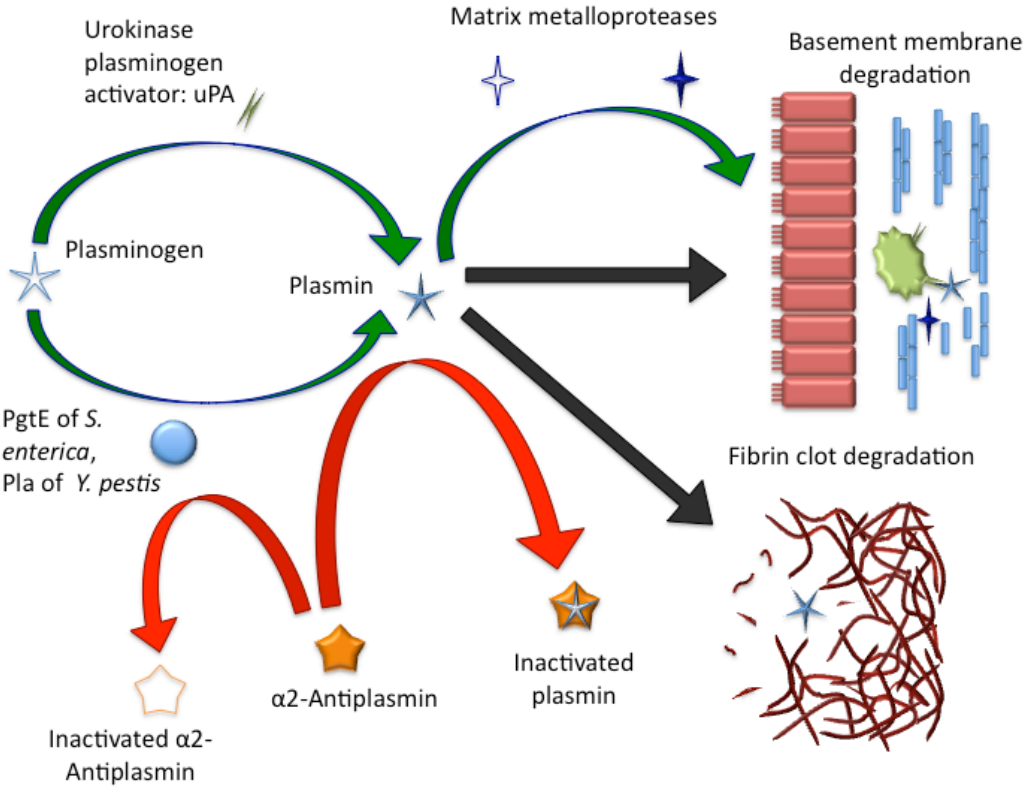

Figure 3: Omptin interactions with the plasminogen system. Plasminogen is cleaved into plasmin by the urokinase plasminogen activator (uPA) on the macrophage cell surface. Plasmin degrades laminin, a major component of the basement membrane, as well as activating matrix metalloproteases that degrade collagens in the basement membrane. This facilitates migration of macrophages. Plasmin also degrades fibrin clots. These processes are carefully controlled by α2-antiplasmin (α_2-AP), which binds and inactivates plasmin. The omptins PgtE of *S. enterica* and Pla of *Y. pestis* are thought to speed their own dissemination through the host by activating plasmin and inactivating α_2-AP[9,12,30]. Activation is depicted in green arrows; inactivation is depicted in red arrows; degradation is depicted in black arrows.

degrades laminin, a major component of the extracellular matrix (ECM), but also activates matrix metalloproteases that degrade ECM collagens. In addition to its ECM-degrading activities, plasmin supports migration by degrading fibrin blood clots. Fibrin clots are a hallmark of inflammation. Their formation around the site of infection forms a barrier to prevent the spread of bacteria. Given the many important roles of active plasmin, it follows that the host must tightly control its protease activity. The protease inhibitor α_2-antiplasmin (α_2-AP) fills this role by binding and inactivating plasmin. There is some evidence that bacterial infection influences host production of plasmin and plasmin inhibitors *in vivo*. Human volunteers exposed to bacterial endotoxins had a surge of plasmin followed by an increase in plasmin inhibitors[29]. The omptins PgtE and Pla are thought to subvert Plg regulation by cleaving and inactivating α_2-AP,[12,9,31] in order to facilitate dissemination[29] through ECM or fibrin clots (Figure **3**), as discussed below.

Tissue factor pathway inhibitor

Tissue factor pathway inhibitor (TFPI) is an essential inhibitor of coagulation that is released from platelets into plasma. TFPI complexes with clotting factor Xa, which then inhibits initiation of blood clotting by tissue factor and factor VIIa. Recently, a research group found that *Y. pestis, S. enterica*, and *E. coli* carrying native omptins all inactivated TFPI two or three orders of magnitude more efficiently than they activated the traditional substrate Plg or inactivated α_2-AP *in vitro*[32]. This would theoretically lead to coagulation surrounding enteric infections. The authors propose that host TFPI evolved to be sensitive to omptins in order to contain infection within blood clots[32]. However, examination of the human, rabbit, rat, and mouse TFPI sequences reveals a high degree of homology even outside of the omptin cleavage site, suggesting a common ancient gene as opposed to convergent evolution towards sensitivity to omptins. Further work may show that omptins take advantage of this shared sensitivity to proteolysis to further deregulate the clotting pathway, in a similar fashion to the prothrombotic function of *Staphylococcus aureus* staphylocoagulase[32].

c. Complement

Omptins may further protect enteric bacteria by disabling the complement

cascade. Complement pathways are essential for innate and adaptive immunity. They function either by direct killing via formation of the membrane attack complex (MAC), or by phagocytosis. Complement components also influence inflammation and migration of phagocytic cells[33]. PgtE has been shown to cleave several complement components, which may be important immediately after release from macrophages, when the O-antigen is too short to provide serum resistance[31,34]. Pla of *Y. pestis* has also been shown to cleave complement *in vitro,* which may increase serum resistance of this extracellular pathogen[35].

d. Tropomyosin

Tropomyosin is a major component of skeletal muscle fibres and is one of the molecules responsible for muscle contraction. Tropomyosin is a non-physiological substrate of OmpT, which alters tropomyosin function by removing the N-terminus between Lys6 and Lys7[36]. Although this does not provide insight into the putative role of OmpT in pathogenesis, the study's authors suggested that OmpT may be useful in functional studies of other proteins with dibasic cleavage sites[36].

As well as the proteolytic capabilities described in this section, omptins have roles in SOS response[37], colicin resistance[38], and adhesive and invasive properties[39]. However these functions fall outside of the scope of this project and are therefore not discussed here.

4. Evolution of omptins

Omptin genes have been passed between species by horizontal gene transfer (HGT). They are most often found on plasmids or in prophages, as seen in Table **1**. In *E. coli*, *ompT* is found on a cryptic prophage in enterohemorrhagic *E. coli* (EHEC) and enteropathogenic *E. coli* (EPEC)[8], and *ompP* is carried on the F plasmid of some strains of *E. coli*[20]. In *Y. pestis*, Pla is found on the pPCP1 plasmid, and *sopA* is located on a *Shigella flexneri* virulence plasmid[8]. There is no report of *pgtE* being located in a prophage, and *croP* is not within any of the prophages or genomic islands recently identified on the *C. rodentium* genome[40]. However, both *pgtE* and *croP* are located between tRNA genes on their respective

Table 1: Summary of enteric omptins, their location in the genome, and their protease functions.

Species	Omptin	Location	Protease function
E. coli	OmpT	Chromosome: cryptic prophage	Various *in vitro* substrates
E. coli	OmpP	F plasmid	Various *in vitro* substrates
S. enterica	PgtE	Chromosome	Plg, α2-AP, TFPI
C. rodentium	CroP	Chromosome	AMPs
Y. pestis	Pla	Plasmid pPCP1	Plg, α2-AP, TFPI
S. flexneri	SopA/IscP	Large virulence plasmid	Cleaves IcsA for intercellular movement

Figure 4: Crop is closely related to OmpP and OmpT. CroP shares 70 – 80 % of its amino acid sequence with OmpP and OmpT, and about 40 % of its amino acid sequence with PgtE and Pla.

genomes. Since insertion sequences and transposons often insert near tRNA genes[41], it is possible that these omptins were also acquired with HGT elements.

Figure **4** shows the omptin family phylogenetic tree. *OmpT* is by far the best-studied omptin. Its close relatives are *ompP* and *croP*, with 70 % identity to *ompT*[8]. The other branch shows that *pgtE* and *pla* are approximately 40 % identical to *croP*. *Pla* is thought to have evolved from *pgtE* after HGT 1 500 – 20 000 years ago, when a strain of *Yersinia pseudotuberculosis* transformed into *Y. pestis*[8]. Omptins have been identified in other bacterial genera and families. *Erwinia pyrifoliae* is an enteric plant pathogen that carries the omptin *plaA*. The plant symbiont *Mesorhizobium* sp. BNC1 is a member of the *Phyllobacteriaceae* family, but it also carries an omptin. Additionally, omptin homologues have been identified in *Erwinia amylovora* and *Y. pseudotuberculosis*. These homologues have substitutions at the catalytic site, hence they are likely to be catalytically inactive[7].

5. Omptin regulation

The OMP OmpT was named for its Temperature-dependent regulation. OmpT's expression is greatly reduced below 32 °C[38], although the mechanism of this regulation is undetermined. Fortunately, there is a wealth of information that links regulation of omptin transcription and expression to virulence and membrane stress in *E. coli*, as described in Figure **5**.

The PhoPQ two-component system is a major regulator of pathogenicity. PhoQ is an inner membrane sensor kinase that is activated by antimicrobial peptides or limiting levels of divalent cations[42], whereupon it phosphorylates the response regulator, PhoP. PhoP up-regulates no less than 200 genes, including *ompT*[43]. In this way, PhoPQ links sensing AMPs at the inner membrane to up-regulation of the AMP-protective omptin. The *E. coli* response regulator EvgA augments the up-regulation of *ompT* transcription by PhoP. EvgA is phosphorylated by its sensor kinase EvgS, in response to an as-yet unidentified environmental signal[43].

Transcription of *ompT* is also indirectly controlled by the σ^E transcription factor, as shown in Figure **5**. σ^E controls aspects of pathogenesis and the development of maximal resistance to environmental stresses. σ^E is activated by temperature

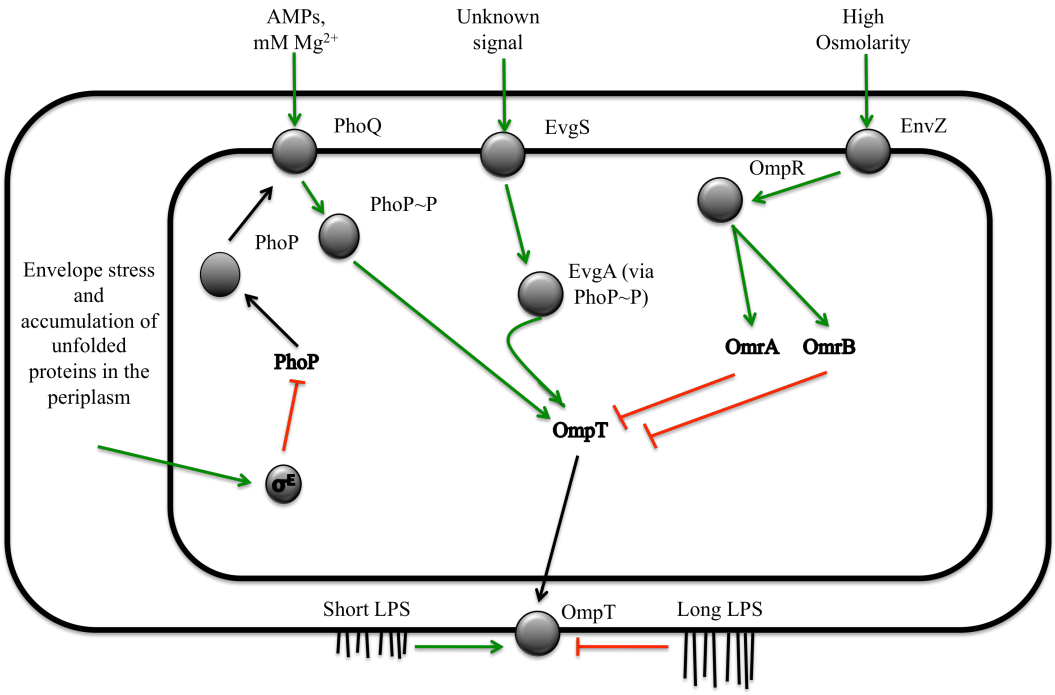

Figure 5: Regulation of omptins is linked to virulence and OM stress[9,43,45,46]. The PhoP/PhoQ two-component system up-regulates transcription of *ompT* in response to AMPs or to mM concentrations of Mg^{2+}; this up-regulation can be augmented by EvgS/EvgA in response to an unknown signal, and is thought to lead to protection of the cell envelope from host AMPs. Conversely, in response to envelope stress due to accumulation of unfolded proteins in the membrane, the σ^E transcription factor induces the sRNA MicA, which binds PhoP mRNA leading to its degradation and therefore indirectly reducing OmpT transcription. Expression of OmpT can also be reduced via EnvZ/OmpR, which sense and respond to high osmolarity envelope stress by increasing transcription of sRNAs OmrA and OmrB. These sRNAs bind OmpT mRNA, leading to its degradation. These last two pathways are thought to stabilize the OM by reducing excess omptin expression. Proteins are depicted as blue circles; mRNAs are depicted as blue text. Activation of proteins and up-regulation of transcription are shown as green arrows, inhibition is shown as red lines.

shock, hyperosmolarity, and accumulation of unfolded OMPs in the periplasm. Upon envelope damage, the σ^E precursor is released from the membrane by proteolysis, yielding active σ^E. Many of the genes that are controlled by σ^E are OMPs. Active σ^E removes OMP mRNAs via sRNAs[44]. In the case of *ompT*, σ^E up-regulates the sRNA MicA, which binds to PhoP mRNA. MicA-bound PhoP mRNA is quickly degraded, indirectly leading to a 3-fold decrease in *ompT* transcription[45]. The net result of the σ^E response is to reduce the flow of new proteins – including omptins - to the stressed OM, preventing further strain from buildup of unassembled OMPs[44].

As illustrated in Figure **5**, degradation of OmpT mRNA is also connected to envelope stress via the sensor kinase EnvZ and its response regulator OmpR. EnvZ senses envelope stress caused by high osmolarity and responds by phosphorylating OmpR. OmpR activates transcription of two highly homologous sRNAs: OmrA and OmrB. OmrA and OmrB negatively regulate *ompT*. Base-pairing between OmrAB and *ompT* mRNA is predicted, but it is not known whether this base-pairing blocks ribosome entry or accelerates decay of mRNA[47]. OmrA and OmrB homologues are reported in *S. enterica*[48], and we have also identified homologues arranged sequentially in the *C. rodentium* genome. Thus, via PhoPQ, σ^E, and EnvZ/OmpR, omptin expression is linked to pathogenesis, AMPs, and outer membrane stress.

6. Omptins of pathogenic *Enterobactereaceae*

Omptin proteases are an example of a homologous group of proteins in which slight modifications in sequence, mainly at the active site and its surrounding loops, have lead to a wide variety of functions. The various functions may contribute to pathogenesis of several species, including *Y. pestis*, *S. enterica, S. flexneri, E. coli*, and *C. rodentium.*

a. *Y. pestis*

The strongest evidence of an omptin as a virulence factor is the case of the Plg activator Pla. *Y. pestis* is one of the most pathogenic bacteria for humans. This bacterium not only caused the Black Plague in medieval Europe, it also infects

thousands of individuals every year in the 21st century[49]. Reservoirs in wild animals are present in the United States, South America, Asia, and Africa. Infection with the bubonic plague begins with a bite of a flea from an infected rodent[49]. From the subcutaneous bite, the bacteria spreads to lymph nodes, and thence to the bloodstream[9] and lungs[29]. Although mortality rates for bubonic plague range from 30 – 70 %, pneumonic or septicaemic plague is nearly always fatal[49]. Most of the bacteria are extracellular during the septicaemic stage; they are then taken up by a flea along with its meal of blood, continuing the infection cycle[49].

The role of Pla in bubonic plague is established in the mouse model. Pla's ability to activate Plg and inactivate α_2-AP has been repeatedly demonstrated *in vitro*[9,12,30]. *In vivo*, the lethal dose for 50 % of mice (LD_{50}) of *Y. pestis pla*$^-$ is 1 x 10^7 colony forming units (CFU), compared to only 50 CFU for wild-type *Y. pestis*. This is true for subcutaneous infection, but not intravenous infection. Plg knockout mice are 100 times more resistant to *Y. pestis,* further supporting a role for Pla's activation of Plg in pathogenesis[29]. In view of Pla's importance in subcutaneous infection, activation of Plg is thought to aid dissemination from the original site of infection to the lymph node[29]. This may be achieved through fibrinolytic or ECM degrading activities of Pla-activated plasmin. Bacterial strains expressing Pla have been shown to promote degradation of fibrin by plasmin *in vitro*, which may allow bacterial movement by disintegrating fibrin clots surrounding the infection[30]. Activation of Plg by Pla has also been shown to facilitate degradation of laminin and human epithelial cell ECM[50].

Other reported *in vitro* activities of Pla include cleavage of complement component C3 and TFPI. Cleavage of C3 may incur serum resistance or reduce production of C5a chemoattractant[35], and TFPI inactivation may either be protective for the host, or constitute further deregulation of the clotting system by Pla[32].

b. *S. enterica*

S. enterica serovar Typhi (*S.* Typhi) causes typhoid fever, which is endemic in many Asia and African countries. Its close relative, *S. enterica* serovar

548 Typhimurium (*S.* Typhimurium) is one of the most common food-borne
549 gastointestinal infections in humans, and causes a typhiod-like disease in mice[51].
550 Initially, *Salmonella* crosses the intestinal epithelium. This leads the bacteria to
551 the macrophages positioned below the epithelium, where *Salmonella* establishes
552 intracellular infection. In macrophages, *Salmonella* survive within a modified
553 phagosome called a *Salmonella* containing vacuole (SCV). Replication of the
554 pathogen within macrophages is a prerequisite for the systemic infection that
555 causes typhoid fever[51].
556 Several lines of evidence point to a role for PgtE in survival in the macrophage.
557 The first is that the PhoPQ system has been shown to control *pgtE* expression[52],
558 and that *S. enterica ΔphoP* had reduced virulence in mice[51]. Moreover, *S. enterica*
559 grown in SCVs showed higher levels of PgtE expression and activity than bacteria
560 grown in broth culture[31]. Finally, these same bacteria demonstrated a reduction in
561 O-antigen length during growth within macrophage-like cell lines[31]. This may
562 allow PgtE to cleave larger substrates in addition to cleaving the AMPs found in
563 the SCV. However, there is some disagreement in the literature as to whether *pgtE*
564 truly confers a survival advantage during growth within macrophages[31,53].
565 These last points leads us to another - not necessarily mutually exclusive -
566 hypothesis for the role of PgtE in *Salmonella* pathogenesis. Several studies have
567 demonstrated cleavage of host proteins *in vitro*. This includes inactivation of
568 complement components C3b, C4b, and C5, which lead to serum resistance[34].
569 Although long O-antigen is traditionally known to protect *Salmonella* from
570 complement[51], one third of *S.* Typhi cells are extracellular[54], presumably after
571 release from macrophages. Since we have seen that *Salmonella* released from
572 SCVs has short O-antigen[31], PgtE may be protective against AMPs or
573 complement during the transition from SCV to serum. PgtE has also been shown
574 to inactivate α_2-AP[31,30] and TFPI[32], and activate Plg[9,31,30]. Inactivation of α_2-AP
575 and activation of Plg may lead to uncontrolled proteolysis of fibrin clots and
576 ECM, allowing rapid dissemination of *Salmonella* infection. Inactivation of
577 clotting inhibitor TFPI may protect the host by sequestering the infection, or it
578 may be another example of deregulation of host clotting factors similar to *S.*

aureus staphylocoagulase[32] activity.

c. *Shigella*

Shigella, which is also known as enteroinvasive *E. coli*, causes bacillary dysentery and bloody diarrhoea. Like *Salmonella,* initial *Shigella* infection involves passage through the M cells and replication in macrophages of the intestinal submucosa. After the macrophages lyse, the bacteria infect enterocytes and continue to spread infection via movement between enterocytes[41]. The autotransporter protein IcsA initiates intracellular movement. IcsA catalyses formation of a comet-like actin tail at one pole of the bacterium. This pushes the bacterium into the adjacent cell. The *Shigella* omptin SopA, or IcsP, is 60% homologous to OmpT. SopA is believed to be a virulence factor because it is required for the localization and cleavage of IcsA, which leads to actin-based intracellular movement in cell culture[55].

d. Attaching and effacing bacteria

The attaching and effacing (A/E) family of pathogens includes EPEC, EHEC*,* rabbit diarrhoeagenic *E. coli* (RDEC), *Escherichia albertii*, which was formerly known as *Hafnia alvei,* and *C. rodentium*[41,56]. *E. coli* infections affect hundreds of millions of people annually. EPEC is a major cause of infant diarrhea in developing nations, whereas contamination of food and water from cattle or beef products leads to EHEC infections in industrialized countries[41]. A/E pathogens tightly attach to intestinal epithelium and destroy (efface) the brush microvilli. Brush microvilli are finger-like projections on the enterocyte surface that are important in nutrient absorption[56]. In fact, malnutrition accounts for 60% of diahrrhoeal deaths world wide[56].

The molecular mechanisms of A/E pathogenesis have been investigated in depth and thoroughly reviewed[41,57]. The locus of enterocyte effacement (LEE) pathogenicity island carries the genes required for the A/E phenotype and is present in the EPEC and EHEC genomes. The step after initial attachment is intimate attachment to enterocytes. The bacterium injects the intimin receptor Tir into the host cell via the Type 3 Secretion System (T3SS). Tir inserts into the host

membrane and associates with intimin on the bacterial surface, forming a close attachment between the two cells. The bacterium then effaces the microvilli and Tir initiates actin re-arrangement to form pedestals beneath the bacterium[41].

The contributions of *E. coli* OmpT to this style of pathogenesis are poorly understood. EPEC and EHEC lack the F plasmid that carries OmpP in some strains of *E. coli.* However there is good evidence that OmpT plays a role in urinary tract infection (UTI) pathogenesis. The strongest support for a role of OmpT in UTIs is *in vitro* and epidemiological. Early work showed that OmpT cleaved and protected from the AMP protamine extracted from salmon sperm *in vitro*[26]. A 1995 study found that *ompT* was associated with other virulence genes in a significant proportion of first-time UTI isolates[58]. Another study found that the majority of 282 clinical isolates carried *ompT.* Overall 77 % of the strains were *ompT*$^{+}$*,* with incidence ranging from 50 % in isolates from stool samples to 100 % in isolates from blood samples[59] More recently, 80 % of 102 *E. coli* isolates from skin and soft-tissue infections were found to carry *ompT*[60]. Additionally, cathelicidin expression in the urinary tract has been linked to defense from *E. coli* infection in humans and mice[61]. Importantly, a recent publication showed that OmpT confers resistance to AMPs isolated from human urine. This bolsters proof for a role in UTIs[62]. These studies suggest that OmpT may indeed be an important virulence factor of *E. coli*. We believe that as in uropathogenic *E. coli* UTIs, OmpT aids EPEC and EHEC evasion of host defense by cleaving cathelicidin in the gut. Moreover, we propose the mouse pathogen *C. rodentium* and its OmpT homologue CroP as a model for this hypothesis.

The murine pathogen *C. rodentium* is a close relative of EPEC and EHEC. In the 1960s, *C. rodentium* was described in North America as an atypical *Citrobacter freundii* and in Japan as mouse pathogenic *E. coli.* These were later confirmed to be the same pathogen, distinct from known *Citrobacter* species. The new species was renamed *C. rodentium*[63]. In adult mice, *C. rodentium* is associated with outbreaks of rectal prolapse, diarrhea, and moderate mortality. However mortality can by high in some lines of inbred mice and in suckling mice. The LEE pathogenicity island of *C. rodentium* is homologous to the one carried by EPEC

and EHEC, and the structure of *C. rodentium* A/E lesions is indistinguishable from that of EPEC and EHEC[63]. As in EPEC and EHEC, bacteria attach to epithelial cells of intestine via binding of intimin and Tir, leading to effacement of the brush border microvilli. *C. rodentium* is the only species outside of *E. coli* to carry the LEE pathogenicity island, as well as being the only LEE-positive species that infects rodents. For these reasons, it is widely accepted as an excellent model for A/E pathogenesis[63].

We are examining the potential role of the *C. rodentium* omptin CroP in pathogenesis. CroP cleavage of the cathelicidin mCRAMP, which is expressed in the mouse colon[15], may protect the bacteria from the innate immune AMPs. Our earlier work has demonstrated that CroP of *C. rodentium* cleaves mCRAMP and provides protection from mCRAMP-mediated killing *in vitro*[21]. Iimura *et al.* investigated the relationship between expression of mCRAMP and infection with *C. rodentium in vivo.* Iimura's group worked with mice that had the mCRAMP-encoding *cnlp* gene knocked out. Lysates of colonic tissue of *clnp*$^{-/-}$ mice killed *C. rodentium* less effectively than lysates from wild-type mice. Expression of mCRAMP prevented epithelial and luminal colonization. These differences were significant at day 7, but not at day 14 post infection, suggesting that protection by mCRAMP is important during the early stages of infection[15].

Introduction

With a potential role for OmpT and CroP in A/E pathogenesis in mind, we set out to compare the functions of different omptins. Our specific goal was to compare the specificities and catalytic activities of previously studied omptins OmpT, OmpP, PgtE, to those of CroP. Cleavage by cells expressing OmpT and OmpP has been shown to mediate resistance to the AMP protamine[26,20]. An *S. enterica* strain expressing PgtE has been reported to cleave C18G, and be more resistant to C18G and LL-37. As well, a *pgtE* knockout strain has been reported to be more sensitive to C18G, LL-37, and mCRAMP than the wild-type[28]. We recently demonstrated that CroP cleaved C18G and mCRAMP, which resulted in protection from AMP killing[21], see Figure **2**. In this work, we examined how the resistance of *E. coli* and *C. rodentium* strains to C18G was affected by expression of the omptins OmpT, OmpP, CroP, or PgtE in disk inhibition assays. Using SDS-PAGE, we studied whether this resistance was mediated by omptin cleavage of AMPs. We also used 1-N-Phenylnaphthylamine (NPN) fluorescence assays to determine how the expression of omptins affected membrane disruption. We observed cleavage of the fluorescent substrate FRET C2 by whole cells expressing CroP or PgtE. Finally we attempted to purify CroP and PgtE by FPLC for a comparison of the enzymes' FRET C2 cleavage.

Materials and Methods

1. Bacterial growth

Bacteria were grown from 1/1000 dilutions of overnight culture into either Luria-Bertani Broth (LB) (10.0 g bio-tryptone, 5.0 g yeast extract, 10.0 g NaCl/L), N-minimal media (20.9 g Bis-Tris pH 7.5, 1.25 g KCl, 7.5 g $(NH_4)SO_4$, 0.07 g KH_2PO_4, 2.78 mL glycerol, 1.0 g casamino acids/L, supplemented with 8 μM Mg^{2+} and 0.2% glucose,) or tryptic soy broth (TSB). Kanamycin was added at a concentration of 25 μg/mL to media with bacteria carrying pWSK 129. Ampicillin was added at a concentration of 50 μg/mL to media with bacteria carrying pET 14 plasmids. Chloramphenicol was used at a concentration of 15 μg/mL during construction of the *C. rodentium ΔcroP*. All growth was carried out at 37 °C with shaking unless otherwise noted.

2. Bacterial strains and construction of plasmids

a. Strains

E. coli XL-1 Blue was obtained from Stratagene. *E. coli* BL21(DE3) was obtained from Novagen. *S. enterica* subspecies *enterica* serovar Typhimurium 14028s was obtained from the *Salmonella* genetic stock centre, University of Calgary. *S. enterica* Δ*pgtE* was a gift from Dr. France Daigle, Université de Montréal. *C. rodentium* ICC168 was a gift from Dr. Samantha Gruenheid, McGill University. *C. rodentium ΔcroP* was developed for this work, as described in the attached manuscript[21]. Briefly, a pRE112 plasmid containing *sacB* and the regions flanking *croP* was conjugated from *E. coli* X7213 to *C. rodentium*. Colonies that took up the plasmid were chloramphenicol resistant. Colonies that recombined the *croP* knockout sequence and lost the *sacB* plasmid were resistant to sucrose. PCR and DNA sequencing verified the presence of the *ΔcroP* deletion. See Table **2** for a list of strains used in this work.

Table 2: Strains of *E. coli, S. enterica,* and *C. rodentium* used in this work.

Species	**Strain**	**Native omptin(s)**
E. coli	XL-1 Blue	*ompT, ompP*
	BL21(DE3)	
	BL21(DE3) pWSK.*ompT*	
	BL21(DE3) pWSK.*ompP*	
	BL21(DE3) pWSK.*croP*	
	BL21(DE3) pWSK.*pgtE*	
	BL21(DE3) pLysE pET.*His-pgtE*	
	BL21(DE3) pLysE pET.*His-croP*	
***S. enterica* serovar Typhimurium**	Wildtype	*pgtE*
	ΔpgtE	
	ΔpgtE pWSK.*pgtE*	
	ΔpgtE pWSK.*croP*	
C. rodentium	Wildtype	*croP*
	ΔcroP	
	ΔcroP pWSK.*ompT*	
	ΔcroP pWSK.*ompP*	
	ΔcroP pWSK.*pgtE*	
	ΔcroP pWSK.*croP*	

b. Plasmids

Plasmids that we used in this work are listed in Table **3**, and the oligonucleotides that we used are described in Table **4.** To construct plasmid pWSK.*ompT*, oligonucleotides 655 and 656 amplified the coding sequence and promoter. The PCR product was cleaved with Xba1 and Pst1 before being inserted into an Xba1- and Pst1-cleaved pWSK 129 plasmid. To construct plasmid pWSK.*ompP*, oligonucleotides 653 and 654 amplified the coding sequence and promoter. The PCR product was cleaved with Xba1 and Pst1 before being inserted into an Xba1- and Pst1-cleaved pWSK 129 plasmid. To construct plasmid pWSK.*pgtE*, oligonucleotides 657 and 658 amplified the coding sequence and promoter. The PCR product was cleaved with Xba1 and Pst1 before being inserted into an Xba1- and Pst1-cleaved pWSK 129 plasmid. To construct plasmid pWSK.*croP*, oligonucleotides 636 and 639 amplified the coding sequence and promoter. The PCR product was cleaved with Xba1 and BamH1 before being inserted into an Xba1- and BamH1-cleaved pWSK 129 plasmid. To construct plasmid pET.*pgtE*, oligonucleotides 746 and 658 amplified the coding sequence without the promoter. The PCR product was cleaved with BamH1 and Pst1 before being inserted into a BamH1- and Pst1-cleaved pET 14b(+) plasmid. To construct plasmid pET.*croP*, oligonucleotides 702 and 703 amplified the coding sequence without the promoter. The PCR product was cleaved with Nde1 and BamH1 before being inserted into a Nde1- and BamH1-cleaved pET 14b(+) plasmid.

Table 3: Plasmids for omptin knockout or expression in *E. coli, S. enterica* and *C. rodentium*. pWSK 129 is a low copy-number plasmid that expressed omptins from their native promoters. pET 14 plasmids expressed omptins from an inducible promoter with N-terminal histidine tags.

Plasmid name (label used in text)	**Vector**	**Omptin gene**
pWSK 129 *ompT (*p*WSK.ompT)*	pWSK 129	*ompT*
pWSK 129 *ompP (*pWSK.*ompP)*	pWSK 129	*ompP*
pWSK 129 *pgtE* Typhimurium *(*pWSK.*pgtE)*	pWSK 129	*pgtE*
pWSK 129 *croP (*pWSK.*croP)*	pWSK 129	*croP*
pET 14 *His-pgtE* Typhimurium *(*pET.*His-pgtE)*	pET 14	Histidine-tagged *pgtE*
pET 14 *His-croP (*pET.*His-CroP)*	pET 14	Histidine-tagged *croP*

Table 4: Oligonucleotides used to construct plasmids and for RT-qPCR.

Target	Forward oligonucleotide name and sequence	Reverse oligonucleotide name and sequence
***ompT*+promoter**	**655:** GCATAGTCTAGACCAACACTTGGCAAGCTGCCCATAAA	**656:** GCATAGCTGCAGTGCCGGCAATTTTGTCAACGCTAGTTT
***ompP*+promoter**	**653:** GCATAGTCTAGATCCTGTAGTTGCGTCAGGCCCTCCA	**654:** GCATAGCTGCAGTCCGGGTAATCCAGGTCCGCCACT
***pgtE*+promoter**	**657:** GCATAGTCTAGATCAGGAGCCGACCCCGCTTG	**658:** GCATAGCTGCAGCACGCGCAGATCCGCAACGA
***croP*+promoter**	**636:** AGCTAGGGTACCTTGGCCTGCTGATTGAACGCG	**639:** AGCTACGAGCTCGCAATACAGGGGATTGAAGGG
pgtE	**746:** GCATAGGGATCCTCAGGAGCCGACCCCGCTTG	**658:** GCATAGCTGCAGCACGCGCAGATCCGCAACGA
croP	**702:** CCTCCACCATATGTCTGGCGAATCCGGTTTGTTTACCCC	**703:** GCATGGATCCTCAGAAGGTATATTTCAGGCCGACAG
***croP* mRNA**	**710:** ATGAACATTACGCTCGCGGGATCA	**711:** TTACGCGACTCCATACGCCTTCAA
***pgtE* mRNA**	**747:** GTTCAATTCATCCGGACACCAG	**748:** TGCGCATGATAATGACGAACAC
***16s* mRNA**	**712:** TGTCTACTTGGAGGTTGTGCCCTT	**713:** TGCAGTCTTCCGTGGATGTCAAGA

3. Disk inhibition assays

Whatman paper disks (3 mm chromatography, 3M) containing 25 µg of C18G were placed on top of an agarose overlay containing 1 x 10^7 CFU of *E. coli* or *C. rodentium* on LB plates. Plates were photographed after overnight incubation at 37 ºC.

4. Minimum inhibitory concentration determinations

The minimum inhibitory concentration corresponds to the lowest concentration of an antibiotic that prevents bacterial growth. Overnight cultures were diluted 1/1000 into TSB. After growth to OD_{595} = 0.430, bacteria were diluted 1/50 into N-minimal medium. In a 96-well plate, 90 µL of antimicrobial peptides in dilutions increasing by half were mixed with 90 µL of diluted bacteria. Control wells containing no bacteria verified that the medium was not contaminated. Plates were covered with parafilm and incubated for 24 h at 37 °C. Wells were scored for presence or absence of visible growth.

5. Proteolytic cleavage of AMPs by cells expressing omptins

C. rodentium strains expressing OmpT, OmpP, PgtE, or CroP were grown in N-minimal media. A volume of 100 µL of bacteria was spun in a tabletop centrifuge at 6 200 *g* for 5 min, and re-suspended in N-minimal media. C18G (10 µg) was incubated with 1 x 10^6 CFU in a total volume of 25 µL for 15 min at room temperature. Cells were removed by centrifugation in a tabletop microcentrifuge at 6 200 *g* for 5 min. Reactions were stopped by adding the supernatant to 5 µL of 4x SDS sample buffer (250 mM Tris/HCl pH 6.8, 40 % glycerol, 8 % SDS, 0.008 % bromophenol blue, 4 % β-mercaptoethanol) and boiling for 2 min. 5 µL of the samples were run on 20 % Tris/Tricine gels. The same protocol was followed for LL-37 cleavage, with 10 µg LL-37 and 1 x 10^7 CFU of *C. rodentium.*

For C18G cleavage by *C. rodentium* and *S. enterica* strains expressing PgtE and CroP, the protocol was modified by growing bacteria in LB media and re-suspending in phosphate-buffered saline (PBS) (Na_2HPO_4, 2.4 g KH_2PO_4, pH 7.5, 80.0 g NaCl, 2.0 g KCl, 14.4 g/L).

6. OM disruption assay with 1-N-phenylnaphthylamine

Outer membrane disruption assays with NPN were carried out as described in the attached manuscript[21].

7. Degradation of tropomyosin by *E. coli* and *C. rodentium* strains expressing omptins

Porcine muscle tropomyosin (15 µg) (Sigma) was incubated with 3 x 10^5 CFU of bacteria for 4 h in PBS pH 7.5, 1 mM dithiothreitol (DTT) at 37 ºC. Total reaction volume was 30 µL. Resultant tropomyosin degradation was visualized by SDS-PAGE.

8. Real-time quantitative PCR

Real-time quantitative PCR (RT-qPCR) was carried out as previously described[21], with the previously used 16S oligonucleotides and the oligonucleotides listed in Table **4** for amplification of *pgtE* and *croP* cDNA.

9. Purification of native CroP

C. rodentium ΔcroP pWSK.*croP* was grown to stationary phase over 6 h in LB broth. Cells were pelleted by centrifugation at 2 300 *g* for 20 min in an IEC Centra GP8R and stored at -20 °C. Frozen pellets were re-suspended in 5 mL of 50 mM Tris/HCl pH 7.5 and sonicated. Debris were removed by centrifugation at 3 500 *g* in an IEC 21000R centrifuge for 15 min. We centrifugued the supernatant to pellet the inner and outer membrane components for 1 h at 100 000 *g* in a Beckman Coulter Omptima™ Max Ultracentrifuge, MLA-80 rotor. The resultant pellet was dissolved in 1 mL of 50 mM Tris/HCl pH 7.5, 0.1% N-lauroyl-sarcosine (sarcosyl), and spun at 100 000 *g* for 1 h, to pellet OMPs. The OM pellet was dissolved in 50 mM Tris/HCl pH 7.5, 10 mM EDTA, 1 % Triton-X 100. Non-solubilized proteins were removed by centrifugation at 225 000 *g* for 20 min. OMPs were analysed by SDS-PAGE.

The sample was bound to a HiTrap™ Q FF column (Amersham Biosciences) with binding buffer (25 mM Tris/HCl pH 8.0, 50 mM NaCl, 0.1% Triton-X 100). Proteins were eluted with a gradient of anion elution buffer (25 mM Tris/HCl pH

8.0, 1 M NaCl, 0.1% Triton-X 100). Fractions were visualized by SDS-PAGE. The fraction containing a 33 kDa band was dialysed against dialysis buffer (10 mM Tris/HCl pH 8.3, 0.1% Triton-X 100, 5 mM EDTA) for 2 h before overnight incubation with a 3 molar excess of *E. coli* EH100 Ra rough LPS (Sigma) at 4 °C.

10. Expression, purification, and refolding of His-PgtE and His-CroP

a. Expression

His-PgtE and His-CroP were expressed from pET 14b(+) vectors in *E. coli* BL21(DE3) pLysE (Table **2**).When the cultures reached an OD_{595} of 0.5-0.7, expression of histidine-tagged omptins was induced by addition of 1mM final concentration of isopropyl β-D-1-thiogalactopyranoside. Antibiotics were also added again at this point. Cells grew for another 4 h before they were centrifuged at 8 000 *g* in an IEC 21000R centrifuge for 10 min. Pellets were frozen at -20 °C.

b. Purification

The frozen pellets were re-suspended in 4 mL binding buffer (0.5 M NaCl, 20 mM Tris/HCl, 5 mM imidazole, pH 7.9), and sonicated twice for 5 sec. Samples were then centrifuged in a tabletop microcentrifuge at 6 200 *g* for 15 min. The resultant pellet was re-suspended in 1 mL of binding buffer, with 5 μg of RNAse and 0.5 mg of lysozyme. Sonication, centrifugation, and Rnase/lysozyme incubation were repeated a total of 3 times. The final pellet was re-suspended in 1 mL of denaturing buffer (20 mM Tris/HCl pH 7.9, 0.5 M NaCl, 5 mM imidazole, 6M Guanidine/HCl or 6 M urea, 1 % CHAPS,), and incubated on ice for 2 h. After a final centrifugation at 18 800 *g* for 30 min, the supernatant containing denatured histidine-tagged omptins was stored at 4 ºC. Fractions were analysed on SDS-PAGE gels.

c. Refolding

A 1/1000 dilution of purified His-CroP in denaturing buffer was dialyzed against PBS pH 7.5 supplemented with 1 mM $DodMe_2NPrSO_3$ and 5 M, 4 M, 3 M, and 0M urea successively. Dialysis was carried out at 12 °C and buffer was changed

twice at every concentration of urea. His-CroP was then incubated overnight with a 3-fold molar excess of *E. coli* EH100 Ra rough LPS (Sigma). We attempted to refold His-PgtE using similar methods.

11. Cleavage of C2 FRET substrate by whole cells or purified omptins

a. Whole cells

Bacterial strains were grown to an OD_{595} of 0.430. 1 mL of the fresh culture was spun down for 5 min at 6 200 *g* in a tabletop microcentrifuge, and re-suspended in 1 mL of PBS, pH 7.5.

Reactions were loaded in triplicate in a black 96 well half-volume plate. Each reaction contained 5 x 10^6 CFU and 3 μM FRET C2. The plate was read by a Spectramax M5 fluorescent microplate reader (Molecular Devices) at 22 °C, with one 5 second shake before the first read. Readings were taken with λ_{ex}= 325; λ_{em}= 430 once per 10 min, over 2 h. Data was exported from SoftMax Pro to Microsoft Excel for analysis.

b. Purified omptins

For native purified CroP, the assay was carried out in a 300 μL cuvette with dialysis buffer (see page 35) and 6 μM FRET C2 substrate. The incubation was 7 min long. For comparison of native purified CroP to refolded histidine-tagged omptins, the assay was similar except it was carried out in a 96 well plate over 2 h and 90 μL of the purified and dialysed omptins were combined with 90 μL PBS.

Results

1. Growth inhibition of *E. coli* and *C. rodentium* strains expressing omptins by C18G.

a. Disk Inhibition

To assess growth inhibition of *E. coli* and *C. rodentium* strains by C18G, we used a disk inhibition assay. This assay measured the dark areas of clearing surrounding the disk, which were zones where C18G prevented bacterial growth. Figure **6** illustrates that inhibition of *E. coli* growth by disks containing C18G was reduced by expression of *ompT, ompP,* or *croP* from a plasmid. *E. coli* XL-1 Blue carries *ompT* and *ompP*. The small zone of clearing implies that this strain survived C18G challenge except at the high concentration immediately surrounding the disk. *E. coli* BL21(DE3) lacks both of the *E. coli* omptin genes. Therefore, the large zone of clearing surrounding the disk, which indicates sensitivity to C18G, was expected. Complementation of *E. coli* BL21(DE3) with pWSK.*ompT*, pWSK.*ompP,* or pWSK.*croP* resulted in growth even at the disk's edge, indicating stronger resistance to C18G than *E. coli* XL-1 Blue. Unlike *E. coli* BL21(DE3) complemented with other omptins, complementation with pWSK.*pgtE* did not significantly reduce the zone of clearing. Therefore, complementation of *E. coli* BL21(DE3) with pWSK.*ompT,* pWSK.*ompP,* or pWSK.*croP* increased resistance to C18G, whereas complementation with pWSK.*pgtE* did not confer resistance to C18G.

Figure **6** shows similar results for *C. rodentium* strains as for *E. coli* strains. The wild-type strain had no growth inhibition around the disk, indicating resistance to C18G. *C. rodentium ΔcroP* did have a broad band of clearing around the disk; it was sensitive to C18G. Complementation of *C. rodentium ΔcroP* with pWSK.*ompT*, pWSK.*ompP,* or pWSK.*croP* restored resistance to C18G. Complementation with pWSK.*pgtE* did not significantly reduce clearing. As in *E. coli* BL21(DE3), *C. rodentium* complemented with pWSK.*ompT,* pWSK.*ompP,* and *pWSK.croP* resisted C18G, but the pWSK.*pgtE* plasmid did not.

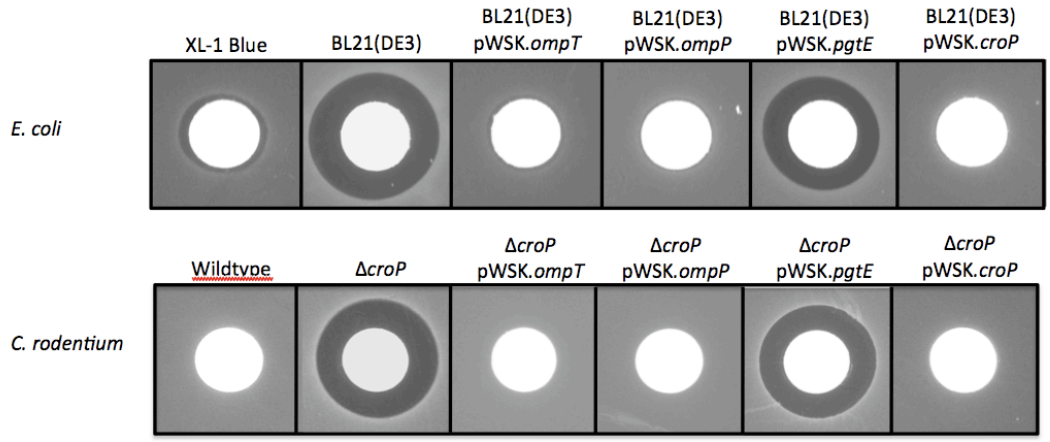

Figure 6: Growth inhibition by C18G of *E. coli* and *C. rodentium* strains expressing omptins. Strains lacking native omptins were sensitive to killing by C18G, as illustrated by the dark zones of clearing. Complementation with *ompT, ompP,* or *croP* restored resistance, whereas complementation with *pgtE* did not. Disks containing 25 µg of C18G were placed on top of an agarose overlay containing 1 x 10^7 CFU. Plates were photographed after overnight incubation at 37 ºC.

b. Minimal inhibitory concentrations

To confirm the results of disk inhibition assays in a more quantitative manner, we established the MICs of *C. rodentium* and *S. enterica* strains for C18G and PMB. The data are summarized in Table **5**. MICs of C18G were affected by the expression of omptin genes; MICs of PMB were not. For C18G, the *S. enterica* wild-type MIC was 4 μg/mL. The MIC was unchanged after deletion of *pgtE*. Complementation of *S. enterica ΔpgtE* with pWSK.*empty* or pWSK.*pgtE* had no affect on the MIC, however complementation with pWSK.*croP* greatly increased the MIC to 128 μg/mL. In agreement with C18G disk inhibition results, *C. rodentium ΔcroP* was sensitive, with a MIC of 4 μg/mL compared to the wild-type MIC of 32 μg/mL. Complementation of *C. rodentium ΔcroP* with pWSK.*ompT* and pWSK.*ompP* restored resistance to 32 μg/mL, whereas complementation with pWSK.*empty* or pWSK.*pgtE* did not. As in *S. enterica*, complementation with pWSK.*croP* increased the MIC to 128 μg/ml. In summary, deletion of the native omptin gene reduced C18G resistance of *C. rodentium,* but not of *S. enterica*. Accordingly, neither species showed increased resistance when complemented with pWSK.*pgE*. However, in *C. rodentium*, strains carrying pWSK.*ompT* or pWSK.*ompP* were slightly more resistant to C18G. Finally, expression of *croP* substantially increased the C18G resistance of *S. enterica* and *C. rodentium*. Overall, these data indicate that in different bacterial species, expression of OmpT, OmpP, and CroP increased resistance to the AMP C18G, but PgtE did not.

In contrast to C18G, neither deletion of omptin genes, nor complementation with pWSK carrying omptins, altered the resistance to PMB. The strains were all sensitive to 1 μg/mL of PMB (Table **5**). Given that PMB is resistant to cleavage by proteases, and that the MICs were unaffected by the presence of omptin genes, these results suggested that the increased resistance to C18G of strains expressing *ompT, ompP,* and *croP* were due to direct C18G cleavage by the omptins. However PgtE did not appear to cleave C18G.

Table 5: MICs of C18G and PMB for *C. rodentium* and *S. enterica* strains. *C. rodentium ΔcroP* had a reduced MIC compared to the wild-type. Complementation with pWSK.*ompT* and pWSK.*ompP* restored survival, whereas complementation with pWSK.*pgtE* did not. The MIC of *S. enterica* was unaffected by deletion of *pgtE.* Complementation with pWSK.*empty* or pWSK.*pgtE* also had no affect on MIC, however complementation with pWSK.*croP* greatly increased survival. All strains were sensitive to 1 µg/mL of PMB. n/d = not done.

Strain	C18G µg/mL	PMB, µg/mL
***S. Typhiumurium* wildtype**	4	1
S. Typhimurium ΔpgtE	4	1
S. Typhimurium ΔpgtE pWSK.empty	4	1
S. Typhimurium ΔpgtE pWSK.pgtE	4	1
S. Typhimurium ΔpgtE pWSK.croP	128	n/d
***C. rodentium* wildtype**	32	1
C. rodentium ΔcroP	4	1
C. rodentium ΔcroP* pWSK.*empty	4	1
C. rodentium ΔcroP* pWSK.*ompT	32	1
C. rodentium ΔcroP* pWSK.*ompP	32	1
C. rodentium ΔcroP* pWSK.*pgtE	4	1
C. rodentium ΔcroP* pWSK.*croP	128	1

2. C18G cleavage by OmpT, OmpP, and CroP

a. C. rodentium

We explored the ability of strains expressing omptins to cleave C18G through peptide cleavage assays visualized on Tris/Tricine gels. Figure **7** shows degradation of C18G on a 20% Tris/Tricine gel after exposure to *C. rodentium* strains expressing *ompT, ompP, pgtE* or *croP*. There was no visible reduction in C18G when it is incubated without bacteria or with *C. rodentium ΔcroP*. Due to our experimental conditions, there was also no visible reduction in C18G when it was incubated with wild-type *C. rodentium,* as discussed below. In agreement with the disk inhibition assays and MICs, *C. rodentium ΔcroP* pWSK.*ompT,* pWSK.*ompP,* and pWSK.*croP* readily cleaved C18G, but the strain complemented with pWSK.*pgtE* did not. These results were confirmed by a time course, seen in Figure 8. *C. rodentium ΔcroP* cells carrying pWSK.*croP* degraded C18G completely after 30 minutes, but cells carrying empty pWSK plasmid or pWSK.*pgtE* did not. In combination with the disk inhibition and MIC data, this demonstrates that cleavage of C18G by OmpT, OmpP, or CroP allowed *C. rodentium* to survive AMP challenge.

b. S. enterica

We also used a Tris/Tricine gel to visualize the ability of *S. enterica* strains expressing omptins to cleave C18G. Figure **8** shows a time course of C18G cleavage by complemented strains of *S. enterica ΔpgtE*. Cells carrying pWSK.*croP* - but not pWSK.*empty* or pWSK.*pgtE* - degraded C18G. This was in agreement with the high MIC of *S. enterica* carrying pWSK.*croP,* and reinforced our belief that protection from C18G was mediated by CroP peptidase activity.

3. LL-37 cleavage by CroP

CroP cleaves LL-37, as shown in Figure **9**. After 30 min, the amount LL-37 incubated with wild-type *C. rodentium* was somewhat reduced compared to the *C. rodentium ΔcroP* control, and LL-37 incubated with C. *rodentium ΔcroP* pWSK.*croP* was nearly all cleaved.

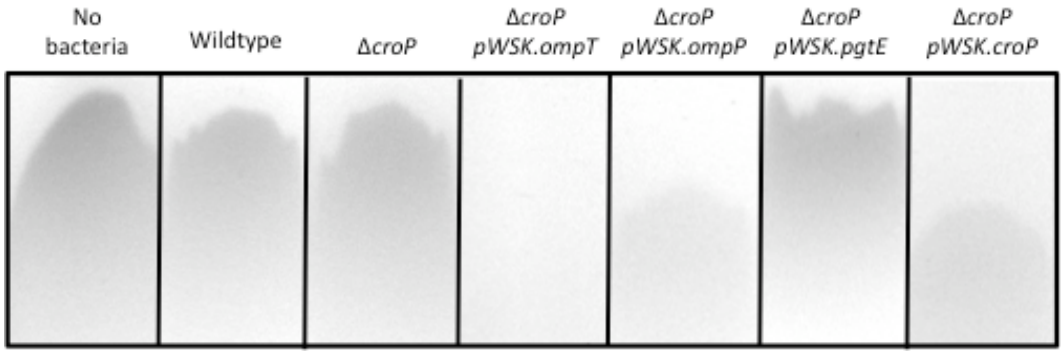

Figure 7: C18G cleavage by *C. rodentium* strains expressing various omptins. Strains complemented with *ompT, ompP,* or *croP* cleaved C18G; those complemented with *pgtE* did not. 10 µg of C18G were incubated with 1 x 10^6 CFU for 15 minutes at room temperature in N-minimal medium. The C18G that remained after this treatment was visualized by Tris/Tricine SDS-PAGE and coomassie staining. For the sake of clarity, these bands were cut from the same gel to create this figure.

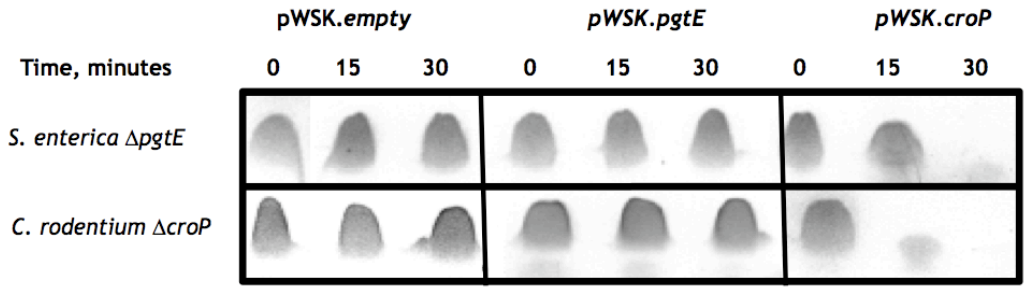

Figure 8: *S. enterica ΔpgtE* and *C. rodentium ΔcroP* cells carrying pWSK.*croP* - but not the pWSK.*empty* or pWSK.*pgtE* - degraded C18G. 10 µg of C18G were incubated with 1 x 10^6 CFU for 0, 15, and 30 min at room temperature in PBS. C18G was visualized by Tris/Tricine SDS-PAGE and coomassie stain.

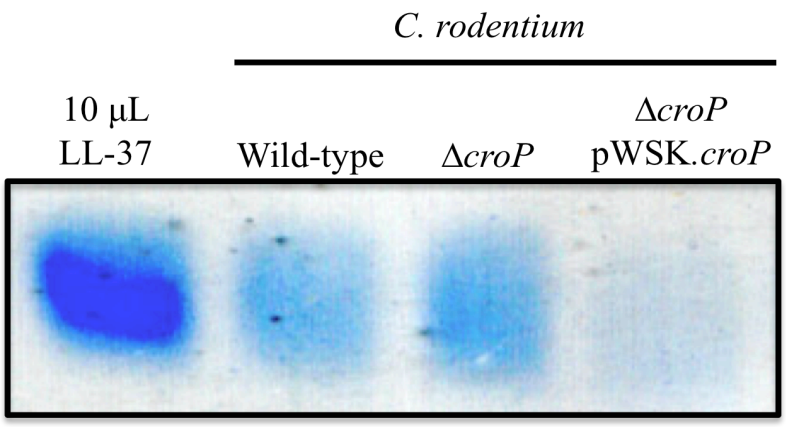

Figure 9: LL-37 cleavage by *C. rodentium* strains expressing CroP. The wild-type *C. rodentium* cleaves some LL-37 over 30 min; *C. rodentium ΔcroP* pWSK.*croP* cleaves most of the LL-37 within 30 min. 10 µg of LL-37 were incubated with 1 x 10^7 CFU for 30 minutes at room temperature in N-minimal medium. The C18G that remained after this treatment was visualized by 20% SDS-PAGE and coomassie staining.

4. Some omptins prevent OM disruption by AMPS

a. NPN without AMPs

To examine membrane disruption, we used NPN as a fluorophore. NPN fluoresces when it contacts the hydrophobic components of the disrupted OM. Figure **10** illustrates fluorescence of 5 μM NPN associated with the OMs of various strains of *C. rodentium*. Neither empty vector, expression of *croP* from the chromosome, nor expression of other omptins lead to fluorescence higher than 100 A.U. Unexpectedly, pWSK.*croP* caused NPN fluorescence to peak close to 600 A.U., suggesting that the OM of *C. rodentium ΔcroP pWSK.croP* was inherently unstable.

b. C18G

To investigate membrane disruption by C18G, we added the AMP to cuvettes containing *C. rodentium* and NPN. Figure **11** shows disruption of the OM of *C. rodentium* strains by 5 μM C18G as measured by fluorescence of 5 μM NPN. *C. rodentium* expressing *ompT, ompP,* or wild-type levels of *croP* had slight membrane disruption, which reduced over time, and with fluorescence remaining below 100 A.U. throughout the experiment In contrast, *C. rodentium ΔcroP* and *C. rodentium ΔcroP pWSK.pgtE* were somewhat disrupted after the addition of C18G, with fluorescence increasing to 200 A.U. However, *C. rodentium ΔcroP* pWSK.*croP* displayed substantial membrane damage even before the addition of C18G, with fluorescence peaking at 550 A.U. These data show that expression of *ompT, ompP,* or wild-type expression of *croP* protected the bacterial OM from disruption by C18G, whereas the AMP disrupted *C. rodentium ΔcroP* and *C. rodentium ΔcroP pWSK.pgtE*. This experiment also confirmed that the OM of *C. rodentium ΔcroP pWSK.croP* was inherently unstable.

c. PMB

To investigate membrane disruption by PMB, we added the AMP to cuvettes containing *C. rodentium* and NPN. Figure **12** shows disruption of the OM of *C. rodentium* strains by 5 μM PMB as measured by fluorescence of 5 μM NPN. Fluorescence increased to between 620 A.U. and 740 A.U. after addition of PMB,

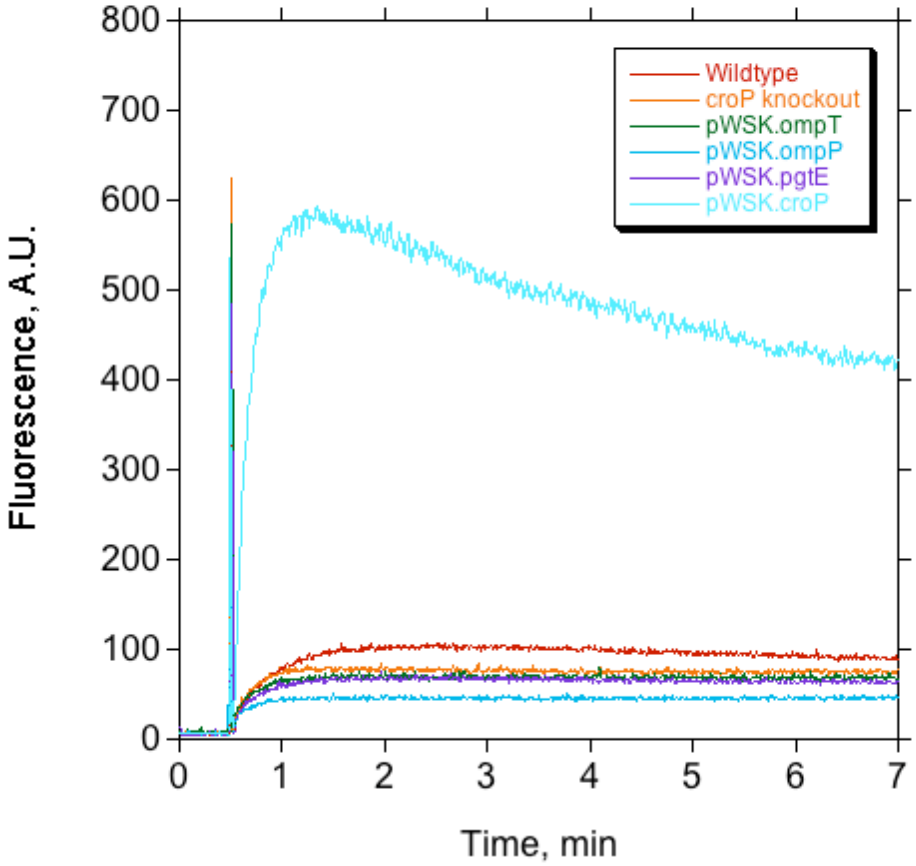

Figure 10: The OM of *C. rodentium ΔcroP pWSK.croP* is inherently unstable. Expression of CroP from pWSK caused high NPN fluorescence due to membrane instability, although expression of CroP at wildtype levels, and expression of other omptins from plasmids did not. NPN was added at 30 sec, to a final concentration of 5 μM.

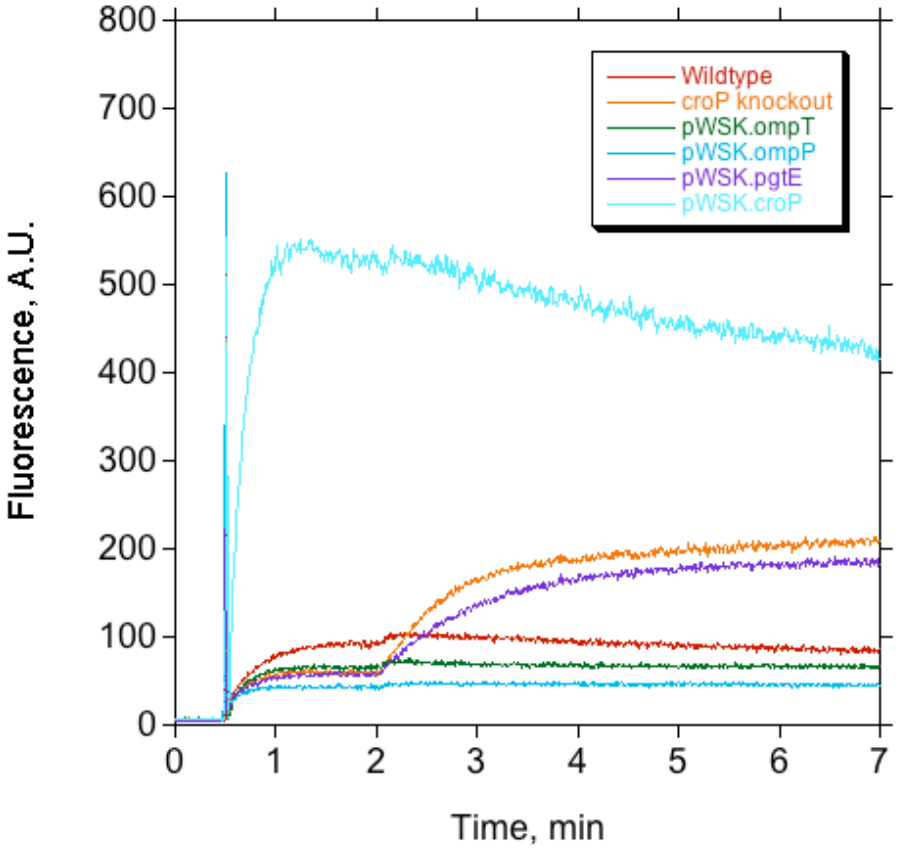

Figure 11: Disruption of the OM of *C. rodentium* strains by C18G, as measured by fluorescence of NPN. The *croP*-complemented strain displayed substantial membrane damage even before the addition of C18G. NPN was added at 30 sec to a final concentration of 5 µM. C18G was added at 2 min to a final concentration of 5 µM.

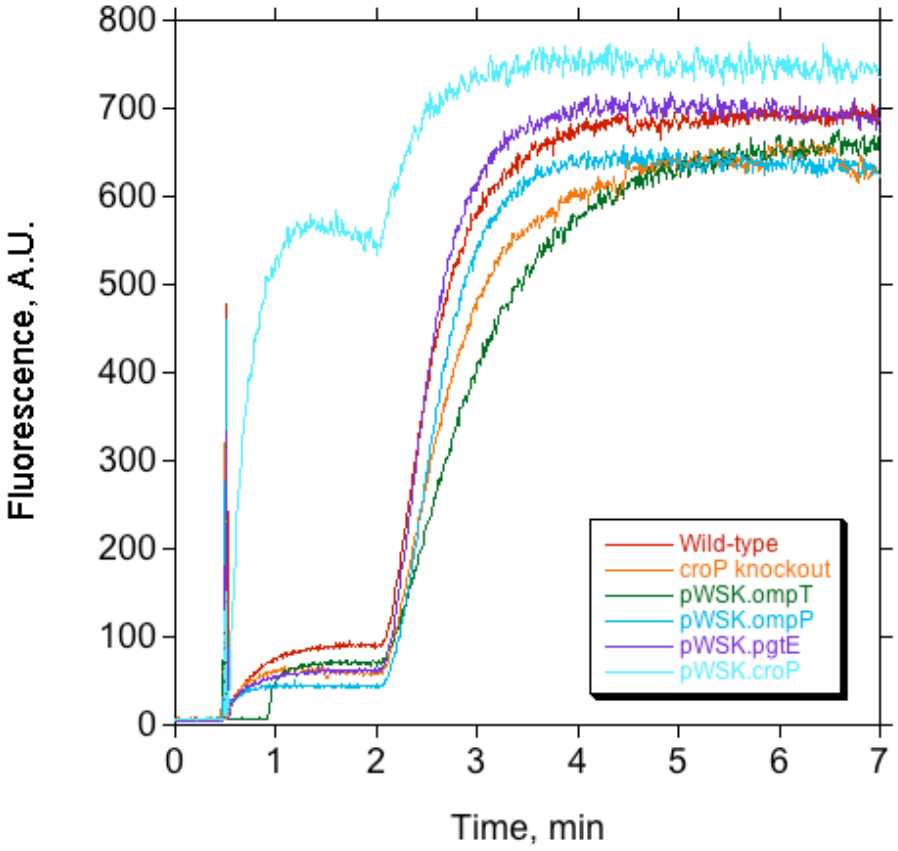

Figure 12: Disruption of the OM of *C. rodentium* by PMB, regardless of omptin expression. NPN fluorescence of wildtype, *ΔcroP*, and *ΔcroP* strains complemented with *ompT, ompP, pgtE,* and *croP* increased drastically after addition of PMB, indicating that omptins were unable to prevent this antimicrobial lipopeptide from disrupting the OM. NPN was added at 30 sec to a final concentration of 5 μM. PMB was added at 2 min to a final concentration of 5 μM.

regardless of omptin expression. The consistently high fluorescence demonstrated that none of the omptins were able to prevent this antimicrobial lipopeptide from disrupting the OM. This is in good agreement with the MIC of PMB that was unaltered by the presence or absence of omptins (Table **5**).

5. Tropomyosin

a. *E. coli* BL21(DE3)

To determine whether PgtE was active at the OM, we examined the ability of *E. coli* and *C. rodentium* strains expressing omptins to cleave the putative substrate tropomyosin. Tropomyosin has been described as a non-physiological protein substrate of OmpT[36]. Given that O-antigen has been reported to interfere with protein degradation by omptins, we investigated tropomyosin cleavage in the rough *E. coli* BL21(DE3) strain as well as in *C. rodentium*, which is smooth[64]. We found that *E. coli* strains expressing any one of four omptins degraded tropomyosin. As shown in Figure 13**,** tropomyosin incubated without bacteria migrated in 2 bands, β-tropomyosin (33.3 kDa) and α-tropomyosin (32.7 kDa)[36]. Wild-type *E. coli* XL-1 Blue, which expresses native *ompT* and *ompP*, cleaved both forms of tropomyosin. As expected, neither wild-type *E. coli* BL21(DE3), nor *E. coli* BL21(DE3) pWSK.*empty* degraded tropomyosin. *E. coli* BL21(DE3) pWSK.*croP* degraded tropomyosin very efficiently, completely eliminating β-tropomyosin and greatly reducing the amount of α-tropomyosin on the gel. *E. coli* BL21(DE3) pWSK.*ompP* cleaved β-tropomyosin and α-tropomyosin both into slightly shorter proteins very effectively, whereas *E. coli* BL21(DE3) pWSK.*ompT* only partially cleaved β-tropomyosin and did not degrade α-tropomyosin. *E. coli* BL21(DE3) pWSK.*pgtE* cleaved both forms, albeit to a lesser degree than *E. coli* BL21(DE3) pWSK.*croP.* Therefore, *E. coli* XL-1 Blue, and *E. coli* BL21(DE3) expressing either *croP, ompT, ompP,* or *pgtE* were able to degrade the protein substrate tropomyosin.

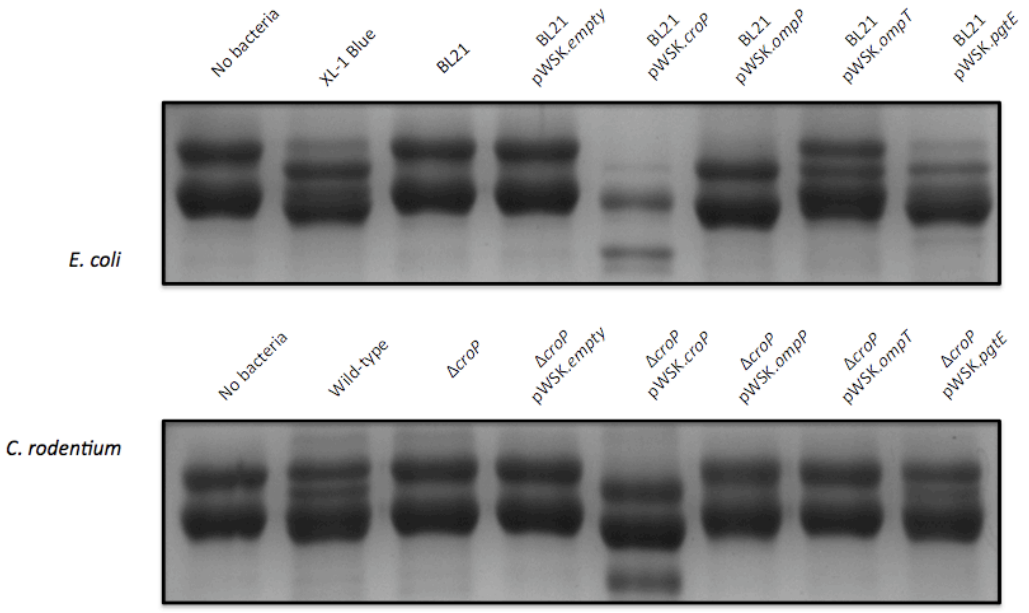

Figure 13: Degradation of tropomyosin by *E. coli* and *C. rodentium* strains expressing omptins. Wildtype *E. coli* XL-1 Blue and wild-type *C. rodentium* degraded tropomyosin slightly, unlike the omptin knockout strains. Cells carrying pWSK.*croP* degraded tropomyosin the most effectively in both species. Strains carrying pWSK.*ompP* and pWSK.*ompT* partially degraded tropomyosin in the *E. coli* BL21(DE3) background, but not in the *C. rodentium ΔcroP* background. 15 µg of tropomyosin were incubated with 3 x 10^5 CFU for 4 hours at 37 ºC. Resultant tropomyosin degradation was visualized by SDS-PAGE and coomassie stain; these gels were run at the same time in the same gel box.

b. *C. rodentium*

As illustrated in Figure 13, *C. rodentium* strains degraded the protein tropomyosin less efficiently than *E. coli* strains. Compared to the control with no bacteria, wild-type *C. rodentium* degraded only a small amount of α- and β-tropomyosin. *C. rodentium ΔcroP* and *C. rodentium ΔcroP* pWSK.*empty* did not degrade either form of tropomyosin. *C. rodentium ΔcroP* pWSK.*croP* was the most effective *C. rodentium* strain for tropomyosin degradation, but it was not as effective as *E. coli* BL21(DE3) pWSK.*croP*. Also in contrast to the equivalent strains in *E. coli* BL21(DE3), *C. rodentium ΔcroP* strains carrying pWSK.*ompT* or pWSK.*ompP* did not degrade tropomyosin. Finally, *C. rodentium ΔcroP* pWSK.*pgtE* only degraded a small amount of tropomyosin. These results demonstrate that PgtE was indeed active at the OM, despite its apparent inability to cleave C18G. Smooth *C. rodentium* strains expressing *croP, ompT, ompP,* or *pgtE* were able to degrade the protein substrate tropomyosin, but to a lesser degree than when the same omptins were expressed in rough *E. coli* BL21(DE3).

6. FRET C2 substrate cleavage

To further demonstrate PgtE's activity, we used the more quantifiable FRET C2 substrate. This substrate is composed of a fluorophore and a quencher joined by a short amino acid sequence based on complement component 2. The amino acid sequence contains a dibasic cleavage site. We compared the ability of *C. rodentium* strains carrying pWSK.*empty,* pWSK.*pgtE,* and pWSK.*croP* to cleave the FRET C2 substrate. Figure **14** illustrates that the fluorescence of wells containing *C. rodentium ΔcroP* pWSK.*empty* did not exceed 100 A.U. at any point over the 2 h incubation. Fluorescence of *C. rodentium ΔcroP* pWSK.*pgtE* reached 250 A.U. after 2 h, showing an ability to cleave the peptide. *C. rodentium ΔcroP* pWSK.*croP* cells cleaved the substrate far more efficiently. It reached 250 A.U. in less than 10 minutes and peaked at 350 A.U. after only 60 minutes. Thus, both *C. rodentium ΔcroP* pWSK.*pgtE* and *C. rodentium ΔcroP* pWSK.*croP* were able to cleave substantially more FRET C2 substrate than *C. rodentium ΔcroP* pWSK.*empty*, but *C. rodentium ΔcroP* pWSK.*croP* had a considerably faster cleavage rate.

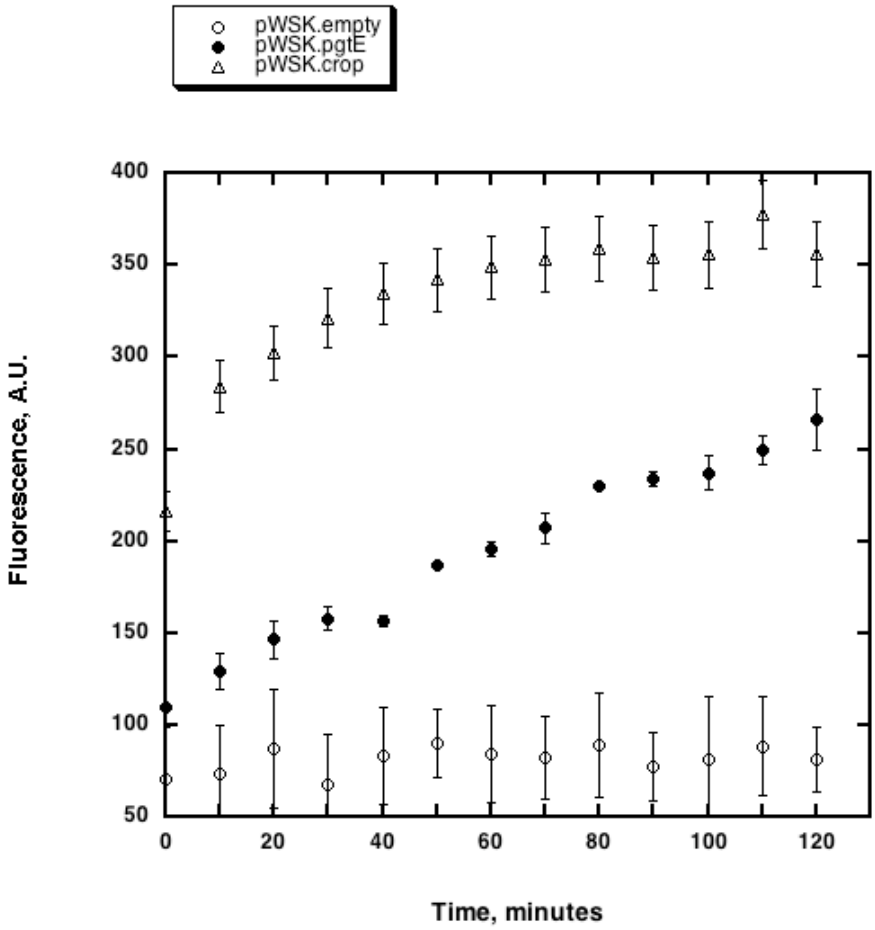

Figure 14: Cleavage of FRET C2 substrate by *C. rodentium ΔcroP* carrying empty plasmid, pWSK.*croP,* or pWSK.*pgtE.* Cells expressing CroP cleaved FRET C2 substrate substantially more efficiently than cells expressing PgtE. 3 μM FRET C2 substrate was incubated for 2 h with 5 x 10^6 bacteria. Values represent mean of 2 biological repeats ± standard error.

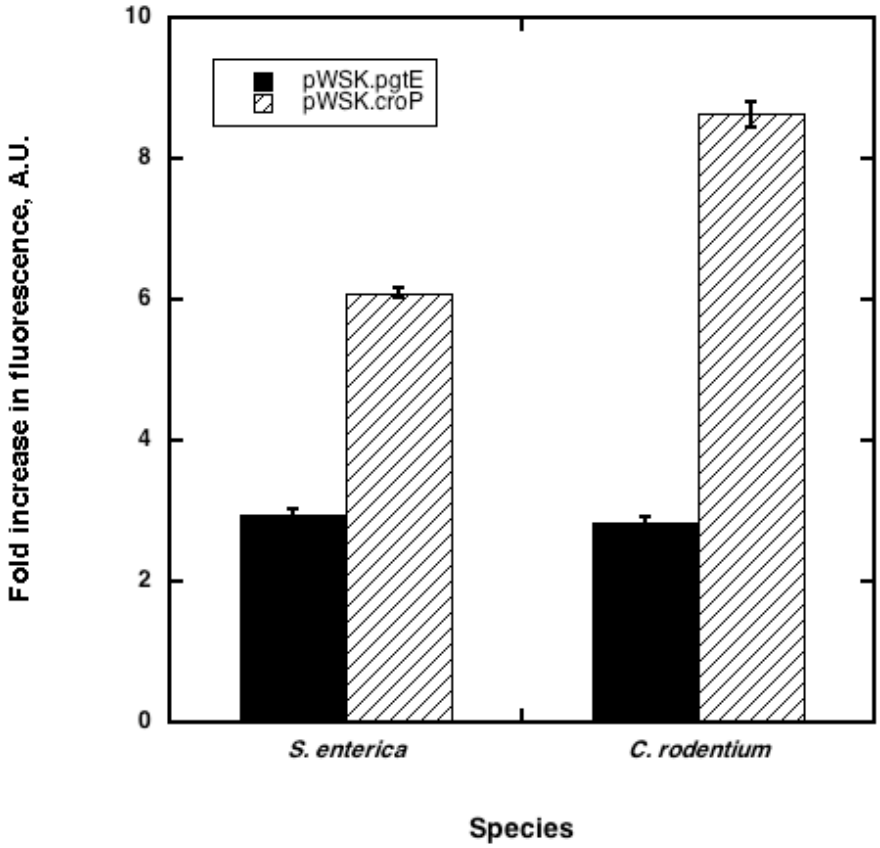

Figure 15: Cleavage of FRET C2 by complemented *S. enterica ΔpgtE* and *C. rodentium ΔcroP* strains. CroP cleaved significantly more FRET C2 than PgtE when expressed in either *S. enterica* or *C. rodentium.* 3 μM FRET C2 substrate was incubated for 1 h with 5 x 10^6 bacteria. Fluorescence is expressed as the mean fold difference of three biological repeats compared to the same strain carrying an empty vector, ± standard error.

The ability of bacterial cells carrying pWSK.*pgtE* and pWSK.*croP* to cleave FRET C2 substrate was tested in *S. enterica.* Figure **15** shows the fold increase in fluorescence compared to *S. enterica ΔpgtE* pWSK.*empty*. *S. enterica ΔpgtE* pWSK.*pgtE* cleaved 3 times more FRET C2 substrate than *S. enterica ΔpgtE* pWSK.*empty* over 1 h. *S. enterica ΔpgtE* pWSK.*croP* cleaved 6 times more of the substrate than *S. enterica ΔpgtE* pWSK.*empty,* which significantly exceeded cleavage by the strain carrying pWSK.*pgtE* (p=0.01). Therefore in *S. enterica* expression of either *pgtE* or *croP* results in FRET C2 substrate cleavage, with *croP* being more active than *pgtE.*

The ability of bacterial cells carrying pWSK.*pgtE* and pWSK.*croP* to cleave FRET C2 substrate was confirmed in *C. rodentium.* In agreement with the results shown in Figure **14**, Figure **15** illustrates that *C. rodentium ΔcroP* pWSK.*pgtE* and *C. rodentium ΔcroP* pWSK.*croP* cleaved 3- and 8.5- times more FRET C2 than *C. rodentium ΔcroP* pWSK.*empty*, respectively. In both species' backgrounds, the strain carrying pWSK.*croP* cleaved significantly more substrate than the strain carrying pWSK.*pgtE.*

7. RT-qPCR

Our results to this point suggested that CroP was either more active than PgtE, or more highly expressed at the OM. Consequently, we set out to determine the relative expression of the omptin genes from pWSK 129 plasmids in *S. enterica* and *C. rodentium*, with the help of our collaborators at l'Université de Montréal. Table **6** shows that many-fold more *croP* mRNA than *pgtE* mRNA is expressed from pWSK 129. There were 15.9 (±2.9), and 12.7 (±2.9) times more *croP* than *pgtE* mRNA in *S. enterica ΔpgtE* and *C. rodentium ΔcroP*, respectively. Given the high levels of *croP* transcription, this data suggested that there was more CroP than PgtE present at the bacterial cell surface in both species' backgrounds. The small difference between the two species was not significant (p=0.05).

8. Omptin expression at the OM

In light of the elevated transcription of *croP,* we examined expression of omptins in OM preparations of *C. rodentium*. Figure **16** shows a 10% SDS-PAGE gel of

Table 6: Over-expression of pWSK.*croP* mRNA compared to pWSK.*pgtE* mRNA in *S. enterica ΔpgtE* and *C. rodentium ΔcroP*. Data generously provided by the Daigle laboratory, Université de Montréal.

	***mRNA croP/pgt*E**
S.enterica ΔpgtE	15.9 (±2.9)
C. rodentium ΔcroP	12.7 (±2.8)

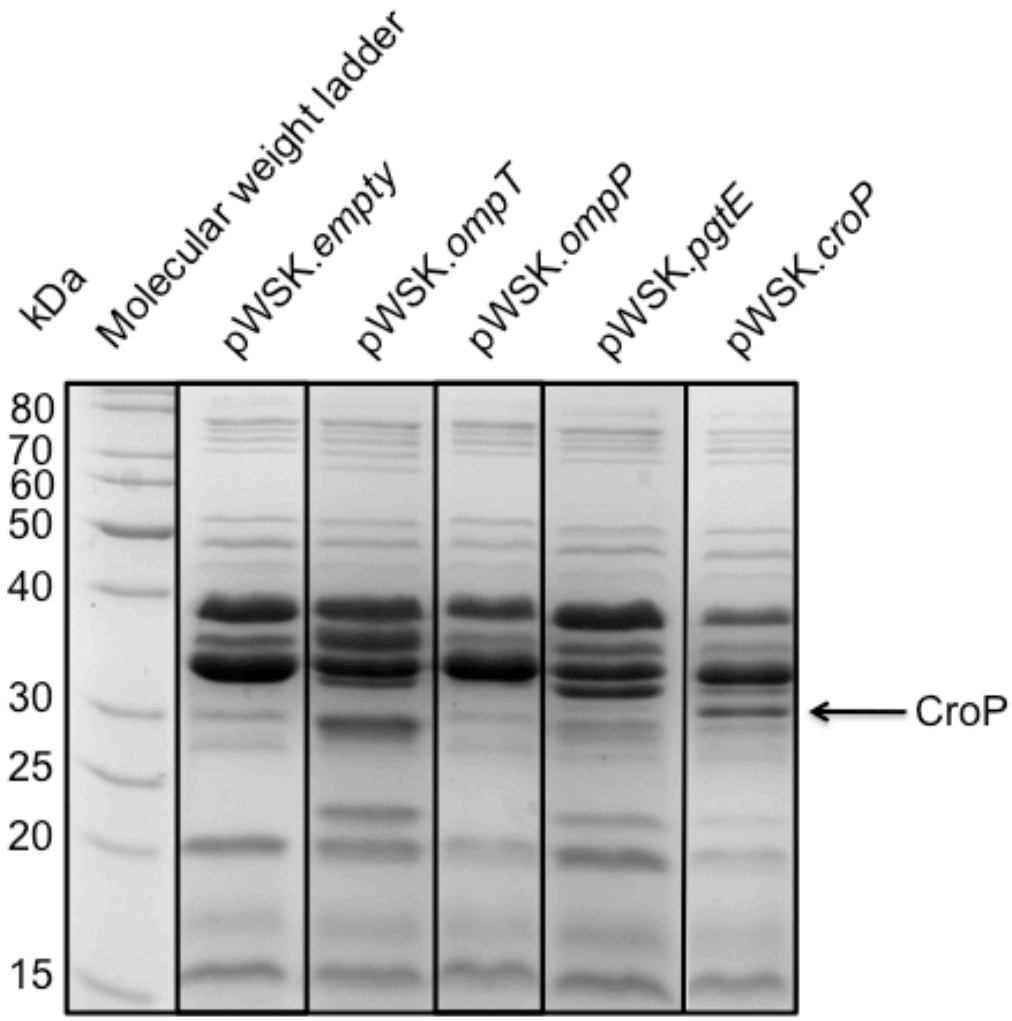

Figure 16: OM preparations of *C. rodentium ΔcroP* strains carrying pWSK.*empty,* pWSK.*ompP*, pWSK.*ompT,* pWSK.*pgtE,* and pWSK.*croP*. Cells expressing pWSK.*ompP* did not show more protein bands than the empty plasmid. However, pWSK.*ompT* had bands at 22 and 34 kDa. Extracts from cells carrying pWSK.*pgtE* had bands at 22, 33 kDa, and 34 kDa. Extracts from cells carrying pWSK.*croP* also had bands at 22, 33, and 34 kDa. For the sake of clarity, these bands were cut from the same gel to create this figure.

OMPs, including omptins, of various strains of *C. rodentium.* In addition to the bands seen in the control OM preparation of *C. rodentium ΔcroP* pWSK.*empty,* OM preparations of *C. rodentium ΔcroP* pWSK.*ompT* had bands at 22 and 34 kDa. 34 kDa is close to the expected molecular weight of OmpT of 33.5 kDa. Despite OmpP's expected molecular weight of 33.1 kDa, *C. rodentium ΔcroP* pWSK.*ompP* had the same pattern of protein bands as the empty vector control, and may be masked behind another OMP, as discussed below. OM preparations from *C. rodentium ΔcroP* pWSK.*pgtE* had bands at 22, 33, and 34 kDa, and PgtE's expected molecular weight is 32.8 kDa. OM preparations from *C. rodentium ΔcroP* pWSK.*croP* had protein bands at 22, 33, and 34 kDa, the second of which corresponds quite closely to the 33.1 kDa expected molecular weight of CroP. Overall, *C. rodentium* strains show the expected omptin protein bands as well as some putative autoprocessing[10,9] and cleavage of other OMPs[55], as described previously and discussed below.

9. Purification and activity of native CroP

In order to quantitatively observe the activity of CroP and PgtE free from the confounding effect of different expression levels, we wished to purify both proteases. Native CroP was purified from OMP preparations by flow-through anion-exchange, which took advantage of the high pI (7.9) of CroP. Figure **17** illustrates an SDS-PAGE gel of purified native CroP. After FPLC, 99% pure CroP was found at 33 kDa, not far from its expected molecular weight of 33.1 kDa. It was slightly smaller than a faint band of 36 kDa that was seen in the preparation from *C. rodentium ΔcroP* pWSK.*empty.* Therefore, after FPLC, native CroP was highly purified and found at the expected molecular weight. The results in Figure **18** clearly illustrate that purified native CroP cleaved C2 FRET substrate effectively because cleavage lead to an increase in fluorescence from 50 A.U. to 900 A.U. after 7 minutes.

10. Purification and activity of His-PgtE and His-CroP

Although the high pI of CroP made purification by flow-through anion-exchange FPLC convenient, the pI of PgtE is 5.5, which is similar to the pI of many other

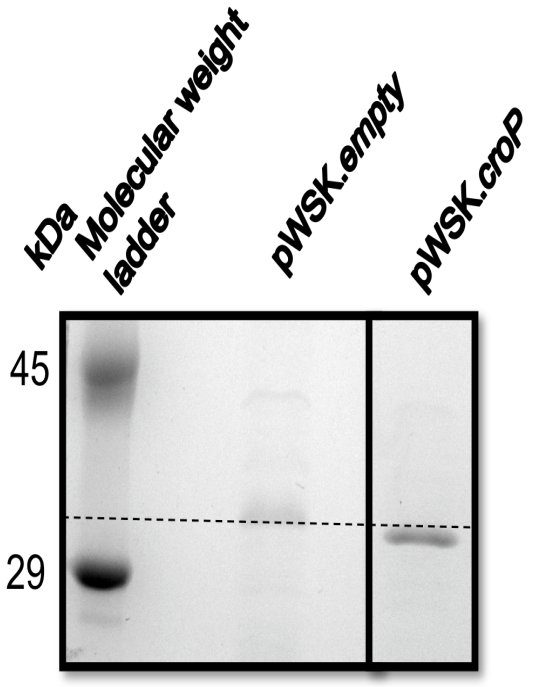

Figure 17: Purified native CroP. OM preparations from *C. rodentium ΔcroP* pWSK.*empty* and pWSK.*croP* were purified by flow-through anion-exchange FPLC. Purified CroP was found at 33 kDa, slightly lower than a faint band of 36 kDa in the preparation from cells carrying the empty plasmid. For the sake of clarity, these bands were cut from the same gel to create this figure.

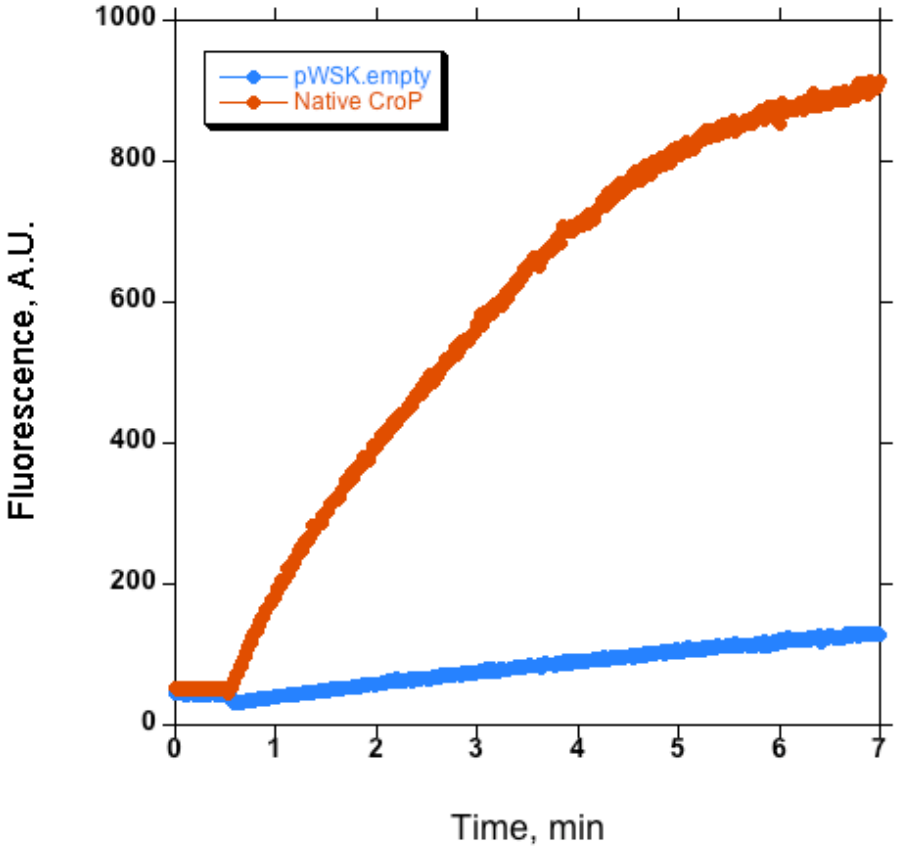

Figure 18: Purified native CroP cleaved FRET C2 substrate. Proteins purified by FPLC from *C. rodentium ΔcroP pWSK.empty* and *pWSK.croP* were incubated with a 3-fold molar excess of rough LPS before incubation with 6 μM FRET C2 substrate from 30 sec to 7 minutes. Values are results from one experiment, representative of 3 experiments.

OMPs and makes it difficult to separate using this method. Instead, we chose to construct histidine-tagged PgtE and CroP. N-terminus histidine-tagged proteins formed inclusion bodies. Inclusion bodies containing mostly His-PgtE or His-CroP were then isolated and refolded for activity assays. Figure **19** shows an SDS-PAGE gel of purified native CroP beside His-PgtE and His-CroP purified from inclusion bodies. Native CroP was seen at 33 kDa, not far from to its expected molecular weight of 33.1 kDa. His-PgtE showed a strong band at 35 kDa, not far from its expected molecular weight of 33.7 kDa. Purified His-CroP was found at 34.0 kDa, close to the expected molecular weight of His-CroP of 33.9 kDa. Both His-PgtE and His-CroP were 99 % pure. Therefore His-PgtE and His-CroP were quite well purified and found at the expected molecular weights.

After they were refolded by dialysis, we verified the peptidase activity of the His-tagged omptins, as seen in Figure 20**.** When FRET C2 substrate was incubated for 2 h with native CroP or refolded His-CroP, the fluorescence increased to 300 A.U. and 240 A.U. respectively, indicating effective cleavage by refolded CroP. However, His-PgtE did not show significantly more activity than the PBS control, suggesting that His-PgtE may not have been properly refolded (p=0.01). Therefore, although His-CroP has been successfully purified and refolded, some work remains to achieve actively purified His-PgtE.

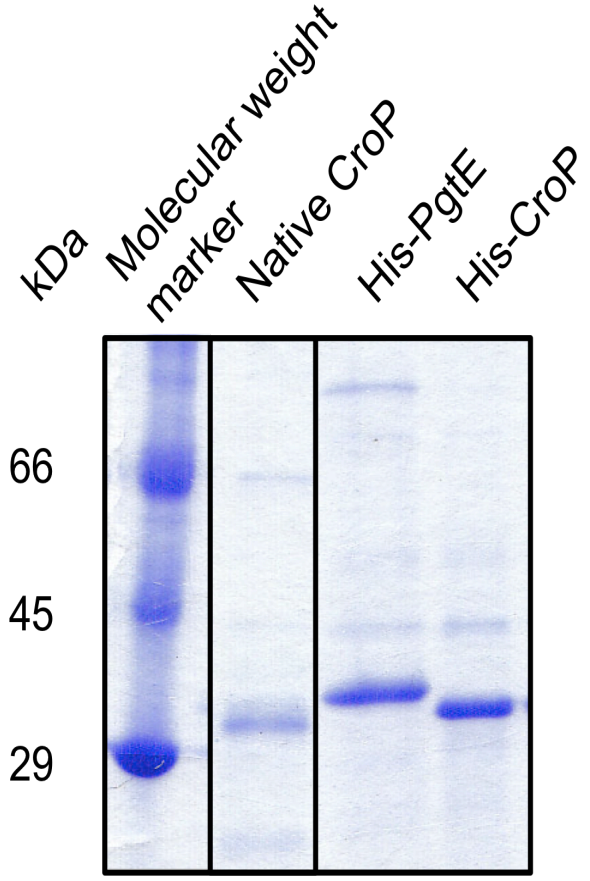

Figure 19: Purified His-CroP and His-PgtE. Native CroP is seen at 33 kDa. His-PgtE showed a strong band at 35 kDa. His-CroP showed a band at 34 kDa. His-CroP and His-PgtE were 99 % pure after isolation from inclusion bodies, as visualized on an SDS-PAGE gel with coomassie stain. For the sake of clarity, these bands were cut from the same gel to create this figure.

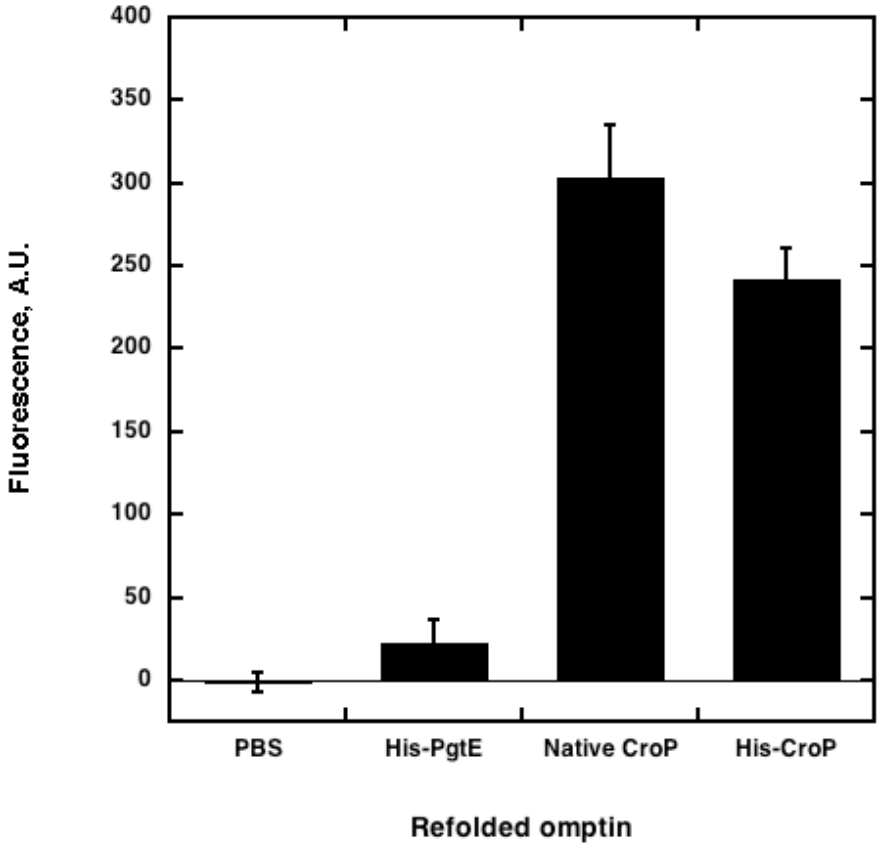

Figure 20: Cleavage of FRET C2 substrate by refolded His-PgtE, native CroP, and refolded His-CroP. Fluorescence of wells containing His-PgtE was not significantly higher than PBS control wells, indicating that His-PgtE was not functional. His-CroP cleaved nearly as much FRET C2 substrate as native CroP after 2 hours of incubation. Native CroP and His-CroP values are not significantly different from one another, but are significantly different from the PBS control and His-PgtE (p = 0.01). Roughly equal quantities of purified omptins were incubated with 3 μM FRET C2 over 2 h; catalytic turnover could not be determined as the exact quantities of enzymes used was not determined. Values represent means of 3 single experiments ± standard error.

Discussion

1. OmpT, OmpP, and CroP conferred resistance to C18G in disk inhibition and MIC assays, PgtE did not

Overall, strains of *E. coli* or *C. rodentium* that lacked omptins were sensitive to killing by C18G in disk inhibition (Figure **6**) and MIC assays (Table **5**). They were rescued by complementation with pWSK.*ompT,* pWSK.*ompP,* or pWSK.*croP*, but not pWSK.*pgtE*. *S. enterica ΔpgtE* was also more resistant to C18G when complemented with *croP*. These results are in agreement with previous work that found OmpT and OmpP to be essential in resistance to the α-helical AMP protamine[26,20] and with our previously published findings that CroP mediated resistance to C18G and mCRAMP[21].

Conversely, our finding that *S. enterica* wild-type and *S. enterica ΔpgtE* were equally sensitive to C18G in MIC assays disagreed with results published by Guina *et al.*[28]. Guina's group worked with constitutively PhoP-activated ($PhoP^C$) strains of *S. enterica* grown in PhoPQ-inducing conditions. They found *ΔpgtE* to be more sensitive to C18G, LL-37, and mCRAMP than $PhoP^C$ with wild-type *pgtE*. They also reported that complementation of *S. enterica* $PhoP^C$ *ΔpgtE* with a high copy number plasmid carrying *pgtE* increased the MIC of C18G and LL-37[28]. The disagreements between our findings and those of Guina *et al.* may be due to constitutive PhoP activation and over-expression of *pgtE* in their work. Indeed, we used a *ΔpgtE* strain expressing wild-type PhoPQ and we used a low copy number plasmid to express PgtE. In agreement with our results, a third group reported that after growth in PhoPQ-inducing conditions, an *S. enterica ΔpgtE* strain was as resistant to the α-helical AMP magainin 2 as the wild-type[65].

In the *E. coli* disk inhibition assay, there was an apparent inconsistency in that XL-1 Blue, which expresses OmpT and OmpP, was more sensitive than the BL21(DE3) strains complemented either OmpT or OmpP (Figure **6**). The most likely explanation for this is that despite the fact that pWSK 129 is a low copy number plasmid, several copies of pWSK.*ompT* and pWSK.*ompP* were expressed in complemented strains, as opposed to the single copy of each omptin gene in *E.*

coli XL-1 Blue. This would result in greater omptin expression at the OM of complemented strains, and therefore stronger resistance to C18G.

It also seemed inconsistent that the disk inhibition assay suggested that *C. rodentium* wild-type, *C. rodentium ΔcroP* pWSK.*ompT, C. rodentium ΔcroP* pWSK.*ompP,* and *C. rodentium ΔcroP* pWSK.*croP* were equally resistant to C18G, whereas the MIC results showed that *C. rodentium* wild-type, *C. rodentium ΔcroP* pWSK.*ompT,* and *C. rodentium ΔcroP* pWSK.*ompP* were more sensitive than *C. rodentium ΔcroP* pWSK.*croP*. However, given that only 25 µg of C18G were applied to the disks, which then diffused into the surrounding agarose, it is logical that the bacteria in the disk inhibition assays were exposed to lower concentrations than in the MICs. This prevented the degree of differentiation that was achieved with MICs. Similarly to *E. coli* pWSK.*ompT*, *C. rodentium ΔcroP* pWSK.*croP* was probably more resistance than the wild-type due to over-expression from pWSK 129. In fact, we have confirmed this by OMP preparation and SDS-PAGE gels (data not shown).

Pla and CroP are known to be unable to cleave the cyclic lipopeptide PMB[66,21]. In agreement with this knowledge, all of the strains that we tested were highly sensitive to PMB (Table **5**).

2. OmpT, OmpP, and CroP cleave C18G, unlike PgtE

The results from disk inhibition and MIC assays suggested that the increased resistance to C18G of strains expressing *ompT, ompP,* and *croP* was due to direct C18G cleavage by the omptins. We explored the ability of strains expressing omptins to cleave C18G through peptide cleavage assays. The C18G peptide (2.0 kDa) was visualized on 20 % acrylamide Tris/Tricine gels. Peptides of this size do not resolve well, resulting in bands that are thicker and more diffuse than larger proteins on SDS-PAGE gels. Our results show that wild-type *C. rodentium,* as well as native omptin knockout strains of *C. rodentium* or *S. enterica* complemented with empty vector or pWSK.*pgtE,* did not cleave large amounts of C18G, whereas strains carrying *ompT, ompP,* or *croP* degraded all or most of the AMP (Figure **7**, Figure **8**). Also, we have shown that *C. rodentium ΔcroP* pWSK.*croP* cleaved the human cathelicidin LL-37 (Figure **9**). These results are in

agreement with the MIC data, in that most of the strains that were resistant to C18G were also shown to cleave this AMP. The exception is wild-type *C. rodentium.* The MIC of C18G for wild-type *C. rodentium* was higher than *C. rodentium ΔcroP* (Table **5**), but the wild-type *C. rodentium* did not appear cleave C18G (Figure **7**). This is despite the fact that we used only $1/50^{th}$ as many bacteria in the MIC assay as in the cleavage assay. However the results may be explained by the fact that the peptide cleavage assay used 400 μg/mL C18G, which is many times the MIC of wild-type *C. rodentium*, 32 μg/mL C18G. Therefore, the amount of C18G that the wild-type strain cleaved in MIC tests was probably too small to visualize in Figure **7**. Nevertheless, moderate LL-37 cleavage by wild-type *C. rodentium* can be seen in Figure **9**. Our findings that cells carrying OmpT and OmpP cleaved C18G agreed with previous reports that a logarithmic phase culture of *E. coli* expressing OmpT can break down 100 μg/mL of protamine in 7 min[26], and that *E. coli* expressing OmpT with OmpP degraded protamine more readily than *E. coli* expressing OmpT alone[20].

However, our cleavage results with regards to PgtE disagreed again with those reported by Guina *et al*. We found that neither *C. rodentium ΔcroP* nor *S. enterica ΔpgtE* carrying pWSK.*pgtE* were able to cleave C18G (Figure **8**). However, Guina's group reported that the *S. enterica ΔpgtE* strain carrying a high copy number *pgtE* plasmid cleaved C18G[28]. Hence, these disagreements are not surprising given the over-expression of *pgtE* under that group's conditions, and in light of the fact that our cleavage assay was 30 min long, compared to their 16 hour incubation[28]. In fact, it is possible that after 16 h of incubation, cytoplasmic proteases are released from dead cells and cleave C18G, as we have seen effective cleavage of FRET C2 substrate during incubation of *C. rodentium ΔcroP* pWSK.*empty* in the presence of membrane-disrupting detergent Triton-X 100 (data not shown). Overall these results show that cells expressing OmpT, OmpP, and CroP are able to cleave C18G, leading to resistance, whereas cells expressing PgtE do not cleave C18G or show increased C18G resistance.

3. Some omptins prevent OM disruption by AMPs

Having shown that OmpT, OmpP, and CroP, but not PgtE, were able to cleave C18G and increase resistance, we wondered if the proteases also reduced the OM disruption that is the first step in AMP-mediated killing[67]. We used NPN as a fluorophore to investigate membrane disruption. NPN fluoresces when it contacts the hydrophobic components of the disrupted OM. In contrast to all other strains measured, NPN was highly fluorescent in combination with *C. rodentium ΔcroP* pWSK.*croP*, as shown in Figure **10**. This implied that the OM of *C. rodentium ΔcroP* pWSK.*croP* was inherently unstable, allowing association with NPN. Several lines of evidence suggest that over-expression of CroP from the low copy number plasmid pWSK 129 at the OM caused this membrane instability. First of all, it is well established that over-expression of OMPs leads to cell envelope stress[44]. Secondly, we observed that wild-type *C. rodentium*, which has a stable OM (Figure **10**), expresses less CroP than the complemented strain. The same was true of another *C. rodentium ΔcroP* strain expressing a functional CroP with a C-terminal histidine tag (data not shown). As well, work in our lab showed that the *C. rodentium ΔcroP* pWSK.*croP* OM was stabilized by the presence of 10 mM Mg^{2+} (data not shown). Mg^{2+} likely allowed closer association of LPS by binding negatively charged phosphates of the LPS[68].

When exposed to C18G, *C. rodentium* expressing *ompT, ompP,* and wild-type levels of *croP* had very low levels of membrane disruption, which quickly returned to the baseline, presumably as the omptins degraded the C18G (Figure **11**). This agreed with our findings that these strains are able to quickly cleave and resist C18G, allowing them to prevent excessive damage and restore membrane organization. In contrast, *C. rodentium ΔcroP* and *C. rodentium ΔcroP pWSK.pgtE* were somewhat disrupted by addition of C18G. These are the strains that were unable to cleave or resist C18G, so it is logical that C18G was able to disrupt their OMs as the first step of AMP-mediated killing. The CroP-complemented strain was highly disrupted before addition of C18G. The OM was so destabilized by the over-expression of CroP that the addition of C18G did not further affect the membrane. From this result alone, we would be unable to

comment upon whether or not C18G reaches and disrupts the *C. rodentium ΔcroP* pWSK.*croP* OM. However, we speculate that although high expression of CroP from pWSK.*croP* caused membrane disruption in and of itself, it did not reduce CroP protease function, explaining the rapid cleavage of C18G and the high resistance to C18G and mCRAMP in MIC assays[21]. As shown in Figure **12**, PMB effectively disrupted the OMs of all strains. This reveals considerably higher levels of membrane disruption by PMB than the same amount of C18G, in agreement with the lower MIC of PMB than C18G. This again supports the ability of *ompT, ompP,* and *croP* to proteolytically inactivate C18G, but not PMB.

4. Tropomyosin

During peptide cleavage assays, we had not seen any evidence that PgtE was expressed or active at the OM. Since PgtE is known to hydrolyse proteins[31], and since tropomyosin is a known OmpT substrate[36], we chose to test the strains' ability to cleave it. We used rough *E. coli* strains and smooth *C. rodentium ΔcroP* strains expressing *ompT, ompP, pgtE,* and *croP* to examine the omptins' ability to cleave tropomyosin in different LPS contexts. In *E. coli,* all omptin-complemented strains cleaved α- and β-tropomyosin (Figure **13**). In fact, the strain that expressed CroP degraded almost all of the tropomyosin present. This confirms previous findings that OmpT can cleave tropomyosin[36]. Of the *C. rodentium* strains, only pWSK.*croP* and pWSK.*pgtE* cleaved tropomyosin, and that was to a lesser degree than in *E. coli*. Assuming similar omptin expression levels in both species, reduced degradation of a large substrate in the presence of smooth LPS confirms previous findings: steric hindrance by O-antigen of degradation of proteins has been reported for OmpT, Pla, and PgtE[9]. Most importantly however, these results demonstrated that PgtE was indeed active at the OM of *E. coli* and *C. rodentium*, despite its apparent inability to cleave C18G. This suggests that whereas OmpT, OmpP, and CroP cleave peptide and protein substrates, PgtE preferentially degrades proteins.

5. Time course of FRET C2 substrate cleavage

Having confirmed the activity of PgtE at the *C. rodentium* OM, we set out to compare PgtE and CroP cleavage of a substrate that was more quantifiable than C18G or tropomyosin. We selected the FRET C2 substrate, which consists of a fluorophore and a quencher connected by an 8 amino acid sequence. The amino acid sequence is based on the complement component C2, and contains the dibasic Arg-Lys cleavage site that is targeted by host complement proteases and is also a cleavage site for omptins. Cleavage of the substrate separates the quencher from the fluorophore and is consequently measured by fluorescence at 430 nm. As shown in Figure **14**, expression of CroP or PgtE from pWSK 129 resulted in substantial cleavage of the FRET C2 substrate compared to the control.

We also examined FRET C2 substrate cleavage by *S. enterica ΔpgtE* alongside *C. rodentium ΔcroP* (Figure **15**). In agreement with Figure **14**, *C. rodentium ΔcroP* or *S. enterica ΔpgtE* carrying pWSK.*croP* cleaved substantially more substrate than strains carrying pWSK.*pgtE.* On the other hand, CroP was significantly more active in the *C. rodentium* background, possibly due to higher expression in its native context than in *S. enterica*. The fact that *pgtE* expressed in either *C. rodentium* or *S. enterica* cleaved substantial amounts of FRET C2 substrate clearly established that PgtE was present and active at the OM.

There are two possible justifications for the fact that PgtE cleaved FRET C2 substrate despite an apparent inability to cleave C18G. The first possibility is an effect of the increased sensitivity of the FRET assay. With this assay, we detected cleavage of less than 3 μM of FRET C2 substrate, as opposed to the C18G Tris/Tricine gels, which could only visualize the presence or absence of 200 μM C18G. Therefore it is possible that we are simply unable to detect the low levels of C18G cleavage. The other possibility is that PgtE did cleave the FRET C2 substrate more easily. PgtE may prefer the Arg-Lys cleavage site to the Lys-Lys sites of C18G. Or it may favour the amino acid sequence surrounding the cleavage site in the FRET C2 peptide. This would not be surprising as OmpT and OmpP have been shown to prefer certain amino acids over others not just at cleavage site, but for a total span of 6 amino acids[69,20]. Finally, the shorter 8-

residue C2 substrate may simply have accessed the PgtE active site more readily than the 18 residues of C18G.

6. RT-qPCR

The FRET C2 substrate cleavage results were in general agreement with the fact that cells expressing CroP cleaved C18G and degraded tropomyosin more quickly than cells expressing PgtE. One outstanding question was whether the apparent increase in activity was truly an effect of higher protease activity and specificity, or merely a result of higher expression of CroP than PgtE. To gain insight into this question, we used RT-qPCR to examine transcription of *croP* and *pgtE.* Both of the omptins were expressed from their native promoters from pWSK 129 plasmids. As shown in Table **6**, there was a many-fold increase in *croP* to *pgtE* mRNA in the *S. enterica ΔpgtE* and *C. rodentium ΔcroP* strains. This suggests that CroP expression at the OM was higher than PgtE expression in both species backgrounds. Therefore it is possible that CroP and PgtE were equally active against FRET C2 substrate, and the increased activity of CroP-expressing strains was simply due to greater numbers of omptins at the cell surface. The differing transcription levels of *croP* and *pgtE* may have been a result of stronger PhoP promotion, or weaker repression by sRNAs such as OmrA and OmrB, which reduce OmpT expression in *E. coli* and have homologues in *S. enterica*[48] and *C. rodentium.* However, since the increase was many-fold, and sRNA control of omptins tends to be moderate[48], a difference in PhoP promotion is the most likely cause. The promoter sequences of these genes are highly divergent, and our lab has identified an inverted PhoP box in the CroP promoter. Site-directed mutations of the promoter would allow for investigation of PhoPQ regulation of CroP. Nonetheless, mRNA level differences do not fully explain the lack of C18G cleavage by PgtE because it is able to degrade tropomyosin and FRET C2 substrate despite low expression.

7. OM preparations

In order to investigate the activities and specificities of PgtE and CroP while avoiding the influence of different expression levels or LPS lengths, we set out to

purify PgtE and CroP. The first step in our purification was to isolate OMPs from *C. rodentium ΔcroP* carrying the empty vector or omptin-expression vectors, as illustrated in Figure **16**. *C. rodentium ΔcroP* pWSK.*pgtE* had a faint band of PgtE. *C. rodentium ΔcroP* pWSK.*croP* had a stronger band of CroP. In light of the lower levels of *pgtE* transcription found by RT-qPCR, it is reasonable that the PgtE band is considerably fainter than the CroP band because there is less *pgtE* mRNA to be translated into protein. Omptins are not clearly visible in preparations from *C. rodentium ΔcroP* pWSK.*ompT* or *C. rodentium ΔcroP* pWSK.*ompP,* which have expected molecular weights of 33.5 kDa and 33.1 kDa respectively. The proteases may have been expressed at too low a level to be visualised, or may be masked behind the 34 kDa OmpA cleavage product. The 34 kDa OmpA cleavage product was visible in lanes with OmpT, PgtE, and CroP. We have confirmed OmpA cleavage by *C. rodentium ΔcroP* pWSK.*croP* by mass spectroscopy analysis of spots separated on a 2D gel[21]. To further support this proposal, the amount of OmpA is reduced in proportion to the amount of 34 kDa cleavage product, and OmpA has a putative dibasic cleave site close to the C-terminus that would result in a 33.8 kDa product.

In addition, bands at 22 kDa were seen in OM preparations containing OmpT, PgtE, and CroP. Although these could be the result of cleavage of other proteins, the 22 kDa bands likely represent autoproteolysis, as has been reported for OmpT and PgtE[12]. Although Kramer *et al.* reported that autoproteolysis of OmpT resulted in a 31 kDa fragment, their figures also show a supplementary band close to 22 kDa[11]. Alternatively, unusual folding may produce a form of Pla that migrates more quickly[12], which may also be the case for our 22 kDa bands. Western blotting could help differentiate between cleavage of larger proteins versus autoproteolysis or alternative folding. Mutations that prevent autoproteolysis could be developed to rule out alternative folding, but these mutants would be unlikely to have wild-type specificities and activities[11,12]. To sum up, SDS-PAGE gels of OMP preparations demonstrated the presence of omptins and in some cases showed evidence of cleavage and autoprocessing. OMP preparations were ready to be used for further purification.

8. Purification and activity of native CroP

Having confirmed the presence of CroP in OMP preparations, our next step was to purify it to homogeneity. We took advantage of the high pI of CroP – 7.9 – for flow-through anion exchange FPLC purification. CroP had a positive charge and flowed through the column. Most other OMPs had a lower pI and therefore a more negative charge, and associated with the column. Purified CroP was found at 33 kDa, slightly lower than a faint band of 36 kDa in the flow-through from a preparation from cells carrying the empty plasmid (Figure **17**). The higher band was likely OmpA, which we have found to be degraded in the presence of CroP[21], explaining its absence from the CroP lane. Native CroP was activated by incubation with a 3-molar excess of rough LPS. The native CroP preparation cleaved FRET C2 substrate very effectively (Figure **18**).

PgtE is unsuitable for purification by the same method because its pI of 5.5 is too similar to the pI of other OMPs. Indeed, attempts to purify native PgtE by binding to the column or collecting it from the flow-through proved unsuccessful.

9. Purification and activity of His-PgtE and His-CroP

Owing to the difficulty in purifying native PgtE, we opted to purify CroP and PgtE from inclusion bodies. We removed the signal sequence and added N-terminal histidine tags. Proteins that lack signal sequences are not properly targeted to the OM, and form inclusion bodies within the cytoplasm[11]. Inclusion bodies can than be easily isolated from other proteins.

As illustrated in Figure **19**, highly purified His-PgtE and His-CroP were isolated in large quantities using this method. His-CroP traveled more quickly on the gel despite its similar size to His-PgtE. This cannot be explained by pI differences that may have been inadequately masked by SDS-PAGE. In fact, at pH 8.8 His-PgtE is expected to carry a charge of -12.8 compared to CroP with -2.8. This would cause His-PgtE to move more quickly through the gel than His-CroP. The unusual migration may instead have been a result of alternate folding, as previously reported[12]. Having purified the histidine-tagged omptins, we were ready to move forward with refolding and activity testing.

10. Refolded omptins

After inclusion body purifications, histidine-tagged proteins were diluted 1/1000 and dialysed to remove urea, in the presence of $DodMe_2NPrSO_3$. $DodMe_2NPrSO_3$ is a detergent that aids refolding of purified omptins[11]. The histidine-tagged omptins were then compared to native CroP by their ability to cleave FRET C2 substrate, as seen in Figure **20**. After 2 hours, native CroP and His-CroP had both cleaved similar amounts of FRET C2 substrate, with a significantly higher fluorescence reading than the PBS control. This not only indicates that His-CroP was properly refolded, but also that the N-terminal histidine tag does not prevent omptin activity, in agreement with previous findings[9,70,71]. However, the amounts of proteases used here were only roughly equal, and it was therefore not possible to compare native CroP and His-CroP rates of cleavage directly, or calculate catalytic activity. The fluorescence produced by His-PgtE was not significantly greater than that of the PBS control, suggesting that His-PgtE was not properly refolded. We observed precipitation during His-PgtE dialysis, which may account for loss of PgtE function (data not shown). In spite of previously published reports of successful His-PgtE and His-Pla refolding[9,70,71], our various attempts at refolding His-PgtE failed. We attempted dialysis against PBS pH 7.5 with concentrations of 6 M, 4 M, 2 M, 1 M, 0.5 M, and 0 M urea, in the presence of 1 mM or 10 mM $DodMe_2NPrSO_3$, and the presence of absence of 0.1 mM DTT without success. Rapid dilution in PBS pH 7.5 3 M or 0 M urea were also unsuccessful. We verified by SDS-PAGE gel that His-PgtE was not inactivated by autoproteolysis and dissociation (data not shown). Future work may involve a more highly diluted initial His-PgtE preparation to reduce precipitation, and employing broader screening techniques with commercially available protein refolding kits. Alternatively, omptins may be purified using a DEAE-cellulose[11] or a hydrophobic column.

11. Final conclusions and future directions

In summary, this work demonstrates that CroP and PgtE have different proteolytic behaviours. CroP cleaves C18G even more effectively than OmpT and OmpP,

leading to increased MICs, and also cleaves LL-37, which is expressed in the human colon. In addition, CroP cleaves FRET C2 substrate more efficiently than other omptins. Despite being active against tropomyosin and FRET C2 substrate - and in disagreement with previous work - PgtE does not cleave C18G or increase resistance. The difference between CroP and PgtE cleavage activity is at least partially due to increased expression of CroP at the OM. To determine the degree to which the differences we have observed are due to protease specificity and catalytic activity as opposed to expression, we must obtain purified, refolded, and quantified CroP and PgtE. Specifically, we plan to purify native PgtE or develop a method for refolding His-PgtE.

Omptins may be excellent targets for protease inhibitors because they seem to be restricted to invasive species and neither human nor commensal bacterial proteases share their unique catalytic site. Moreover, in light of increasing worldwide resistance to traditional antibiotics that target the cell wall or protein synthesis[72], we hope that a stronger understanding of omptin proteases with relation to degradation of host AMPs will lay the path for development of novel pharmaceuticals such as protease inhibitors for A/E pathogens.

References

1. Vogel, J. & Papenfort, K. Small non-coding RNAs and the bacterial outer membrane. *Curr. Opin. Microbiol* **9**, 605-611 (2006).
2. Galván, E.M., Chen, H. & Schifferli, D.M. The Psa fimbriae of *Yersinia pestis* interact with phosphatidylcholine on alveolar epithelial cells and pulmonary surfactant. *Infect. Immun* **75**, 1272-1279 (2007).
3. Janakiraman, A., Fixen, K.R., Gray, A.N., Niki, H. & Goldberg, M.B. A genome-scale proteomic screen identifies a role for DnaK in chaperoning of polar autotransporters in *Shigella*. *J. Bacteriol* **191**, 6300-6311 (2009).
4. Benjelloun-Touimi, Z., Sansonetti, P.J. & Parsot, C. SepA, the major extracellular protein of *Shigella flexneri*: autonomous secretion and involvement in tissue invasion. *Mol. Microbiol* **17**, 123-135 (1995).
5. Vandeputte-Rutten, L. et al. Crystal structure of the outer membrane protease OmpT from *Escherichia coli* suggests a novel catalytic site. *EMBO J* **20**, 5033-5039 (2001).
6. Varadarajan, N., Rodriguez, S., Hwang, B., Georgiou, G. & Iverson, B.L. Highly active and selective endopeptidases with programmed substrate specificities. *Nat. Chem. Biol* **4**, 290-294 (2008).
7. Rawlings, N.D., Morton, F.R., Kok, C.Y., Kong, J. & Barrett, A.J. MEROPS: the peptidase database. *Nucleic Acids Res* **36**, D320-325 (2008).
8. Hritonenko, V. & Stathopoulos, C. Omptin proteins: an expanding family of outer membrane proteases in Gram-negative *Enterobacteriaceae*. *Mol. Membr. Biol* **24**, 395-406 (2007).
9. Kukkonen, M. et al. Lack of O-antigen is essential for plasminogen activation by *Yersinia pestis* and *Salmonella enterica*. *Mol. Microbiol* **51**, 215-225 (2004).
10. Kramer, R.A., Dekker, N. & Egmond, M.R. Identification of active site serine and histidine residues in *Escherichia coli* outer membrane protease OmpT. *FEBS Lett* **468**, 220-224 (2000).
11. Kramer, R.A., Zandwijken, D., Egmond, M.R. & Dekker, N. In vitro folding, purification and characterization of *Escherichia coli* outer membrane protease ompT. *Eur. J. Biochem* **267**, 885-893 (2000).
12. Kukkonen, M. et al. Protein regions important for plasminogen activation and inactivation of alpha$_2$-antiplasmin in the surface protease Pla of *Yersinia pestis*. *Mol. Microbiol* **40**, 1097-1111 (2001).
13. Bucki, R., Leszczyńska, K., Namiot, A. & Sokołowski, W. Cathelicidin LL-37: a multitask antimicrobial peptide. *Arch. Immunol. Ther. Exp. (Warsz.)* **58**, 15-25 (2010).
14. Hancock, R.E.W. & Sahl, H. Antimicrobial and host-defense peptides as new anti-infective therapeutic strategies. *Nat. Biotechnol* **24**, 1551-1557 (2006).
15. Iimura, M. et al. Cathelicidin mediates innate intestinal defense against colonization with epithelial adherent bacterial pathogens. *J. Immunol* **174**,

4901-4907 (2005).
16. Rosenberger, C.M., Gallo, R.L. & Finlay, B.B. Interplay between antibacterial effectors: A macrophage antimicrobial peptide impairs intracellular Salmonella replication. *Proc Natl Acad Sci U S A* **101**, 2422-2427 (2004).
17. Pestonjamasp, V.K., Huttner, K.H. & Gallo, R.L. Processing site and gene structure for the murine antimicrobial peptide CRAMP. *Peptides* **22**, 1643-1650 (2001).
18. Hase, K. et al. Expression of LL-37 by human gastric epithelial cells as a potential host defense mechanism against *Helicobacter pylori*. *Gastroenterology* **125**, 1613-1625 (2003).
19. Gudmundsson, G.H., Bergman, P., Andersson, J., Raqib, R. & Agerberth, B. Battle and balance at mucosal surfaces - The story of *Shigella* and antimicrobial peptides. *Biochemical and Biophysical Research Communications* **396**, 116-119 (2010).
20. Hwang, B. et al. Substrate Specificity of the *Escherichia coli* Outer Membrane Protease OmpP. *J Bacteriol* **189**, 522-530 (2007).
21. Le Sage, V. et al. An outer membrane protease of the omptin family prevents activation of the *Citrobacter rodentium* PhoPQ two-component system by antimicrobial peptides. *Mol. Microbiol* **74**, 98-111 (2009).
22. Pranting, M. & Andersson, D.I. Mechanisms and physiological effects of protamine resistance in *Salmonella enterica* serovar Typhimurium LT2. *J. Antimicrob. Chemother.* **65**, 876-887 (2010).
23. Darveau, R.P. et al. Peptides related to the carboxyl terminus of human platelet factor IV with antibacterial activity. *J. Clin. Invest* **90**, 447-455 (1992).
24. Bader, M.W. et al. Recognition of antimicrobial peptides by a bacterial sensor kinase. *Cell* **122**, 461-472 (2005).
25. Peschel, A. & Sahl, H. The co-evolution of host cationic antimicrobial peptides and microbial resistance. *Nat. Rev. Microbiol* **4**, 529-536 (2006).
26. Stumpe, S., Schmid, R., Stephens, D.L., Georgiou, G. & Bakker, E.P. Identification of OmpT as the Protease That Hydrolyzes the Antimicrobial Peptide Protamine before It Enters Growing Cells of *Escherichia coli. J. Bacteriol.* **180**, 4002-4006 (1998).
27. Hwang, B. et al. Substrate specificity of the *Escherichia coli* outer membrane protease OmpP. *J. Bacteriol* **189**, 522-530 (2007).
28. Guina, T., Yi, E.C., Wang, H., Hackett, M. & Miller, S.I. A PhoP-regulated outer membrane protease of *Salmonella enterica* serovar typhimurium promotes resistance to alpha-helical antimicrobial peptides. *J. Bacteriol* **182**, 4077-4086 (2000).
29. Lähteenmäki, K., Edelman, S. & Korhonen, T.K. Bacterial metastasis: the host plasminogen system in bacterial invasion. *Trends Microbiol* **13**, 79-85 (2005).
30. Haiko, J., Kukkonen, M., Ravantti, J.J., Westerlund-Wikström, B. & Korhonen, T.K. The single substitution I259T, conserved in the plasminogen activator Pla of pandemic *Yersinia pestis* branches, enhances fibrinolytic activity. *J. Bacteriol* **191**, 4758-4766 (2009).

31. Lähteenmäki, K., Kyllönen, P., Partanen, L. & Korhonen, T.K. Antiprotease inactivation by *Salmonella enterica* released from infected macrophages. *Cell. Microbiol* **7**, 529-538 (2005).
32. Yun, T.H., Cott, J.E., Tapping, R.I., Slauch, J.M. & Morrissey, J.H. Proteolytic inactivation of tissue factor pathway inhibitor by bacterial omptins. *Blood* **113**, 1139-1148 (2009).
33. Duncan, R.C., Wijeyewickrema, L.C. & Pike, R.N. The initiating proteases of the complement system: controlling the cleavage. *Biochimie* **90**, 387-395 (2008).
34. Ramu, P. et al. The surface protease PgtE of *Salmonella enterica* affects complement activity by proteolytically cleaving C3b, C4b and C5. *FEBS Lett* **581**, 1716-1720 (2007).
35. Sodeinde, O.A. et al. A surface protease and the invasive character of plague. *Science* **258**, 1004-1007 (1992).
36. Kluwe, L. et al. Rabbit skeletal muscle alpha alpha-tropomyosin expressed in baculovirus-infected insect cells possesses the authentic N-terminus structure and functions. *J. Muscle Res. Cell. Motil* **16**, 103-110 (1995).
37. Sedliaková, M., Masek, F., Slezáriková, V. & Pirsel, M. The effect of the OmpT protease on excision repair in UV-irradiated *Escherichia coli*. *J. Photochem. Photobiol. B, Biol* **41**, 245-248 (1997).
38. Grodberg, J. & Dunn, J.J. ompT encodes the *Escherichia coli* outer membrane protease that cleaves T7 RNA polymerase during purification. *J. Bacteriol* **170**, 1245-1253 (1988).
39. Lähteenmäki, K., Kukkonen, M. & Korhonen, T.K. The Pla surface protease/adhesin of *Yersinia pestis* mediates bacterial invasion into human endothelial cells. *FEBS Lett* **504**, 69-72 (2001).
40. Petty, N.K. et al. The *Citrobacter rodentium* Genome Sequence Reveals Convergent Evolution with Human Pathogenic *Escherichia coli*. *J. Bacteriol.* **192**, 525-538 (2010).
41. Croxen, M.A. & Finlay, B.B. Molecular mechanisms of *Escherichia coli* pathogenicity. *Nat. Rev. Microbiol* **8**, 26-38 (2010).
42. Goldberg, S.D., Clinthorne, G.D., Goulian, M. & DeGrado, W.F. Transmembrane polar interactions are required for signaling in the *Escherichia coli* sensor kinase PhoQ. *Proc. Natl. Acad. Sci. U.S.A* **107**, 8141-8146 (2010).
43. Eguchi, Y. et al. Signal Transduction Cascade between EvgA/EvgS and PhoP/PhoQ Two-Component Systems of *Escherichia coli*. *J Bacteriol* **186**, 3006-3014 (2004).
44. Papenfort, K. et al. SigmaE-dependent small RNAs of *Salmonella* respond to membrane stress by accelerating global omp mRNA decay. *Mol. Microbiol* **62**, 1674-1688 (2006).
45. Coornaert, A. et al. MicA sRNA links the PhoP regulon to cell envelope stress. *Mol Microbiol* (2010).doi:10.1111/j.1365-2958.2010.07115.x
46. Eguchi, Y. & Utsumi, R. Introduction to bacterial signal transduction networks. *Adv. Exp. Med. Biol* **631**, 1-6 (2008).
47. Vogel, J. & Papenfort, K. Small non-coding RNAs and the bacterial outer

membrane. *Curr. Opin. Microbiol* **9**, 605-611 (2006).
48. Guillier, M. & Gottesman, S. Remodelling of the *Escherichia coli* outer membrane by two small regulatory RNAs. *Mol. Microbiol* **59**, 231-247 (2006).
49. Stenseth, N.C. et al. Plague: Past, Present, and Future. *PLoS Med* **5**, e3 (2008).
50. Lahteenmaki, K., Virkola, R., Saren, A., Emody, L. & Korhonen, T.K. Expression of Plasminogen Activator Pla of *Yersinia pestis* enhances bacterial attachment to the mammalian extracellular matrix. *Infect. Immun.* **66**, 5755-5762 (1998).
51. Lahiri, A., Lahiri, A., Iyer, N., Das, P. & Chakravortty, D. Visiting the cell biology of *Salmonella* infection. *Microbes and Infection* **In Press, Uncorrected Proof**,
52. Navarre, W.W. et al. Co-regulation of *Salmonella enterica* genes required for virulence and resistance to antimicrobial peptides by SlyA and PhoP/PhoQ. *Mol. Microbiol* **56**, 492-508 (2005).
53. Pietilä, T.E. et al. Activation, cytokine production, and intracellular survival of bacteria in *Salmonella*-infected human monocyte-derived macrophages and dendritic cells. *J. Leukoc. Biol* **78**, 909-920 (2005).
54. Wain, J. et al. Quantitation of bacteria in blood of typhoid fever patients and relationship between counts and clinical features, transmissibility, and antibiotic resistance. *J. Clin. Microbiol.* **36**, 1683-1687 (1998).
55. Egile, C., d'Hauteville, H., Parsot, C. & Sansonetti, P.J. SopA, the outer membrane protease responsible for polar localization of IcsA in *Shigella flexneri. Mol. Microbiol* **23**, 1063-1073 (1997).
56. Viswanathan, V.K., Hodges, K. & Hecht, G. Enteric infection meets intestinal function: how bacterial pathogens cause diarrhoea. *Nat. Rev. Microbiol* **7**, 110-119 (2009).
57. Kaper, J.B., Nataro, J.P. & Mobley, H.L. Pathogenic *Escherichia coli*. *Nat. Rev. Microbiol* **2**, 123-140 (2004).
58. Foxman, B., Zhang, L., Palin, K., Tallman, P. & Marrs, C.F. Bacterial virulence characteristics of *Escherichia coli* isolates from first-time urinary tract infection. *J. Infect. Dis* **171**, 1514-1521 (1995).
59. Lundrigan, M.D. & Webb, R.M. Prevalence of *ompT* among *Escherichia coli* isolates of human origin. *FEMS Microbiology Letters* **97**, 51-56 (1992).
60. Petkovsek, Z., Elersic, K., Gubina, M., Zgur-Bertok, D. & Starcic Erjavec, M. Virulence potential of Escherichia coli isolates from skin and soft tissue infections. *J. Clin. Microbiol* **47**, 1811-1817 (2009).
61. Chromek, M. et al. The antimicrobial peptide cathelicidin protects the urinary tract against invasive bacterial infection. *Nat. Med* **12**, 636-641 (2006).
62. Hui, C. et al. *Escherichia coli* outer membrane protease OmpT confers resistance to urinary cationic peptides. *Microbiol. Immunol* **54**, 452-459 (2010).
63. Luperchio, S.A. & Schauer, D.B. Molecular pathogenesis of *Citrobacter rodentium* and transmissible murine colonic hyperplasia. *Microbes Infect* **3**, 333-340 (2001).
64. MacLean, L.L. & Perry, M.B. Structural studies on the O-polysaccharide of

the lipopolysaccharide produced by *Citrobacter rodentium* (ATCC 51459). *Eur. J. Biochem* **268**, 5740-5746 (2001).
65. Shi, Y., Cromie, M.J., Hsu, F., Turk, J. & Groisman, E.A. PhoP-regulated *Salmonella* resistance to the antimicrobial peptides magainin 2 and polymyxin B. *Mol. Microbiol* **53**, 229-241 (2004).
66. Galván, E.M., Lasaro, M.A.S. & Schifferli, D.M. Capsular antigen fraction 1 and Pla modulate the susceptibility of *Yersinia pestis* to pulmonary antimicrobial peptides such as cathelicidin. *Infect. Immun* **76**, 1456-1464 (2008).
67. Brogden, K.A. Antimicrobial peptides: pore formers or metabolic inhibitors in bacteria? *Nat. Rev. Microbiol* **3**, 238-250 (2005).
68. Moore, R.A., Bates, N.C. & Hancock, R.E. Interaction of polycationic antibiotics with *Pseudomonas aeruginosa* lipopolysaccharide and lipid A studied by using dansyl-polymyxin. *Antimicrob. Agents Chemother* **29**, 496-500 (1986).
69. McCarter, J.D. et al. Substrate specificity of the *Escherichia coli* outer membrane protease OmpT. *J. Bacteriol* **186**, 5919-5925 (2004).
70. Ramu, P. et al. Activation of pro-matrix metalloproteinase-9 and degradation of gelatin by the surface protease PgtE of *Salmonella enterica* serovar Typhimurium. *Int. J. Med. Microbiol* **298**, 263-278 (2008).
71. Suomalainen, M. et al. Temperature-Induced Changes in the Lipopolysaccharide of *Yersinia pestis* Affect Plasminogen Activation by the Pla Surface Protease. *Infect Immun* (2010).doi:10.1128/IAI.01329-09
72. Supuran, C.T., Scozzafava, A. & Clare, B.W. Bacterial protease inhibitors. *Medicinal Research Reviews* **22**, 329-372 (2002).

Attached paper

An outer membrane protease of the omptin family prevents activation of the *Citrobacter rodentium* PhoPQ two-component system by antimicrobial peptides.

Valerie Le Sage, Lei Zhu, Christine Lepage, Andrea Portt, Charles Viau, France Daigle, Samantha Gruenheid, Hervé Le Moual

Mol. Microbiol 74, 98-111 (2009)

Molecular Microbiology (2009) 74(1), 98–111 ■
doi:10.1111/j.1365-2958.2009.06854.x
First published online 2 September 2009

An outer membrane protease of the omptin family prevents activation of the *Citrobacter rodentium* PhoPQ two-component system by antimicrobial peptides

Valerie Le Sage,[1] Lei Zhu,[1] Christine Lepage,[2] Andrea Portt,[1] Charles Viau,[1] France Daigle,[2] Samantha Gruenheid[1] and Hervé Le Moual[1,3]*
[1]*Department of Microbiology and Immunology and*
[3]*Faculty of Dentistry, McGill University, Montreal, QC, H3A 2B4, Canada.*
[2]*Department of Microbiology and Immunology, University of Montreal, Montreal, QC, H3C 3J7, Canada.*

Summary

The PhoPQ two-component system of the intracellular pathogen *Salmonella enterica* senses and controls resistance to α-helical antimicrobial peptides (AMPs) by regulating covalent modifications of lipid A. A homologue of the *phoPQ* operon was found in the genome of the murine enteric extracellular pathogen, *Citrobacter rodentium*. Here we report that *C. rodentium* PhoPQ was apparently unable to mediate activation of target genes in the presence of α-helical AMPs. However, these AMPs activated *C. rodentium* PhoPQ expressed in a *S. enterica* Δ*phoPQ* mutant. Analysis of the outer membrane (OM) fractions of the *C. rodentium* wild-type and Δ*phoPQ* strains led to the identification of an omptin family protease (CroP) that was absent in Δ*phoPQ*. Deletion of *croP* in *C. rodentium* resulted in higher susceptibility to α-helical AMPs, indicating a direct role of CroP in AMP resistance. CroP greatly contributed to the protection of the OM from AMP damage by actively degrading α-helical AMPs before they reach the periplasmic space. Accordingly, transcriptional activation of PhoP-regulated genes by α-helical AMPs was restored in the Δ*croP* mutant. This study shows that resistance to α-helical AMPs by the extracellular pathogen *C. rodentium* relies primarily on the CroP OM protease.

Introduction

Antimicrobial peptides (AMPs) are important components of the innate immune system that are involved in host defence against microorganisms (Hancock and Lehrer, 1998; Zasloff, 2002; Hancock and Sahl, 2006). Although diverse in sequence and structure, AMPs are characterized by their small size, amphipathic properties and cationic net charges. There are two major classes of mammalian AMPs, the cathelicidins, such as human LL-37 and mouse CRAMP that form α-helices, and the α and β-defensins that adopt a β-sheet structure (Ganz, 2003; Zanetti, 2004). Various cell types including phagocytic cells, goblet cells and epithelial cells produce AMPs in a constitutive or inducible manner. In Gram-negative bacteria, AMPs interact first with the lipid A moiety of lipopolysaccharide (LPS) to disrupt the outer membrane (OM) and gain access to the periplasmic space. Most AMPs appear to exert their bactericidal function by disrupting the cytoplasmic membrane (Brogden, 2005; Melo *et al.*, 2009). Bacterial pathogens have developed several mechanisms to resist killing by AMPs. These resistance mechanisms include the protease-mediated inactivation of AMPs, the export of AMPs by efflux pumps and the covalent modification of bacterial membrane components that results in a decrease of the overall negative charge and, in turn, minimize membrane interaction with cationic AMPs (Miller *et al.*, 2005; Peschel and Sahl, 2006).

The PhoPQ two-component system (TCS) is composed of the sensor kinase PhoQ and the cognate response regulator PhoP. PhoPQ is found in a variety of Gram-negative pathogens, including the facultative intracellular *Salmonella enterica*. PhoPQ of *S. enterica*, which is by far the best-characterized PhoPQ system, is a master regulator of virulence that is critical for bacterial survival within macrophage phagosomes (Groisman *et al.*, 1989; Miller *et al.*, 1989). PhoQ, like most sensor kinases, possesses both kinase and phosphatase activities that play opposite roles in controlling the phosphorylation level of PhoP. These activities are regulated by several environmental cues that are sensed by the PhoQ periplasmic domain. Limiting concentrations of the divalent cations Mg^{2+} and Ca^{2+} were shown to promote PhoQ autophosphorylation and, in turn, PhoP phosphorylation (Garcia Vescovi *et al.*, 1996; Castelli *et al.*, 2000; Montagne *et al.*, 2001; Sanowar and Le Moual, 2005). Recent studies revealed that PhoQ also responds to α-helical AMPs and acidic pH,

Accepted 7 August, 2009. *For correspondence. E-mail herve.lemoual@mcgill.ca; Tel. (+1) 514 398 6235; Fax (+1) 514 398 7052.

leading to the activation of the PhoPQ signalling pathway (Bader *et al.*, 2005; Prost *et al.*, 2007). Acidic pH and α-helical AMPs are likely the physiologically relevant ligands of *S. enterica* PhoQ, since the vacuolar environment of phagosomes is characterized by the presence of AMPs, a pH in the range of 5.0–6.5 and a constant concentration of Mg^{2+} around 1 mM (Alpuche Aranda *et al.*, 1992; Martin-Orozco *et al.*, 2006; Prost and Miller, 2008). In agreement, PhoPQ has been shown to be critical for *S. enterica* resistance to the antimicrobial activity of CRAMP in murine macrophages (Rosenberger *et al.*, 2004). PhoQ-activating signals, such as α-helical AMPs, promote structural modifications of the lipid A moiety of LPS (Miller *et al.*, 2005). PhoP directly regulates the expression of the lipid A-modifying enzymes *lpxO*, *pagL* and *pagP*. The PmrAB TCS regulates expression of other lipid A-modifying enzymes such as the *pmrC* gene and the *pmrHFIJKLM* operon (renamed the *arn* operon). In *S. enterica*, PhoPQ promotes activation of PmrA-regulated genes by transcriptionally activating the expression of the PmrD protein, which in turn prevents PmrA dephosphorylation (Kox *et al.*, 2000; Kato and Groisman, 2004).

The involvement of PhoPQ in resistance to various AMPs has also been reported for other pathogens of the family *Enterobacteriaceae*. These include the mammalian pathogens *Yersinia pseudotuberculosis* and *Yersinia pestis* (Marceau *et al.*, 2004; Winfield *et al.*, 2005), *Shigella flexneri* (Moss *et al.*, 2000), as well as the insect pathogen *Photorhabdus luminescens* (Derzelle *et al.*, 2004) and the plant pathogen *Erwinia chrysanthemi* (Llama-Palacios *et al.*, 2003). In contrast, *Pseudomonas aeruginosa* PhoQ is not activated by AMPs but responds to both divalent cations and acidic pH (Prost *et al.*, 2008). This discrepancy was attributed to the absence of a cluster of acidic amino acids from the *P. aeruginosa* PhoQ periplasmic domain. Thus, a PhoQ response to AMPs can be directly correlated with the presence of this acidic cluster in the PhoQ periplasmic domain (Bader *et al.*, 2005; Cho *et al.*, 2006; Prost and Miller, 2008).

The role of OM proteases in bacterial resistance to AMPs is less well established than that of lipid A modifications. OM proteases of the omptin family are found in various Gram-negative pathogens including *S. enterica* (PgtE), *Y. pestis* (Pla), *S. flexneri* (SopA) and *Escherichia coli* (OmpT and OmpP) (Kukkonen and Korhonen, 2004; Hritonenko and Stathopoulos, 2007; Haiko *et al.*, 2009a). Although *S. enterica* PgtE cleaves AMPs such as the synthetic α-helical peptide L-C18G *in vitro*, its contribution to AMP resistance appears to be marginal when expressed from a single chromosomal copy (Guina *et al.*, 2000). *In vivo*, *Y. pestis* Pla activity is essential to tissue invasion (Sodeinde *et al.*, 1992; Lathem *et al.*, 2007). Pla promotes degradation of fibrin clots by activating plasminogen into plasmin and inactivating the α_2-antiplasmin inhibitor (Kukkonen and Korhonen, 2004). A recent study revealed that Pla was also able to inactivate AMPs such as LL-37 and CRAMP, *in vitro* (Galvan *et al.*, 2008). Furthermore, *E. coli* OmpT was reported to efficiently degrade the AMP protamine (Stumpe *et al.*, 1998).

Citrobacter rodentium is an extracellular enteric pathogen that causes transmissible murine colonic hyperplasia (Schauer and Falkow, 1993). Similar virulence factors make *C. rodentium* an excellent model organism for the study of the human pathogens enteropathogenic *E. coli* (EPEC) and enterohaemorrhagic *E. coli* (EHEC). Colonization of the intestine by these food-borne pathogens produces attaching and effacing (A/E) lesions (Mundy *et al.*, 2005), which are characterized by intimate bacterial attachment to intestinal epithelial cells, formation of actin-rich pedestals underneath adherent bacteria and destruction of brush border microvilli. Host defences against these pathogens include the secretion of AMPs such as β-defensins and cathelicidins (O'Neil *et al.*, 1999; Hase *et al.*, 2002; Schauber *et al.*, 2003). During infection, *C. rodentium* resides in close proximity to colonic epithelial cells expressing CRAMP, which has antimicrobial activity against this pathogen (Iimura *et al.*, 2005).

Having identified a homologue of the *phoPQ* operon in the *C. rodentium* genome sequence, we examined whether *C. rodentium* PhoQ recognizes α-helical AMPs and responds accordingly by promoting resistance. We present evidence that *C. rodentium* PhoQ is not activated by α-helical AMPs because they are degraded by CroP, an OM protease of the omptin family, before they reach the periplasmic space. This study shows that *C. rodentium* and *S. enterica* use different strategies to resist the deleterious effect of α-helical AMPs.

Results

C. rodentium *PhoQ responds to* Mg^{2+} *and pH acidification but not to α-helical AMPs*

Open reading frames (ORFs) with high identities to the amino acid sequences of *S. enterica* PhoP (82%) and PhoQ (78%) were identified from the *C. rodentium* genome sequence (http://www.sanger.ac.uk/Projects/C_rodentium). As in the *S. enterica phoPQ* operon, the two ORFs overlapped by one nucleotide, suggesting that they are part of the same transcriptional unit. To determine whether the *C. rodentium* and *S. enterica* PhoQ sensor kinases respond to the same environmental cues, we constructed chromosomal β-galactosidase fusions with the *mgtA* gene in both the wild-type and Δ*phoPQ C. rodentium* strains. As in *S. enterica* and *E. coli*, the *mgtA* gene, which codes for a Mg^{2+} transporter, harbours a PhoP box (TGTATAxxxxxCGTTTA) that contains all the essential

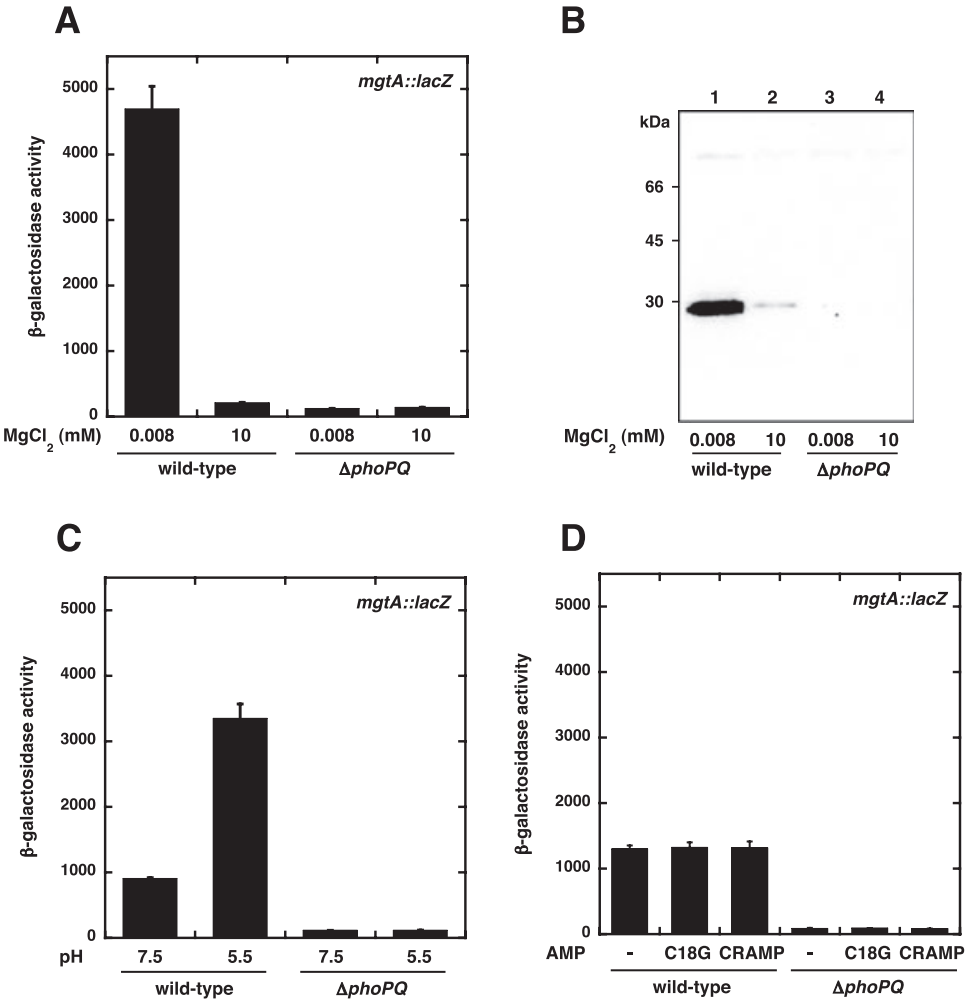

Fig. 1. C. *rodentium* PhoPQ responds to Mg^{2+} deprivation and acidic pH but not AMPs.
A. Regulation of the *mgtA*::*lacZ* transcriptional fusion in response to external Mg^{2+}. Overnight cultures of the *C. rodentium* wild-type and Δ*phoPQ* mutant were diluted 1:100 in N-minimal medium (pH 7.5) containing 10 mM $MgCl_2$ and grown at 37°C. At an OD_{600} of 0.4, cells were washed twice in N-minimal medium, re-suspended in fresh media containing either 8 μM or 10 mM $MgCl_2$ and incubated at 37°C for an additional 90 min. Values are mean ± standard deviation of cultures grown in triplicate and are representative of at least three independent trials.
B. Expression of *C. rodentium* PhoP is regulated by external Mg^{2+}. Anti-PhoP immunoblot of crude bacterial extracts isolated from wild-type or Δ*phoPQ* cells grown in N-minimal medium containing either 8 μM or 10 mM $MgCl_2$.
C. pH acidification upregulates *mgtA*::*lacZ* transcriptional activity. Cultures were grown to an OD_{600} of 0.4 in N-minimal medium (pH 7.5) supplemented with 1 mM $MgCl_2$. Cells were washed and re-suspended in fresh media supplemented with 1 mM $MgCl_2$ and buffered with 100 mM Bis-Tris at either pH 7.5 or pH 5.5. Cells were grown for an additional 90 min at 37°C. No pH fluctuations were observed over the course of the experiment.
D. The *mgtA*::*lacZ* transcriptional activity is unresponsive to α-helical AMPs. Bacterial strains were grown in N-minimal medium (pH 7.5) supplemented with 1 mM $MgCl_2$. At an OD_{600} of 0.4, 2 μM L-C18G or 10 μM CRAMP was added and cultures were incubated at 37°C for an additional 60 min.

nucleotides (underlined) for PhoP recognition (Yamamoto *et al.*, 2002). To examine the PhoQ response to external Mg^{2+}, the *mgtA*::*lacZ* reporter strains were grown under PhoQ-activating (8 μM $MgCl_2$) and PhoQ-repressing (10 mM $MgCl_2$) conditions. The β-galactosidase activity produced by the wild-type strain grown in the presence of 8 μM $MgCl_2$ was 22-fold higher than that of cells grown in the presence of 10 mM $MgCl_2$ (Fig. 1A). Mg^{2+}-mediated regulation of the *mgtA*::*lacZ* reporter was not observed in the Δ*phoPQ* strain. Western blot analysis of whole-cell lysates from wild-type *C. rodentium* grown in media containing either 8 μM or 10 mM $MgCl_2$ is shown in Fig. 1B. The PhoPQ-inducing condition (8 μM $MgCl_2$) produced elevated levels of PhoP (lane 1), while the expression of PhoP under the PhoPQ-repressing condition (10 mM $MgCl_2$) was drastically repressed (lane 2). As expected, no expression was observed in the Δ*phoPQ* mutant under either growth condition (lanes 3 and 4). As described

Table 1. Minimum inhibitory concentrations (MICs) of AMPs for *C. rodentium* strains.

Strain	MIC (μg ml^{-1})			
	L-C18G	D-C18G	CRAMP	PMB
C. rodentium wild-type	32	4	128	0.5
C. rodentium Δ*phoPQ*	4	4	32	0.5
C. rodentium Δ*phoPQ*-pCR*phoPQ*	16	n/d	128	n/d
C. rodentium Δ*croP*	4	4	32	0.5
C. rodentium Δ*croP*-pCR*croP*	128	n/d	> 128	n/d

n/d, not determined.

previously for *S. enterica* and *E. coli*, these data indicate that *C. rodentium* PhoPQ responds to external Mg^{2+} and suggest that *C. rodentium* PhoP autoregulates its own promoter (Soncini *et al.*, 1995; Garcia Vescovi *et al.*, 1996; Kato *et al.*, 1999). Accordingly, a consensus PhoP box that consists of the two half-sites GGTTTA and TGTTTA separated by five nucleotides was identified 58 nucleotides upstream of the *C. rodentium phoP* gene start codon.

Acidic pH was tested as a PhoQ-activating cue, since *S. enterica* PhoQ has been shown to respond to pH acidification. *C. rodentium* strains were grown in N-minimal medium containing 1 mM $MgCl_2$, as described previously for *S. enterica* (Prost *et al.*, 2007). A 3.7-fold increase in *mgtA::lacZ* gene transcription was observed when wild-type cells were transferred from a medium buffered with Bis-Tris at pH 7.5 to one at pH 5.5 (Fig. 1C). A similar response to pH acidification was obtained using media buffered with MOPS (2.5-fold increase in *mgtA*::*lacZ* activation) (data not shown). With both buffer systems, pH was stable over the course of the experiment. Acidic pH did not induce reporter activation in the Δ*phoPQ* mutant (Fig. 1C), indicating that *C. rodentium* PhoQ responds to acidic pH, as does its *S. enterica* homologue. The effect of the α-helical AMPs L-C18G and CRAMP on the expression of the *mgtA*::*lacZ* fusions was measured, as *S. enterica* PhoQ was previously shown to sense these AMPs (Bader *et al.*, 2005). Strikingly, the addition of sublethal concentrations of L-C18G or CRAMP did not affect expression of the *mgtA*::*lacZ* fusion in *C. rodentium* wild-type (Fig. 1D). Expression of a *phoP*::*lacZ* transcriptional fusion in *C. rodentium* wild-type in the absence and presence of these AMPs confirmed this result (data not shown). The apparent unresponsiveness of *C. rodentium* PhoPQ to α-helical AMPs is in sharp contrast to what was observed for *S. enterica* PhoPQ under similar experimental conditions (Fig. 3A) (Bader *et al.*, 2005) and might suggest that *C. rodentium* PhoQ is unable to recognize AMPs.

C. rodentium *PhoPQ is involved in the adaptive response to α-helical AMPs*

To further investigate the role of *C. rodentium* PhoPQ in AMP resistance, we compared the susceptibility of *C. rodentium* wild-type and Δ*phoPQ* to the α-helical AMPs L-C18G and CRAMP, and the cyclic lipopeptide polymyxin B (PMB) by determining minimum inhibitory concentration (MIC) values. As shown in Table 1, the *C. rodentium* Δ*phoPQ* mutant was more susceptible than wild-type to L-C18G or CRAMP, while complementation of the Δ*phoPQ* mutant with pCR*phoPQ* restored, at least partly, resistance to both peptides. Interestingly, we observed that the *C. rodentium* wild-type and Δ*phoPQ* mutant strains were equally susceptible to PMB (Table 1), indicating that, in contrast to *S. enterica* PhoPQ, *C. rodentium* PhoPQ is not involved in resistance to PMB. Similar results were obtained by disk diffusion assays using increasing amounts of L-C18G, CRAMP and PMB (data not shown). Together, these results indicate that *C. rodentium* PhoPQ is important for the adaptive response to α-helical AMPs, although *C. rodentium* PhoQ does not appear to sense these AMPs.

The C. rodentium *PhoQ periplasmic domain binds L-C18G*

The sequence of the *S. enterica* PhoQ periplasmic domain ($PhoQ_{Peri}$) contains a cluster of acidic amino acids (EDDDDAE) that has been proposed to be involved in the recognition of both divalent cations and AMPs (Bader *et al.*, 2005; Cho *et al.*, 2006). Alignment of the amino acid sequences of the *C. rodentium* and *S. enterica* PhoQ periplasmic domains showed that this acidic cluster is strictly conserved (Fig. 2A). A construct of *C. rodentium* $PhoQ_{Peri}$, corresponding to residues 45–190 of the periplasmic sensor domain, was expressed in *E. coli* and purified to homogeneity. $PhoQ_{Peri}$ was used to measure the binding of the dansylated derivative of L-C18G (dC18G) by monitoring fluorescence emission, as described previously (Bader *et al.*, 2005). As shown in Fig. 2B, dC18G fluoresces with a λ_{max} of 550 nm (line b). The fluorescence intensity of dC18G increased by approximately threefold upon addition of equimolar amounts of *C. rodentium* $PhoQ_{Peri}$ (line c). In addition, the λ_{max} was blue-shifted from 550 to 520 nm (lines b and c). These changes in fluorescence reflect movement of the dansyl group to a more hydrophobic environment and

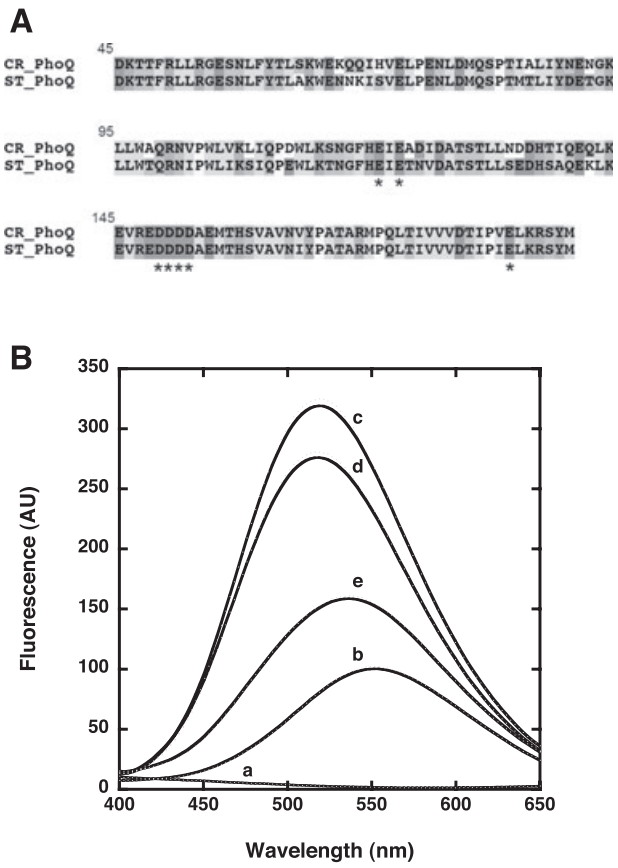

Fig. 2. The *C. rodentium* PhoQ periplasmic domain has features required for AMP recognition.
A. Amino acid sequence alignment of the *C. rodentium* (CR) and *S. enterica* (ST) PhoQ periplasmic domains. Stars indicate residues that have been proposed to be important for recognition of both divalent cations and AMPs in *S. enterica* PhoQ.
B. dC18G interacts with the *C. rodentium* PhoQ periplasmic domain. dC18G (1 μM) was excited at 340 nm and emission spectra were recorded (b). $PhoQ_{Peri}$ (1 μM) was incubated with dC18G in the absence (c) or in the presence of $MgCl_2$ at a concentration of 1 mM (d) or 10 mM (e). The emission spectrum of the protein control (1 μM $PhoQ_{Peri}$) is shown as (a). AU, arbitrary units.

illustrate that dC18G binds to *C. rodentium* $PhoQ_{Peri}$. The addition of 10 mM $MgCl_2$ caused a reduction in the fluorescence intensity and a red-shift of the λ_{max} to 537 nm (line e), confirming that Mg^{2+} effectively competes with dC18G for binding to $PhoQ_{Peri}$. These results are very similar to those obtained previously using the *S. enterica* $PhoQ_{Peri}$ protein (Bader *et al.*, 2005). The ability of *C. rodentium* $PhoQ_{Peri}$ to bind dC18G in combination with its sequence identity to *S. enterica* strongly suggests that *C. rodentium* PhoQ has the potential to recognize AMPs.

C. rodentium *PhoPQ responds to AMPs when expressed in* S. enterica

To further demonstrate that *C. rodentium* PhoQ can respond to AMPs, we complemented the Δ*phoPQ* mutant strains of *S. enterica* and *C. rodentium* with plasmids pCR*phoPQ* and pST*phoPQ* respectively. The activation of PhoPQ was measured by monitoring the β-galactosidase activity of the *mgtA::lacZ* fusion. Interestingly, in the context of the *S. enterica* Δ*phoPQ* strain, complementation with *C. rodentium phoPQ* mediated a 2.4- and 1.8-fold increase in β-galactosidase activity in the presence of L-C18G and CRAMP respectively (Fig. 3A). This level of activation was comparable to that obtained by complementation of the *S. enterica* Δ*phoPQ* strain with its native *phoPQ* operon (Fig. 3A). Conversely, *S. enterica phoPQ* introduced in the *C. rodentium* Δ*phoPQ* mutant was unable to activate transcription of the *mgtA::lacZ* fusion in response to either L-C18G or CRAMP (Fig. 3B). These data clearly show that the differential regulation of *mgtA::lacZ* in response to α-helical AMPs between *C. rodentium* and *S. enterica* is not due to differences in the respective PhoPQ systems.

Disruption of the C. rodentium *OM by AMPs*

Initially, AMPs interact with LPS and then penetrate the OM by self-promoted uptake to access the cytoplasmic membrane (Hancock and Lehrer, 1998). NPN (1-*N*-phenylnaphthylamine), which fluoresces in the hydrophobic environment of damaged membranes, was used as a probe to measure OM disruption induced by L-C18G, CRAMP or PMB (Loh *et al.*, 1984). Addition of PMB to wild-type *C. rodentium* caused a rapid increase in fluorescence intensity that reached a plateau after 30 s (Fig. 4A). In contrast, both L-C18G and CRAMP had a moderate effect on the integrity of the *C. rodentium* OM. L-C18G caused a biphasic disruption of the *C. rodentium* OM characterized by a slight burst followed by a sustained decrease in fluorescence intensity (Fig. 4A). In contrast, the OM of the *C. rodentium* Δ*phoPQ* mutant was disrupted to a much greater extent than that of wild-type upon addition of either L-C18G or CRAMP (Fig. 4B). There was no significant difference between the *C. rodentium* wild-type and Δ*phoPQ* strains in the OM disruption produced by PMB (Fig. 4A and B). Together, these results are in good agreement with the MIC values obtained for the *C. rodentium* wild-type and Δ*phoPQ* strains (Table 1). These data show that α-helical AMPs barely disrupt the OM of *C. rodentium* wild-type, and suggest that these AMPs may not be able to reach the periplasmic space and activate PhoQ. In addition, they confirm that *C. rodentium* PhoPQ controls resistance to α-helical AMPs.

Identification of a C. rodentium *OM protease involved in AMP resistance*

The OM protein fractions of the *C. rodentium* wild-type and Δ*phoPQ* strains were analysed by SDS-PAGE. As

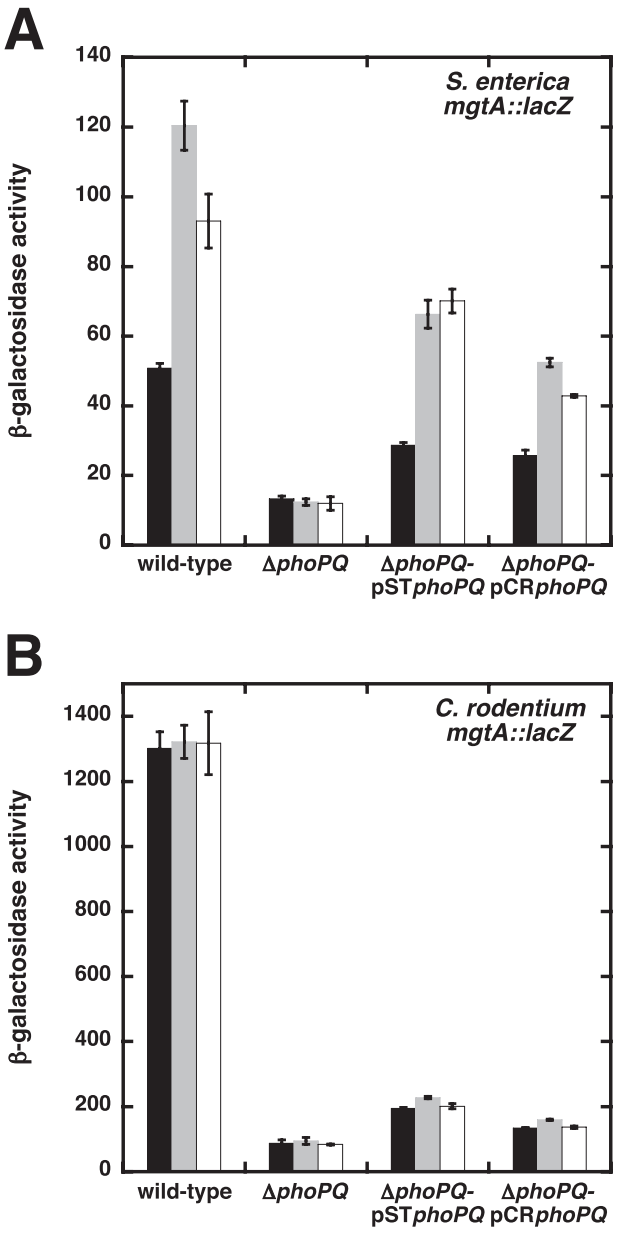

Fig. 3. *C. rodentium* PhoQ is activated by α-helical AMPs when expressed in *S. enterica*. β-Galactosidase activity produced by *S. enterica* (A) and *C. rodentium* (B) strains harbouring a chromosomal *mgtA::lacZ* fusion and complemented or not with the indicated plasmids. Cultures were grown in N-minimal medium containing 1 mM $MgCl_2$ without AMP (black bars) or with 2 μM L-C18G (grey bars) and 10 μM CRAMP (white bars). Values are mean ± standard deviation of cultures grown in triplicate and are representative of at least three independent trials.

shown in Fig. 5A, the protein profiles were essentially similar with the exception of one band having an approximate molecular weight of 33 kDa that was absent from the Δ*phoPQ* mutant. Coomassie-stained bands were cut from lanes 1 and 2, trypsin-digested and submitted to liquid chromatography electrospray ionization tandem mass spectrometry (LC-MS/MS). Mass fingerprinting identified the protein migrating at 33 kDa in the wild-type strain as a homologue of the *E. coli* OM protease OmpP. A BLAST search of the *C. rodentium* genome identified an ORF coding for an OM protease of the omptin family

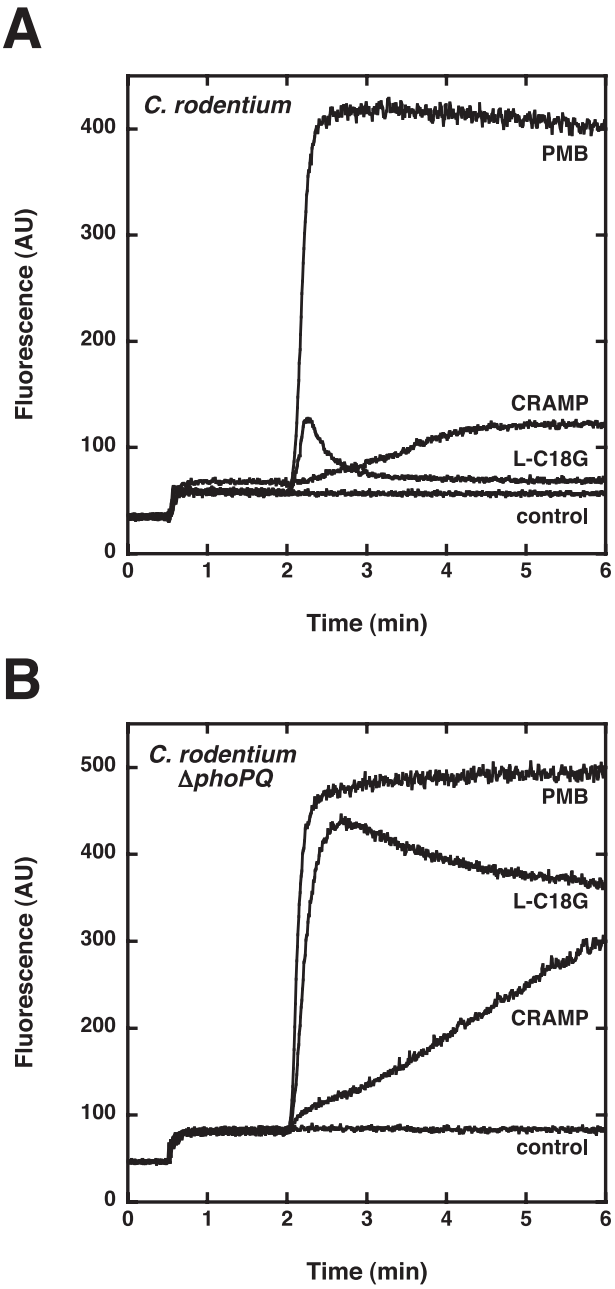

Fig. 4. PhoPQ protects the *C. rodentium* OM from disruption by α-helical AMPs. *C. rodentium* wild-type (A) and Δ*phoPQ* (B) cells were exposed to either 2 μM L-C18G, 10 μM CRAMP or 0.7 μM PMB. The OM uptake of NPN was monitored by measuring fluorescence over time. NPN and AMPs were added 30 s and 2 min, respectively, after the beginning of the experiment. Each experiment is representative of at least three independent trials. AU, arbitrary units.

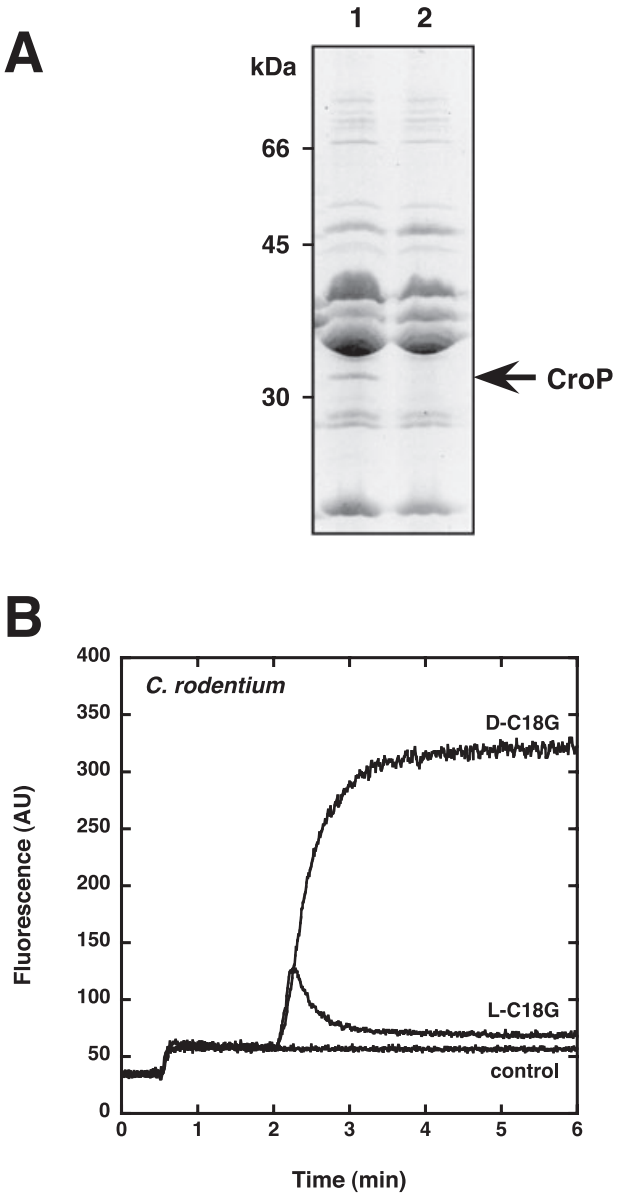

Fig. 5. Identification and stereospecificity of the CroP OM protease.
A. SDS-PAGE of OM protein fractions isolated from *C. rodentium* wild-type (lane 1) and Δ*phoPQ* (lane 2) cultures grown in LB for 6 h. The arrow indicates the band corresponding to the CroP OM protease identified by mass fingerprinting.
B. Disruption of the *C. rodentium* OM in response to L- and D-C18G. Wild-type *C. rodentium* cells were exposed to 2 μM of either L- or D-C18G and NPN fluorescence was measured over time. Each experiment is representative of at least three independent trials. AU, arbitrary units.

(Accession No. ROD20151), hereafter named CroP (*C. rodentium* outer-membrane protease). The protein sequence of the *croP* gene shared 73% and 74% amino acid sequence identity with *E. coli* OmpP and OmpT, respectively, and 40% sequence identity with *S. enterica* PgtE. The CroP sequence contained the conserved residue pairs (Asp-103–Asp-105 and Asp-230–His-232) that constitute the omptin active site (Hritonenko and Stathopoulos, 2007).

We hypothesized that if CroP was a functional OM protease degrading α-helical AMPs, it would display stereospecificity with respect to its substrates. To test our hypothesis, the enantiomer of L-C18G (D-C18G) was synthesized from all D-amino acids. As shown in Table 1, wild-type *C. rodentium* was eightfold more susceptible to D-C18G than L-C18G, suggesting that D-C18G is not degraded by CroP. Furthermore, the Δ*phoPQ* mutant exhibited similar MIC values for L-C18G and D-C18G, suggesting that PhoPQ controls *croP* expression and/or CroP activity. In addition, D-C18G caused a rapid increase in NPN fluorescence, indicating extensive damage to the wild-type *C. rodentium* OM (Fig. 5B). Altogether, our results are indicative of a stereospecific mechanism of AMP resistance that is consistent with the enzymatic activity of the CroP OM protease. A Δ*croP* deletion mutant was generated to better define the role of CroP in resistance to α-helical AMPs.

PhoPQ regulates croP *expression and the presence of CroP at the OM*

To determine whether PhoP regulates expression of the *croP* gene at the transcriptional level, RNA was isolated from the *C. rodentium* wild-type, Δ*phoPQ* and Δ*croP* strains grown under PhoPQ-inducing conditions. Real-time quantitative PCR (qPCR) was performed using the 16S rRNA gene as the reference gene for normalization. Compared with the wild-type strain, transcription of *croP* was reduced by 184- and 33 000-fold in the Δ*phoPQ* and Δ*croP* strains respectively. These results indicate that *croP* expression is partly, but not entirely, under the control of PhoP. The absence of a prototypical PhoP box in the *croP* promoter may indicate that PhoPQ-mediated regulation of *croP* is indirect. Subsequently, the presence of the CroP protein at the OM was investigated by isolating OM protein fractions from strains grown under PhoPQ-inducing or PhoPQ-repressing conditions. Wild-type and complemented Δ*croP* mutant strains grown in the presence of 8 μM $MgCl_2$ showed a Coomassie-stained band corresponding to CroP (Fig. 6). This band was undetectable for cells grown in the presence of 10 mM $MgCl_2$. The presence of active CroP at the OM was further demonstrated by the appearance of an OmpA degradation product (OmpA*) that was identified by mass fingerprinting (Fig. 6). Both the CroP and OmpA* bands were absent from OM protein fractions isolated from the Δ*croP* mutant (Fig. 6). Additional bands missing from OM fractions of cells grown under PhoPQ-repressing conditions may correspond to CroP conformational isoforms or autoprocessed forms (Haiko *et al.*, 2009b). Together these data

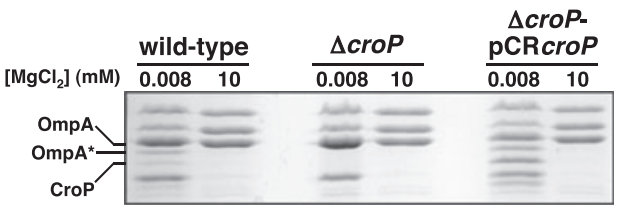

Fig. 6. External Mg^{2+} regulates the presence of CroP at the OM. OM protein fractions of *C. rodentium* wild-type, Δ*croP* and Δ*croP* complemented strains grown under PhoPQ-inducing (8 μM $MgCl_2$) or PhoPQ-repressing conditions (10 mM $MgCl_2$) were analysed by SDS-PAGE. Bands corresponding to the CroP and OmpA proteins are indicated. OmpA* corresponds to an OmpA degradation product, as determined by mass fingerprinting.

suggest that PhoPQ regulates both expression of *croP* at the transcriptional level and the presence of CroP at the OM at a post-transcriptional level. The latter regulation level is consistent with the previous observation that localization of *S. enterica* PgtE to the OM is PhoPQ-dependent (Guina *et al.*, 2000).

CroP contributes to the protection of the OM from AMP damage

Minimum inhibitory concentration values were determined for the *C. rodentium* Δ*croP* mutant, which was found to be as susceptible as the Δ*phoPQ* mutant to L-C18G and CRAMP (Table 1). Complementation of the Δ*croP* mutant with plasmid pCR*croP* restored resistance to L-C18G and CRAMP to a greater extent than wild-type (Table 1). Similar results were obtained by disk diffusion assays (data not shown). In agreement with these results, L-C18G and CRAMP were able to disrupt the OM of the Δ*croP* mutant, as illustrated by the increase in NPN fluorescence that follows the addition of these AMPs (Fig. 7A). Interestingly, the addition of L-C18G or CRAMP to the Δ*croP* mutant complemented with pCR*croP* produced the same baseline signal as the control without AMP, suggesting complete proteolytic inactivation of AMPs (Fig. 7B). As shown in Fig. 7A and B, the addition of PMB to both the Δ*croP* and the pCR*croP*-complemented strains caused the same rapid increase in fluorescence intensity as the wild-type strain (Fig. 4A), indicating that PMB is not a CroP substrate. Taken together, these results show that CroP plays a crucial role in resistance to α-helical AMPs, likely through its proteolytic activity.

CroP degrades AMPs

To verify that CroP was directly responsible for the proteolytic inactivation of AMPs, cleavage of L-C18G and CRAMP was assayed using the wild-type, Δ*phoPQ*, Δ*croP* and complemented Δ*croP* strains. As shown in Fig. 8, L-C18G was completely degraded when incubated for 30 min with wild-type *C. rodentium* cells (lane 2). In sharp contrast, no degradation was observed when L-C18G was incubated with either Δ*phoPQ* or Δ*croP* mutant cells (lanes 3 and 4). As expected, complementation of the Δ*croP* mutant with pCR*croP* led to the complete degradation of L-C18G (lane 5). Similar results were obtained using CRAMP as a CroP substrate (Fig. 8B). The results shown in Fig. 5B and Table 1 correlate with D-C18G not

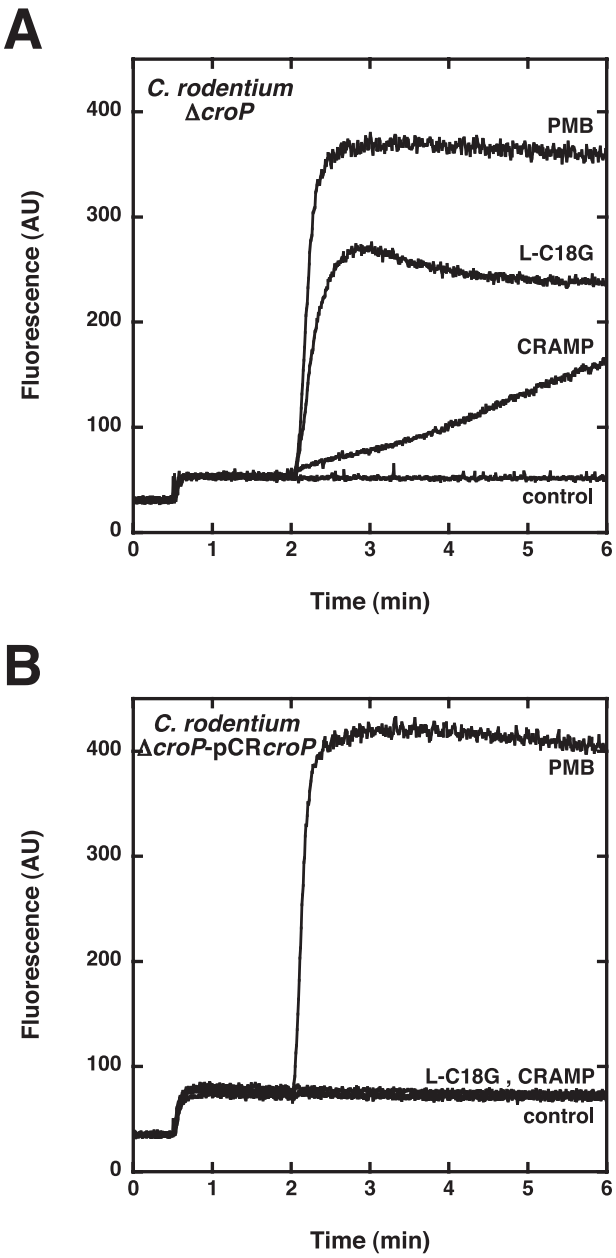

Fig. 7. Involvement of the CroP OM protease in resistance to α-helical AMPs. OM disruption of the *C. rodentium* Δ*croP* (A) and Δ*croP* complemented (B) strains in the presence of AMPs. Bacterial cells were exposed to either 2 μM L-C18G, 10 μM CRAMP or 0.7 μM PMB and NPN fluorescence was measured over time. Each experiment is representative of at least three independent trials.

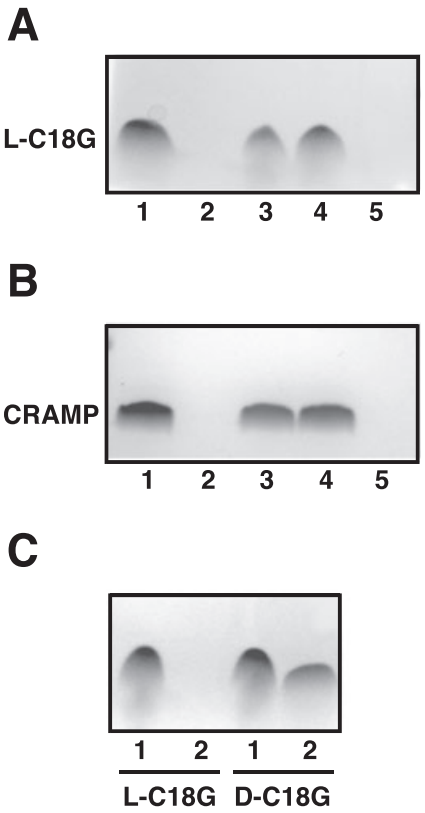

Fig. 8. Proteolytic degradation of α-helical AMPs by *C. rodentium* CroP.
A and B. Degradation of L-C18G (A) and CRAMP (B) by *C. rodentium* strains. L-C18G or CRAMP (10 μg) was incubated for 30 min at 37°C in the absence of bacterial cells (lanes 1) or in the presence of the *C. rodentium* wild-type (lanes 2), Δ*phoPQ* (lanes 3), Δ*croP* (lanes 4) and Δ*croP* complemented (lanes 5) strains. Aliquots were analysed by Tris-Tricine SDS-PAGE and subsequently stained with Coomassie blue.
C. D-C18G is not degraded by CroP. L-C18G or D-C18G (10 μg) was incubated for 30 min at 37°C in the absence of bacterial cells (lanes 1) or in the presence of *C. rodentium* wild-type cells (lanes 2).

being degraded when incubated with *C. rodentium* wild-type cells (Fig. 8C). These data clearly show that the proteolytic activity of CroP, present at the *C. rodentium* OM, is responsible for the degradation of α-helical AMPs.

CroP inhibits PhoQ recognition of AMPs

To ascertain whether AMPs could activate PhoPQ in the context of the *C. rodentium* Δ*croP* mutant, we assayed the expression of *mgtA::lacZ* and *phoP::lacZ* in the presence of L-C18G and CRAMP. As shown in Fig. 9, the addition of L-C18G and CRAMP induced a 2.5- and 2.1-fold increase in *mgtA::lacZ* activity and a 1.8- and 1.9-fold increase in *phoP::lacZ* activity respectively. To further confirm this result, qPCR was performed on RNA samples isolated from the *C. rodentium* Δ*croP* mutant exposed or not to L-C18G for 15 min. The presence of L-C18G enhanced expression of the *mgtA* and *phoP* genes by 12- and 5-fold respectively. Thus, α-helical AMPs activate *C. rodentium* PhoQ in the absence of CroP. These data demonstrate that the presence of CroP at the *C. rodentium* OM is responsible for the unresponsiveness of PhoQ to α-helical AMPs, which are degraded before they reach the periplasmic space and activate PhoQ.

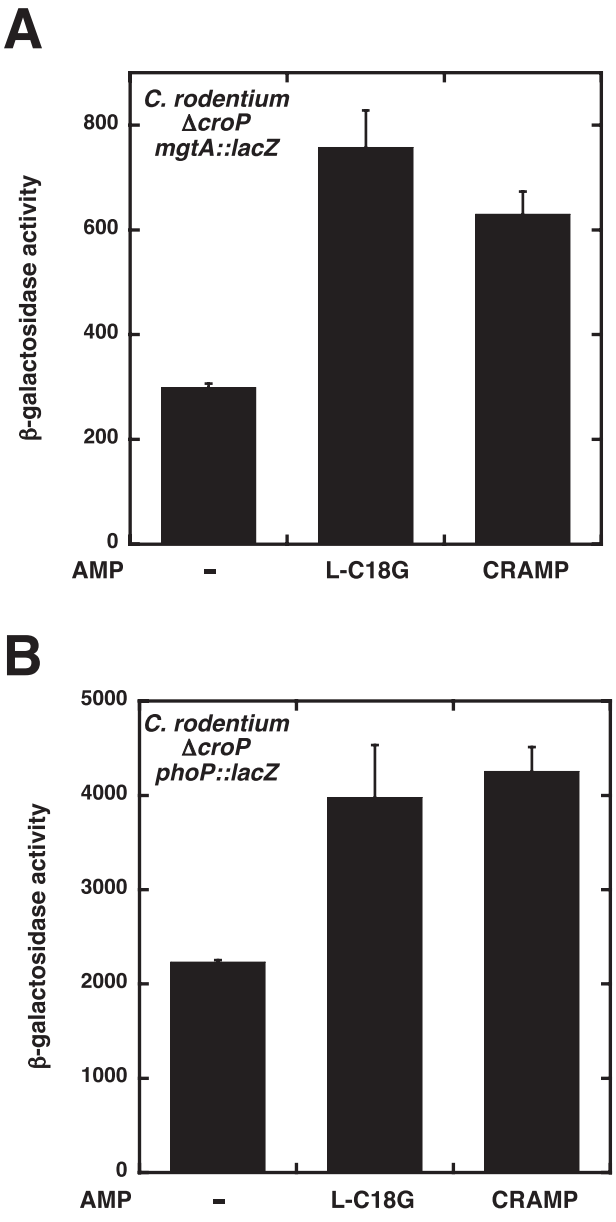

Fig. 9. *C. rodentium* PhoPQ responds to α-helical AMPs in the Δ*croP* mutant. β-Galactosidase activity from chromosomal *mgtA::lacZ* (A) and *phoP::lacZ* (B) transcriptional fusions expressed by *C. rodentium* Δ*croP* strains. Cells were grown in N-minimal medium supplemented with 1 mM $MgCl_2$ in the absence or presence of either 2 μM C18G or 10 μM CRAMP. Values are mean ± standard deviation of cultures grown in triplicate and are representative of at least three independent trials.

Discussion

Antimicrobial peptides are an important means of defence against bacterial pathogens. The mouse colonic environment inhabited by *C. rodentium* contains CRAMP, an α-helical AMP that has been shown to have antimicrobial activity against this extracellular pathogen (Iimura *et al.*, 2005). PhoQ is a chief sensor of the host environment that responds to divalent cations, pH and AMPs in *S. enterica*. It remains unclear whether all PhoQ homologues respond to the same cues. To determine whether *C. rodentium* PhoPQ plays a role in resistance to AMPs, including CRAMP, we characterized this TCS and compared it with its homologue in *S. enterica*. The activities of both *C. rodentium* and *S. enterica* PhoPQ systems were repressed by millimolar concentrations of Mg^{2+} and activated by acidic pH. In addition, both Δ*phoPQ* mutants showed increased susceptibility to α-helical AMPs. However, our study revealed a striking difference between the *C. rodentium* and *S. enterica* PhoPQ systems. The *C. rodentium* PhoQ sensor was apparently unresponsive to α-helical AMPs such as CRAMP and L-C18G, whereas these AMPs were shown to activate the *S. enterica* PhoPQ system upon recognition by PhoQ (Bader *et al.*, 2005).

We have found that sublethal concentrations of α-helical AMPs do not activate PhoPQ in *C. rodentium* wild-type. However, this study provides several lines of evidence showing that *C. rodentium* PhoQ has all the features needed for recognizing and being activated by AMPs. First, *C. rodentium* PhoQ possesses the acidic cluster that participates in the binding of both divalent cations and AMPs in *S. enterica* PhoQ (Fig. 2A) (Bader *et al.*, 2005; Cho *et al.*, 2006). The isolated PhoQ periplasmic sensor domain bound dC18G, much like its *S. enterica* homologue (Fig. 2B) (Bader *et al.*, 2005). AMPs activated PhoPQ when the *C. rodentium phoPQ* operon was expressed in a *S. enterica* Δ*phoPQ* mutant (Fig. 3A). Finally, *C. rodentium* PhoPQ was activated by AMPs in a Δ*croP* mutant (Fig. 9). Thus, the observed difference in response to α-helical AMPs between the *C. rodentium* and *S. enterica* PhoQ proteins is attributable to the CroP OM protease in *C. rodentium*. Our study also provides compelling evidence that CroP is a key player in resistance to α-helical AMPs. First, susceptibility to α-helical AMPs was largely increased in the Δ*croP* mutant (Table 1). NPN fluorescence experiments showed that CroP prevents α-helical AMPs from crossing the OM (Fig. 7). Lastly, L-C18G and CRAMP were readily degraded when incubated with bacteria expressing CroP at their OM (Fig. 8). Thus, CroP protects the *C. rodentium* OM from disruption induced by α-helical AMPs by degrading them before they reach the periplasmic space and activate PhoQ.

The PgtE OM protease of *S. enterica* shares 40% amino acid sequence identity with CroP, but did not prevent AMPs from reaching the periplasmic space and activating PhoPQ (Fig. 3A). In the study by Guina *et al.* PgtE appeared to have a minor effect on *S. enterica* survival in the presence of L-C18G when expressed from a single chromosomal copy. Only when *pgtE* was overexpressed on a high-copy-number plasmid was susceptibility of *S. enterica* to L-C18G decreased (Guina *et al.*, 2000). It is a possibility that PgtE is far less efficient than CroP at degrading L-C18G for several reasons. First, the *croP* and *pgtE* genes may be expressed at different levels when their respective bacteria are grown in laboratory media. In support of this, previous studies have shown that *pgtE* expression and PgtE activity were enhanced during the intracellular growth of *S. enterica* in macrophages (Eriksson *et al.*, 2003; Lahteenmaki *et al.*, 2005). In addition, the highly divergent promoter regions of the *croP* and *pgtE* genes suggest that transcription could be regulated by different factors. A second explanation is that the CroP and PgtE OM proteases exhibit different substrate specificities and/or catalytic efficiencies. The fact that the CroP amino acid sequence is only 40% identical to that of PgtE is consistent with the possibility that CroP degrades primarily biologically active AMPs, whereas PgtE preferentially cleaves larger protein substrates (A. Portt, unpublished). Interestingly, our data indicate that CroP does not degrade all AMPs, as the cyclic lipopeptide PMB causes OM disruption regardless of the presence of CroP (Fig. 7). The resistance of PMB to enzymatic proteolysis may be due to peptide cyclization and/or the presence of the unusual amino acid analogue 2,4-diaminobutyric acid.

The important contribution of *S. enterica* lipid A modifications to AMP resistance has been extensively documented. Strikingly, many genes that encode LPS-modifying enzymes in *S. enterica* are absent from the *C. rodentium* genome. Of the *S. enterica* PhoP-regulated genes *lpxO*, *pagL* and *pagP*, only *pagP* is present in the *C. rodentium* genome. The PhoP-regulated *pmrD* gene, whose gene product connects the *S. enterica* PhoPQ and PmrAB regulatory pathways, is absent from the *C. rodentium* genome. In addition, the PmrA-regulated *pmrHFIJKLM* operon is missing from the *C. rodentium* genome. This operon is responsible for the addition of 4-aminoarabinose to lipid A, a modification that is essential to PMB resistance (Gunn *et al.*, 1998). These findings are consistent with PhoPQ not playing a role in PMB resistance (Table 1). Although it is possible that LPS-modifying genes are harboured by *C. rodentium* virulence plasmids, it appears that *C. rodentium* possesses only the *pagP* and *pmrC* genes that are responsible for the transfer of palmitate and the addition of phosphoethanolamine to lipid A respectively. This limited number of lipid A modifications may not allow *C. rodentium* to strengthen the permeability barrier of its OM to an extent compatible with AMP resistance. These observations suggest that

C. rodentium may rely primarily on the CroP OM protease to resist AMPs and that LPS modifications play a secondary role. Thus, *C. rodentium* and *S. enterica* appear to use different strategies to resist AMPs. Nonetheless, PhoPQ remains a central regulator of AMP resistance for both organisms.

In summary, this work provides an alternative mechanism by which the extracellular enteric pathogen, *C. rodentium*, resists AMPs. This mechanism relies upon the proteolytic inactivation of AMPs by an OM protease of the omptin family.

Experimental procedures

Bacterial strains and growth conditions

Bacterial strains and plasmids used in this study are listed in Table S1. Bacterial cultures were grown at 37°C in Luria–Bertani (LB) broth, Tryptic Soy Broth (TSB) or N-minimal medium supplemented with 0.2% glucose (Nelson and Kennedy, 1971). When appropriate, media were supplemented with the following antibiotics: ampicillin (100 μg ml^{-1}), chloramphenicol (30 μg ml^{-1}), kanamycin (50 μg ml^{-1}), streptomycin (30 μg ml^{-1}) and gentamicin (20 μg ml^{-1}).

Construction of C. rodentium *deletion mutants*

Plasmid purification, cloning and transformation were performed according to standard procedures (Sambrook *et al.*, 1989). All oligonucleotide primers are listed in Table S2. The *C. rodentium* Δ*phoPQ* and Δ*croP* deletion mutants were generated by *sacB* gene-based allelic exchange (Donnenberg and Kaper, 1991). The upstream and downstream sequences of the *phoPQ* operon were PCR-amplified from *C. rodentium* genomic DNA using primers CR400, CR401, CR402 and CR403. To generate plasmid pCR001, a three-way ligation was performed with the two digested fragments (XbaI–NdeI and NdeI–SacI) and plasmid pRE118 previously cleaved with XbaI and SacI. The constructed plasmid pCR001 was confirmed by sequencing and transformed by electroporation into *C. rodentium* DBS100. Transformants were grown on LB agar with kanamycin to select for plasmid insertion into the chromosome of *C. rodentium*. The 5′ and 3′ flanking regions of *croP* were amplified using primers CR636, CR637, CR638 and CR639. A two-step ligation was used to insert the digested fragments (XbaI–EcoRV and EcoRV–SacI) into the XbaI and SacI sites of pRE112. The resulting plasmid, pCR002, was transformed into the *E. coli* donor strain χ7213 and conjugated into the *C. rodentium* wild-type strain. Plasmid insertion was selected for using LB agar supplemented with chloramphenicol. Clones of each deletion mutant were grown on peptone agar containing 2% sucrose to select for sucrose-resistant colonies that were either Kan^s or Cm^s, indicating that allelic exchange resulted in the loss of the wild-type copy of *phoPQ* and *croP*, respectively, along with the plasmid vehicle. Insertions were confirmed by PCR and sequencing.

Plasmid construction

Plasmid pCR*phoPQ* was constructed by amplifying the *phoPQ* operon and its promoter from *C. rodentium* genomic DNA using *Pfx* DNA polymerase (Invitrogen) and primers CR541 and CR430. The resulting PCR product was cloned into the XbaI and BamHI restriction sites of plasmid pWSK129. Similarly, pST*phoPQ* was obtained by cloning the PCR-amplified *S. enterica phoPQ* operon and its promoter (primers ST565 and ST564) into pWSK129 previously digested with XbaI and BamHI. The *C. rodentium croP* gene and its promoter were PCR-amplified using primers CR634 and CR639 and cloned into the XbaI and SacI sites of pWSK129, generating plasmid pCR*croP*.

Construction of chromosomal lacZ *transcriptional fusions and β-galactosidase assay*

Chromosomal transcriptional fusions between the *mgtA* or *phoP* promoters and the *lacZ* reporter gene were generated in *C. rodentium* and *S. enterica* using the suicide vector pFUSE (Baümler *et al.*, 1996). The *mgtA::lacZ* fusion was constructed by PCR amplifying the *mgtA* promoter using *C. rodentium* genomic DNA and primers CR542 and CR543. The PCR product was digested with XbaI and SmaI and cloned into the corresponding sites of pFUSE. The resulting construct was transferred into the *C. rodentium* wild-type, Δ*phoPQ* and Δ*croP* strains by conjugation and integrated by homologous recombination, as previously described (Daigle *et al.*, 2001). A similar strategy was used to integrate the *phoP*::*lacZ* fusion (primers CR540 and CR541) into the *C. rodentium* wild-type and Δ*croP* strains. The *S. enterica mgtA*::*lacZ* fusion (primers ST459 and ST458) was integrated into the chromosome of both *S. enterica* wild-type and Δ*phoPQ*. β-Galactosidase activity assays were performed in triplicate, as previously described (Miller, 1972).

MIC determination and disk diffusion assay

CRAMP (GLLRKGGEKIGEKLKKIGQKIKNFFQKLVPQPEQ) and L-C18G (ALYKKLLKKLLKSAKKLG) were synthesized with a purity of > 85% (BioChemia). D-C18G, the all D-amino acid enantiomer of L-C18G, was synthesized at the Sheldon Biotechnology Centre, McGill University. Dansylated C18G was a gift from S.I. Miller (University of Washington). PMB was purchased from Sigma. MICs were determined by the broth microdilution method in 96-well microtitre plates, as previously described (Wiegand *et al.*, 2008). Bacterial cultures were grown in TSB and diluted to 5×10^5 cfu ml^{-1} in N-minimal medium containing 1 mM $MgCl_2$. Serial dilutions of AMPs were added and plates were incubated at 37°C for 24 h. The lowest concentration of AMP that completely inhibited growth was identified as the MIC. For disk diffusion assays, aliquots (80 μl) of overnight cultures were inoculated into 1% agarose (20 ml) and poured into 15 cm Petri dishes containing LB agar. Disks containing increasing amounts of AMP were layered on top of the agarose and incubated overnight at 37°C.

Cloning, expression and purification of the C. rodentium *PhoQ periplasmic domain*

The *C. rodentium* PhoQ periplasmic domain ($PhoQ_{Peri}$) was amplified by PCR using primers CR562 and CR563 from

genomic DNA. The PCR fragment was digested with BamHI and XbaI and ligated into plasmid pET11a digested with the same enzymes to generate plasmid $pCRQ_{Peri}$. The *C. rodentium* $PhoQ_{Peri}$ protein was expressed in *E. coli* ArcticExpress™ (DE3)RIL cells (Stratagene) according to the manufacturer's instructions. Cells were harvested and re-suspended in 20 mM sodium phosphate buffer (pH 7.5) containing 500 mM NaCl, 20 mM imidazole and PMSF (17 μg ml^{-1}). Cells were disrupted by sonication, centrifuged at 216 000 *g* for 30 min and the supernatant was applied to a Ni^{2+}-NTA affinity chromatography column (GE Healthcare). Purified protein was dialysed against 20 mM Tris-HCl (pH 7.5) containing 150 mM NaCl. Protein concentration was determined using the BCA protein assay (Pierce).

Fluorescence spectroscopy

Peptide binding assays were performed as previously described (Bader *et al.*, 2005). $PhoQ_{Peri}$ at a final concentration of 1 μM was incubated with 1 μM dansylated C18G (dC18G) in the absence or presence of $MgCl_2$ for 20 min at room temperature. Excitation of dC18G was at 340 nm and fluorescence emission spectra were recorded from 400 to 650 nm using 10 nm slit widths. Each spectrum was the mean of 10 consecutive scans.

OM disruption assay

Bacterial cells were grown to an OD_{600} of 0.5–0.6 in N-minimal medium containing 1 mM $MgCl_2$. Cells were diluted to an OD_{600} of 0.37 with 5 mM HEPES (pH 7.5) and transferred into a quartz cuvette equipped with a stir bar. NPN (Sigma) was added 30 s after the start of the experiment at a concentration of 5 μM and AMPs were added 90 s later. Samples were excited at 350 nm and emitted fluorescence was recorded over time at 420 nm using 5 nm slit widths.

OM protein extraction

Outer membrane protein fractions were isolated as previously described (Hernandez-Alles *et al.*, 1999). Briefly, cells were collected by centrifugation, re-suspended in 10 mM Tris-HCl (pH 7.5) containing 5 mM $MgCl_2$ and disrupted by sonication. Unbroken cells were removed by centrifugation at 3300 *g* for 10 min. Cell membranes were collected by high-speed centrifugation at 100 000 *g* for 1 h. The pellet was re-suspended in 10 mM Tris-HCl (pH 7.5), 5 mM $MgCl_2$ containing 2% sodium lauryl sarcosinate and incubated for 30 min at 25°C. OM proteins were collected by centrifugation at 100 000 *g* for 1 h. Following a second treatment with sodium lauryl sarcosinate, OM proteins were re-suspended in SDS sample buffer before being resolved on a 12.5% SDS-PAGE gel and stained with Coomassie blue. In-gel trypsin digestion, mass spectrometry and analysis by MASCOT software were carried out at the McGill University and Génome Québec Innovation Centre, Montreal, Canada.

Real-time quantitative RT-PCR (qPCR)

Bacterial strains were grown to an OD_{600} of 0.5 in N-minimal medium supplemented with 1 mM $MgCl_2$. Total RNA was isolated using TRIzol reagents (Invitrogen) and treated with the DNA-free kit (Ambion) to remove any trace of DNA. The absence of contaminating DNA was confirmed by qPCR using primers CR712 and CR713 (Table S2). RNA (1 μg) was reverse-transcribed using Superscript II (Invitrogen) with 0.5 μg of random hexamer primers (Sigma). As a negative control, a reaction without Superscript II was also included (NRT). qPCR reactions were performed in a Rotor-Gene 3000 thermal cycler (Corbett Research) by using the QuantiTect SYBR Green PCR kit (Qiagen), according to manufacturer's instructions. Primers used are listed in Table S2. The transcriptional level of the genes of interest under each condition was normalized against the reference gene (16S rRNA) and analysed by applying the $2^{-\Delta\Delta CT}$ method (Livak and Schmittgen, 2001). For each condition, reverse transcription was performed three times independently, and the NRT sample was used as a negative control.

Proteolytic cleavage of AMPs by CroP

Bacterial cells were grown to an OD_{600} of 0.5–0.6 in N-minimal medium with 1 mM $MgCl_2$. Culture aliquots (20 μl) were incubated with 10 μg of AMP for 30 min at 37°C in a total volume of 25 μl. Bacterial cells were pelleted by centrifugation. The supernatant was removed and an equal volume of Tricine sample buffer (2×) was added. Aliquots (10 μl) were analysed by Tris-Tricine SDS-PAGE (10–20% acrylamide, Bio-Rad) and Coomassie staining.

Western blotting

Wild-type *C. rodentium* cells were grown at 37°C to an OD_{600} of 0.8 in N-minimal medium (pH 7.5) containing either 8 μM or 10 mM $MgCl_2$. Cells were harvested and re-suspended in 100 mM sodium phosphate buffer (pH 7.5), 5 mM EDTA and 10% glycerol. Cells were lysed by sonication and cell debris was removed by centrifugation at 100 000 *g* for 30 min. Equal amounts of whole cell lysates were run on a 10% SDS-PAGE gel and transferred to a nitrocellulose membrane. The blot was developed with an antiserum against *S. enterica* PhoP (1:1000), an anti-rabbit IgG horseradish peroxidase-linked antibody (1:5000) and the Immobilon Western reagent (Millipore).

Acknowledgements

We are grateful to Samuel I. Miller (University of Washington Medical School, Seattle, WA, USA) for providing dansylated L-C18G. This work was supported by the Canadian Institutes of Health Research (CIHR, MOP-15551) and the Natural Sciences and Engineering Research Council (NSERC, 217482). A.P. was the recipient of an Ontario–Quebec exchange fellowship and a F.C. Harrison fellowship. C.V. was supported by a studentship from Fonds de la Recherche en Santé du Québec (FRSQ).

References

Alpuche Aranda, C.M., Swanson, J.A., Loomis, W.P., and Miller, S.I. (1992) *Salmonella typhimurium* activates viru-

lence gene transcription within acidified macrophage phagosomes. *Proc Natl Acad Sci USA* **89:** 10079–10083.
Bader, M.W., Sanowar, S., Daley, M.E., Schneider, A.R., Cho, U., Xu, W., *et al.* (2005) Recognition of antimicrobial peptides by a bacterial sensor kinase. *Cell* **122:** 461–472.
Baümler, A.J., Tsolis, R.M., van der Velden, A.W., Stojiljkovic, I., Anic, S., and Heffron, F. (1996) Identification of a new iron regulated locus of *Salmonella typhi*. *Gene* **183:** 207–213.
Brogden, K.A. (2005) Antimicrobial peptides: pore formers or metabolic inhibitors in bacteria? *Nat Rev Microbiol* **3:** 238–250.
Castelli, M.E., Garcia Vescovi, E., and Soncini, F.C. (2000) The phosphatase activity is the target for Mg^{2+} regulation of the sensor protein PhoQ in *Salmonella*. *J Biol Chem* **275:** 22948–22954.
Cho, U.S., Bader, M.W., Amaya, M.F., Daley, M.E., Klevit, R.E., Miller, S.I., and Xu, W. (2006) Metal bridges between the PhoQ sensor domain and the membrane regulate transmembrane signaling. *J Mol Biol* **356:** 1193–1206.
Daigle, F., Graham, J.E., and Curtiss, R., 3rd (2001) Identification of *Salmonella typhi* genes expressed within macrophages by selective capture of transcribed sequences (SCOTS). *Mol Microbiol* **41:** 1211–1222.
Derzelle, S., Turlin, E., Duchaud, E., Pages, S., Kunst, F., Givaudan, A., and Danchin, A. (2004) The PhoP–PhoQ two-component regulatory system of *Photorhabdus luminescens* is essential for virulence in insects. *J Bacteriol* **186:** 1270–1279.
Donnenberg, M.S., and Kaper, J.B. (1991) Construction of an *eae* deletion mutant of enteropathogenic *Escherichia coli* by using a positive-selection suicide vector. *Infect Immun* **59:** 4310–4317.
Eriksson, S., Lucchini, S., Thompson, A., Rhen, M., and Hinton, J.C. (2003) Unravelling the biology of macrophage infection by gene expression profiling of intracellular *Salmonella enterica*. *Mol Microbiol* **47:** 103–118.
Galvan, E.M., Lasaro, M.A., and Schifferli, D.M. (2008) Capsular antigen fraction 1 and Pla modulate the susceptibility of *Yersinia pestis* to pulmonary antimicrobial peptides such as cathelicidin. *Infect Immun* **76:** 1456–1464.
Ganz, T. (2003) Defensins: antimicrobial peptides of innate immunity. *Nat Rev Immunol* **3:** 710–720.
Garcia Vescovi, E., Soncini, F.C., and Groisman, E.A. (1996) Mg^{2+} as an extracellular signal: environmental regulation of *Salmonella* virulence. *Cell* **84:** 165–174.
Groisman, E.A., Chiao, E., Lipps, C.J., and Heffron, F. (1989) *Salmonella typhimurium phoP* virulence gene is a transcriptional regulator. *Proc Natl Acad Sci USA* **86:** 7077–7081.
Guina, T., Yi, E.C., Wang, H., Hackett, M., and Miller, S.I. (2000) A PhoP-regulated outer membrane protease of *Salmonella enterica* serovar Typhimurium promotes resistance to alpha-helical antimicrobial peptides. *J Bacteriol* **182:** 4077–4086.
Gunn, J.S., Lim, K.B., Krueger, J., Kim, K., Guo, L., Hackett, M., and Miller, S.I. (1998) PmrA–PmrB-regulated genes necessary for 4-aminoarabinose lipid A modification and polymyxin resistance. *Mol Microbiol* **27:** 1171–1182.
Haiko, J., Suomalainen, M., Ojala, T., Lahteenmaki, K., and Korhonen, T.K. (2009a) Breaking barriers – attack on innate immune defences by omptin surface proteases of enterobacterial pathogens. *Innate Immun* **15:** 67–80.
Haiko, J., Kukkonen, M., Ravantti, J.J., Westerlund-Wikstrom, B., and Korhonen, T.K. (2009b) The single substitution I259T, conserved in the plasminogen activator Pla of pandemic *Yersinia pestis* branches, enhances fibrinolytic activity. *J Bacteriol* **191:** 4758–4766.
Hancock, R.E., and Lehrer, R. (1998) Cationic peptides: a new source of antibiotics. *Trends Biotechnol* **16:** 82–88.
Hancock, R.E., and Sahl, H.G. (2006) Antimicrobial and host-defense peptides as new anti-infective therapeutic strategies. *Nat Biotechnol* **24:** 1551–1557.
Hase, K., Eckmann, L., Leopard, J.D., Varki, N., and Kagnoff, M.F. (2002) Cell differentiation is a key determinant of cathelicidin LL-37/human cationic antimicrobial protein 18 expression by human colon epithelium. *Infect Immun* **70:** 953–963.
Hernandez-Alles, S., Alberti, S., Alvarez, D., Domenech-Sanchez, A., Martinez-Martinez, L., Gil, J., *et al.* (1999) Porin expression in clinical isolates of *Klebsiella pneumoniae*. *Microbiology* **145:** 673–679.
Hritonenko, V., and Stathopoulos, C. (2007) Omptin proteins: an expanding family of outer membrane proteases in Gram-negative *Enterobacteriaceae*. *Mol Membr Biol* **24:** 395–406.
Iimura, M., Gallo, R.L., Hase, K., Miyamoto, Y., Eckmann, L., and Kagnoff, M.F. (2005) Cathelicidin mediates innate intestinal defense against colonization with epithelial adherent bacterial pathogens. *J Immunol* **174:** 4901–4907.
Kato, A., and Groisman, E.A. (2004) Connecting two-component regulatory systems by a protein that protects a response regulator from dephosphorylation by its cognate sensor. *Genes Dev* **18:** 2302–2313.
Kato, A., Tanabe, H., and Utsumi, R. (1999) Molecular characterization of the PhoP–PhoQ two-component system in *Escherichia coli* K-12: identification of extracellular Mg^{2+}-responsive promoters. *J Bacteriol* **181:** 5516–5520.
Kox, L.F., Wosten, M.M., and Groisman, E.A. (2000) A small protein that mediates the activation of a two-component system by another two-component system. *EMBO J* **19:** 1861–1872.
Kukkonen, M., and Korhonen, T.K. (2004) The omptin family of enterobacterial surface proteases/adhesins: from housekeeping in *Escherichia coli* to systemic spread of *Yersinia pestis*. *Int J Med Microbiol* **294:** 7–14.
Lahteenmaki, K., Kyllonen, P., Partanen, L., and Korhonen, T.K. (2005) Antiprotease inactivation by *Salmonella enterica* released from infected macrophages. *Cell Microbiol* **7:** 529–538.
Lathem, W.W., Price, P.A., Miller, V.L., and Goldman, W.E. (2007) A plasminogen-activating protease specifically controls the development of primary pneumonic plague. *Science* **315:** 509–513.
Livak, K.J., and Schmittgen, T.D. (2001) Analysis of relative gene expression data using real-time quantitative PCR and the $2^{-\Delta\Delta CT}$ method. *Methods* **25:** 402–408.
Llama-Palacios, A., Lopez-Solanilla, E., Poza-Carrion, C., Garcia-Olmedo, F., and Rodriguez-Palenzuela, P. (2003) The *Erwinia chrysanthemi phoP–phoQ* operon plays an important role in growth at low pH, virulence and bacterial survival in plant tissue. *Mol Microbiol* **49:** 347–357.

Loh, B., Grant, C., and Hancock, R.E. (1984) Use of the fluorescent probe 1-*N*-phenylnaphthylamine to study the interactions of aminoglycoside antibiotics with the outer membrane of *Pseudomonas aeruginosa*. *Antimicrob Agents Chemother* **26:** 546–551.

Marceau, M., Sebbane, F., Ewann, F., Collyn, F., Lindner, B., Campos, M.A., *et al.* (2004) The *pmrF* polymyxin-resistance operon of *Yersinia pseudotuberculosis* is upregulated by the PhoP–PhoQ two-component system but not by PmrA–PmrB, and is not required for virulence. *Microbiology* **150:** 3947–3957.

Martin-Orozco, N., Touret, N., Zaharik, M.L., Park, E., Kopelman, R., Miller, S., *et al.* (2006) Visualization of vacuolar acidification-induced transcription of genes of pathogens inside macrophages. *Mol Biol Cell* **17:** 498–510.

Melo, M.N., Ferre, R., and Castanho, M.A. (2009) Antimicrobial peptides: linking partition, activity and high membrane-bound concentrations. *Nat Rev Microbiol* **7:** 245–250.

Miller, J.H. (1972) *Experiments in Molecular Genetics*. Cold Spring Harbor, NY: Cold Spring Harbor Laboratory.

Miller, S.I., Kukral, A.M., and Mekalanos, J.J. (1989) A two-component regulatory system (*phoP phoQ*) controls *Salmonella typhimurium* virulence. *Proc Natl Acad Sci USA* **86:** 5054–5058.

Miller, S.I., Ernst, R.K., and Bader, M.W. (2005) LPS, TLR4 and infectious disease diversity. *Nat Rev Microbiol* **3:** 36–46.

Montagne, M., Martel, A., and Le Moual, H. (2001) Characterization of the catalytic activities of the PhoQ histidine protein kinase of *Salmonella enterica* serovar Typhimurium. *J Bacteriol* **183:** 1787–1791.

Moss, J.E., Fisher, P.E., Vick, B., Groisman, E.A., and Zychlinsky, A. (2000) The regulatory protein PhoP controls susceptibility to the host inflammatory response in *Shigella flexneri*. *Cell Microbiol* **2:** 443–452.

Mundy, R., MacDonald, T.T., Dougan, G., Frankel, G., and Wiles, S. (2005) *Citrobacter rodentium* of mice and man. *Cell Microbiol* **7:** 1697–1706.

Nelson, D.L., and Kennedy, E.P. (1971) Magnesium transport in *Escherichia coli*. Inhibition by cobaltous ion. *J Biol Chem* **246:** 3042–3049.

O'Neil, D.A., Porter, E.M., Elewaut, D., Anderson, G.M., Eckmann, L., Ganz, T., and Kagnoff, M.F. (1999) Expression and regulation of the human beta-defensins hBD-1 and hBD-2 in intestinal epithelium. *J Immunol* **163:** 6718–6724.

Peschel, A., and Sahl, H.G. (2006) The co-evolution of host cationic antimicrobial peptides and microbial resistance. *Nat Rev Microbiol* **4:** 529–536.

Prost, L.R., and Miller, S.I. (2008) The Salmonellae PhoQ sensor: mechanisms of detection of phagosome signals. *Cell Microbiol* **10:** 576–582.

Prost, L.R., Daley, M.E., Le Sage, V., Bader, M.W., Le Moual, H., Klevit, R.E., and Miller, S.I. (2007) Activation of the bacterial sensor kinase PhoQ by acidic pH. *Mol Cell* **26:** 165–174.

Prost, L.R., Daley, M.E., Bader, M.W., Klevit, R.E., and Miller, S.I. (2008) The PhoQ histidine kinases of *Salmonella* and *Pseudomonas* spp. are structurally and functionally different: evidence that pH and antimicrobial peptide sensing contribute to mammalian pathogenesis. *Mol Microbiol* **69:** 503–519.

Rosenberger, C.M., Gallo, R.L., and Finlay, B.B. (2004) Interplay between antibacterial effectors: a macrophage antimicrobial peptide impairs intracellular *Salmonella* replication. *Proc Natl Acad Sci USA* **101:** 2422–2427.

Sambrook, J., Fritsch, E.F., and Maniatis, T. (1989) *Molecular Cloning: A Laboratory Manual.* New York: Cold Spring Harbor Laboratory Press.

Sanowar, S., and Le Moual, H. (2005) Functional reconstitution of the *Salmonella typhimurium* PhoQ histidine kinase sensor in proteoliposomes. *Biochem J* **390:** 769–776.

Schauber, J., Svanholm, C., Termen, S., Iffland, K., Menzel, T., Scheppach, W., *et al.* (2003) Expression of the cathelicidin LL-37 is modulated by short chain fatty acids in colonocytes: relevance of signalling pathways. *Gut* **52:** 735–741.

Schauer, D.B., and Falkow, S. (1993) The *eae* gene of *Citrobacter freundii* biotype 4280 is necessary for colonization in transmissible murine colonic hyperplasia. *Infect Immun* **61:** 4654–4661.

Sodeinde, O.A., Subrahmanyam, Y.V., Stark, K., Quan, T., Bao, Y., and Goguen, J.D. (1992) A surface protease and the invasive character of plague. *Science* **258:** 1004–1007.

Soncini, F.C., Vescovi, E.G., and Groisman, E.A. (1995) Transcriptional autoregulation of the *Salmonella typhimurium phoPQ* operon. *J Bacteriol* **177:** 4364–4371.

Stumpe, S., Schmid, R., Stephens, D.L., Georgiou, G., and Bakker, E.P. (1998) Identification of OmpT as the protease that hydrolyzes the antimicrobial peptide protamine before it enters growing cells of *Escherichia coli*. *J Bacteriol* **180:** 4002–4006.

Wiegand, I., Hilpert, K., and Hancock, R.E. (2008) Agar and broth dilution methods to determine the minimal inhibitory concentration (MIC) of antimicrobial substances. *Nat Protoc* **3:** 163–175.

Winfield, M.D., Latifi, T., and Groisman, E.A. (2005) Transcriptional regulation of the 4-amino-4-deoxy-L-arabinose biosynthetic genes in *Yersinia pestis*. *J Biol Chem* **280:** 14765–14772.

Yamamoto, K., Ogasawara, H., Fujita, N., Utsumi, R., and Ishihama, A. (2002) Novel mode of transcription regulation of divergently overlapping promoters by PhoP, the regulator of two-component system sensing external magnesium availability. *Mol Microbiol* **45:** 423–438.

Zanetti, M. (2004) Cathelicidins, multifunctional peptides of the innate immunity. *J Leukoc Biol* **75:** 39–48.

Zasloff, M. (2002) Antimicrobial peptides of multicellular organisms. *Nature* **415:** 389–395.

Supporting information

Additional supporting information may be found in the online version of this article.

Please note: Wiley-Blackwell are not responsible for the content or functionality of any supporting materials supplied by the authors. Any queries (other than missing material) should be directed to the corresponding author for the article.

